

**This dissertation has been  
microfilmed exactly as received**

69-11,056

WEST, Harry Harding, 1943-  
OPTIMAL FEEDFORWARD-FEEDBACK CONTROL.

The University of Oklahoma, Ph.D., 1969  
Engineering, chemical

University Microfilms, Inc., Ann Arbor, Michigan

THE UNIVERSITY OF OKLAHOMA  
GRADUATE COLLEGE

OPTIMAL FEEDFORWARD-FEEDBACK CONTROL

A DISSERTATION  
SUBMITTED TO THE GRADUATE FACULTY  
in partial fulfillment of the requirements for the  
degree of  
DOCTOR OF PHILOSOPHY

BY  
HARRY HARDING WEST  
Norman, Oklahoma

1969

OPTIMAL FEEDFORWARD-FEEDBACK CONTROL

APPROVED BY

*Michael J. Griffin*

\_\_\_\_\_  
*E. J. Blech*

\_\_\_\_\_  
*Arthur Bernhart*

\_\_\_\_\_  
*Paul J. Rook*

\_\_\_\_\_  
*Chesleywood*

DISSERTATION COMMITTEE

## ABSTRACT

Optimal control equations are developed and applied to the chemical process regulator problem. The method of optimization uses a parametric expansion of the dynamic programming partial differential equation. This formulation requires the time domain state-variable approach to system dynamics. Composite feedforward-feedback controllers are shown to be optimum in the quadratic sense. The effect of system delay time, signal-to-noise ratio, and model misidentification is presented. Results from the experimental heat exchange process show that this design method can be used to obtain controllers which reduce control signal saturation with only a small reduction in effectiveness from that of the "ideal" feedforward and feedback. This optimal controller design was shown to be superior to the previously used frequency domain methods.

## ACKNOWLEDGEMENT

I wish to express my gratitude to my advisor, Dr. M. L. McGuire for his constant availability and assistance throughout my years of association with him.

I can not overstate my appreciation for my colleague Dr. R. A. Sims, who was an enormous help in the experimental phase of this work.

The assistance of other personnel of the Process Dynamics Laboratory, J. L. Goldsberry, K. Sanders, and W. Woodard was also appreciated.

The financial support of The National Aeronautics and Space Administration and the Dow Chemical Company is gratefully acknowledged.

Finally, I must thank my wife, Betty, for her patience and encouragement which made this work possible.

## TABLE OF CONTENTS

	Page
LIST OF TABLES . . . . .	vii
LIST OF ILLUSTRATIONS. . . . .	viii
 Chapter	
I. INTRODUCTION. . . . .	1
Statement of the Problem. . . . .	3
Literature Review . . . . .	5
II. MATHEMATICAL BACKGROUND . . . . .	9
Review of Statistical Design Concepts . . . . .	9
Mean Square Evaluation. . . . .	13
Solution of Matrix Differential Equations . . . . .	14
Dynamic Programming . . . . .	16
III. OPTIMAL CONTROLLER DESIGN EQUATIONS . . . . .	20
Problem Formation . . . . .	21
Parametric Expansion Solution . . . . .	26
Separable Load Disturbance. . . . .	30
Time Invariant Systems. . . . .	32
Constraints . . . . .	36
Controller Specifications . . . . .	37
Summary of Optimal Controller Equations . . . . .	39
IV. FIRST ORDER SYSTEM ANALYSIS . . . . .	41
The First Order Model . . . . .	43
A Particular System . . . . .	52

Chapter	Page
Constraints on the Integral of the State Variable. . . . .	60
Effect of Feedback Noise. . . . .	68
Effect of Model Error . . . . .	75
Process Time Delay. . . . .	80
Effect of Control Delay . . . . .	89
V. EXPERIMENTAL STUDIES. . . . .	98
Experimental Description. . . . .	99
Dynamic Mathematical Model. . . . .	106
Controller Results. . . . .	110
VI. ANALOG COMPUTER SIMULATIONS . . . . .	126
Third Order Models. . . . .	128
Controller Results. . . . .	132
VII. RECOMMENDATIONS AND CONCLUSIONS . . . . .	138
BIBLIOGRAPHY . . . . .	141
APPENDICES . . . . .	146
A. VECTOR EQUATIONS FROM TRANSFER FUNCTIONS. . . . .	146
B. DERIVATION OF CONTROLLER PARAMETER EQUATIONS. . . . .	152
C. SOLVING THE MATRIX RICCATI EQUATION . . . . .	156
D. SOLUTION OF THE OPTIMAL FEEDFORWARD EQUATION. . . . .	160
E. MATRIX EXPONENTIAL EVALUATION . . . . .	165
F. MEAN SQUARE CALCULATION . . . . .	168
G. THEORETICAL MODEL OF THE EXPERIMENTAL PROCESS . . . . .	171
H. NOMENCLATURE. . . . .	176
I. DIGITAL COMPUTER PROGRAMS . . . . .	179

## LIST OF TABLES

Table	Page
5.1 Optimal Controller Equations Corresponding to Markings on the Performance Diagram for Oil Disturbed System. . . . .	113
5.2 Controller Efficiency for Oil Disturbed System. .	119
5.3 Optimal Controller Equations Corresponding to Markings on the Performance Diagram for Coolant Disturbed System. . . . .	121
6.1 Optimal Controller Equations for the Third Order Model and the First Order Approximate Model . .	131
G.1 List of Experimental System Constants . . . . .	175



## LIST OF ILLUSTRATIONS

Figure	Page
1-1. Block Diagram of the Controlled System . . . . .	4
3-1. Response Trajectory of the Feedback Parameter, $K(\mu)$ . . . . .	34
4-1. Perfectly Stirred Heating Tank . . . . .	42
4-2. Response Characteristics of Optimally Controlled System for Various Disturbance Frequency . . .	54
4-3. Performance Diagram with Various Portions of the Optimal Controller Deleted . . . . .	55
4-4. Output Efficiency in Relation to the Amount of Control Effort Expended. . . . .	56
4-5. Contribution of Each Portion of the Optimal Con- troller to Overall System Attenuation. . . . .	59
4-6. Contribution of Each Portion of the Optimal Con- troller to Overall Control Effort. . . . .	61
4-7. Performance Diagram for Both the Output and the Integral Output. . . . .	63
4-8. Effect of Integral Constraints on the Mean Square Output . . . . .	64
4-9. Unit Step Response of a First Order System with Proportional-Integral Controllers. . . . .	67
4-10. A Typical Control Signal Trajectory for a System Containing a Dead Band . . . . .	70
4-11. Block Diagram of a Controlled System with Measurement Noise in Feedback. . . . .	72
4-12. The Performance Diagram of a First Order System with Various Levels of Feedback Noise Present.	73

Figure	Page
4-13. The Effect of Model Error on the Mean Square Output of an Optimally Controlled First Order System . . . . .	79
4-14. Block Diagram of a First Order Time Delay System	84
4-15. The Performance Diagram of a First Order System Showing the Points of Instability. . . . .	86
4-16. The Effect of Time Delay on the Mean Square Output of a First Order System Using the Same Integral Weighting Factor . . . . .	88
4-17. Sensitivity of a First Order Time Delay System to Errors in the Value of the Model Time Lag .	90
4-18. The Influence of Time Delay on the Point of Instability which Occurs when the Minor Feedback is Deleted. . . . .	91
4-19. The Effect of Control Time Delay on the Performance Diagram of a First Order System . . . . .	95
5-1. Schematic Flow Sheet of Experimental System. . .	100
5-2. Detail of Reactor. . . . .	101
5-3. Oil Flow Control System. . . . .	104
5-4. Coolant Flow Control System. . . . .	105
5-5. Wall Temperature Measuring System. . . . .	107
5-6. Response of the Wall Temperature of the Experimental System and the Model to a Step Change in Coolant Flow Rate . . . . .	109
5-7. Response of the Wall Temperature of the Experimental System and the Model to a Step Change in Oil Flow Rate . . . . .	111
5-8. Performance Diagram of the Experimental System Model with Coolant Flow Rate as Manipulative Variable . . . . .	112
5-9. Response of Experimental System to Disturbances in Oil Flow Rate . . . . .	115
5-10. Response of Optimally Controlled Experimental System to Disturbances in Oil Flow Rate. . . .	116

Figure	Page
5-11. Performance Diagram of the Experimental System Model with Oil Flow Rate as Manipulative Variable . . . . .	120
5-12. Response of Experimental System to Disturbances in Coolant Flow Rate . . . . .	123
6-1. A Comparison of the Unit Step Response Trajectories of 1st and 3rd Order Systems. . . . .	127
6-2. Analog Computer Circuit for Simulation of the Experimental Transfer Function . . . . .	129
6-3. Performance Diagram for Third Order Model. . . . .	130
6-4. Response of the Third Order Analog Model to Disturbances . . . . .	133
6-5. Response of the Third Order Analog Model to Disturbances . . . . .	134
6-6. Unit Step Response of the Transport Delay Generator. . . . .	135

# OPTIMAL FEEDFORWARD-FEEDBACK CONTROL

## CHAPTER I

### INTRODUCTION

Optimal control theory has advanced at an unbelievable rate since the pioneering work of Wiener in the 1940's. It is one of the unique scientific fields in which the theory has preceded application and has generally maintained this gap through the years. The electronic industry has always been the leader in applying the newly developed control techniques. The ability to obtain accurate mathematical models and make precise measurements has provided the impetus for the electrical engineering involvement in optimal control theory. The chemical process industry has not followed this field closely and is rather slow to try new developments in control theory. The reason for this tardiness can be traced to the nature of chemical processes. Dynamic elements of chemical systems, such as heat transfer and fluid flow are relatively slow. These slow, unpredictable disturbances can introduce enough uncertainty so that the advantage gained by using a sophisticated controller is considerably reduced. The present work describes an application of an existing control technique which has been

modified to fit the requirements of chemical processes.

There are two different types of problems that are frequently encountered by control engineers. The servomechanism control problem is associated with a change in operating conditions. The objective is to control the chemical process as it moves from one steady-state to another. The start-up and shut-down of systems fall in this category. In an optimal servomechanism controller design, the engineer is faced with several choices. The major optimization variable can be time or energy, i.e., start-up a process in the least amount of time or with the least amount of energy expended over a given length of time.

The regulator problem is concerned with controlling a system at a steady-state level in the presence of load disturbances. The optimal regulator problem is concerned with maintaining control subject to constraints on the allowable operating range of some of the parameters. An infinite time interval is used in the optimization procedure.

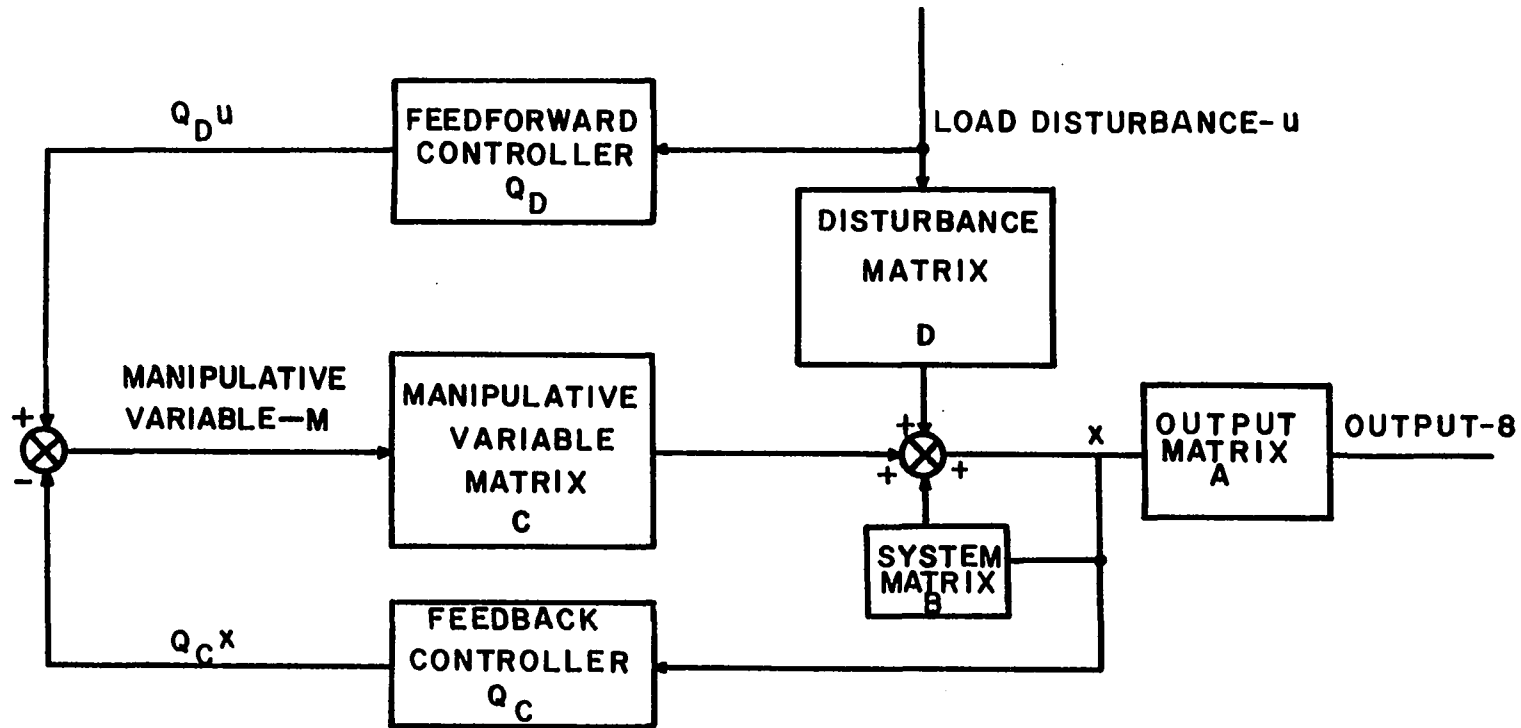
It is this latter category - the regulator problem - which is of interest in this work. There are two different variables with which to implement a controller. A feedback controller monitors the system output and corrects for any deviation. The feedforward controller monitors the disturbance and corrects for any change in this variable. Both types of controllers are used in the chemical process today.

The advantage in using a composite feedforward-feedback controller is that the undesirable characteristics of each individual controller is de-emphasized. The big limitations to obtaining good control with feedback alone are process time delays and noisy output measurements while feedforward controllers are sensitive to errors in the dynamic mathematical model. Since chemical processes usually contain all these limiting factors, the composite controller seems to be the best way to regulate the process.

#### Statement of the Problem

The mathematical model of the systems under consideration must be linear. There are no adequate methods for treating large classes of non-linear control problems. When a regulator problem is under consideration, the usual linearization procedure used to modify non-linear system dynamics is not unreasonable. The reason for this successful linearization is inherent in the regulatory problems because the objective is to control a variable at a particular steady state condition. If the system moves too far from this steady-state, the controller isn't doing a good job and the linear approximation errors would not be significant in the overall controller design.

Figure (1-1) shows a block diagram of the overall controlled system. The vector-matrix notation is used for the system dynamics.



**BLOCK DIAGRAM OF PLANTS AND CONTROLLERS  
UNDER CONSIDERATION**

Figure 1-1. Block diagram of the controlled system.

$$\dot{x}(t) = Bx(t) + Cm(t) + Du(t) \quad (1.1)$$

$$q(t) = Ax(t) \quad (1.2)$$

where  $x, m, u$ , and  $q$  are vectors and  $A, B, C$ , and  $D$  are continuous, time varying matrices. This representation allows multi-variable systems as well as single-input, single-output systems.

The manipulative signal is represented by

$$m(t) = Q_D u(t) - Q_C x(t) \quad (1.3)$$

where  $Q_D$  is the matrix of feedforward gains and  $Q_C$  is the matrix of feedback gains.

The load disturbance,  $u(t)$ , is a random variable. Laning and Battin (11) have presented a discussion on various statistical characterizations of physically observed systems. The great majority of load disturbances were found to be approximately gaussian. Therefore the later portion of the optimal controller design will be limited to gaussian load noise.

### Literature Review

Feedback control has been used in industrial processes for many years, while feedforward control is a relative newcomer to the control scene. Articles concerning the use of feedforward control started to appear only within the last twenty years. The early pioneers of control theory were electrical engineers. However, because of the nature of their electrical devices, feedforward control did not



hold their interest.

Bollinger and Lamb (B9) used the ideal feedforward or mirror image control and then added a small feedback to correct for drifts and small errors. Harris and Schecter (H1) presented a similar application of feedforward control to the linearized dynamics of a chemical reactor. In either case, no optimum feedback control was attempted. Haskins and Sliepcevich (H2) showed how certain classes of system non-linearities can be accounted for in the feedforward controller. Luyben and Gerster (L8) examined the application of feedforward control to distillation columns. Distillation is a process which would be a prime target for the use of feedforward control because the outlet variables are concentrations which usually can not be continuously monitored. Shinskey and MacMullen (M2) reported some experiments with feedforward control of distillation columns. Cadman, Rothfus, and Kermode (C1) examined the effect of linearization of the dynamic distillation column model on the feedforward controller. Recently, Luyben (L9) presented a method for calculating non-linear feedforward controllers for the non-linear continuous stirred tank chemical reactor.

While none of these investigators tried to use any optimization techniques, Rozonoer (R2) has shown that the ideal feedforward controller is indeed an optimal one when no constraints are placed upon the system. So in the study of feedforward controllers, one is dealing with a type of

optimal control.

Optimization techniques applied to feedback control systems dominate the literature. The great majority of reported work is concerned with various methods to obtain optimum feedback control for a servomechanism problem. This work is usually carried out by aeronautical and electrical engineers who are working in the aerospace industry. Most of their problems fall within the servomechanism category.

Most of the work on optimal feedback control utilizes one of the four prevailing optimization techniques.

1. Variational Calculus (N1)
2. Optimal Search (B1)
3. Mathematical Programming (B2)
4. Maximum Principle (K1)

One reference is provided for each of these techniques. The vast amount of literature on the many facets of these concepts precludes an exhaustive review.

There have been two studies which have looked at some type of optimal composite feedforward-feedback control. Johansen (L3) used the results of Kalman (K1) to define an optimal feedback control system in the presence of measurement and load noise. Although his interests lay more with filtering the noise in a model-following controller than with providing a feedforward controller, the method of attack of both problems is very similar. As usual Johansen's work was

directed toward a servomechanism problem, i.e., airplane navigation. One disadvantage of Kalman's method is that the problem formulation requires matrix partitioning which doubles the dimensionality of the problem and always causes computer difficulties for even low dimensional problems.

Heidemann (H4) was interested in composite control of a distillation column. He used the discrete form of the maximum principle as presented by Kalman (K1). However, Heidemann only calculated an optimal feedback controller and then added the ideal feedforward controller. In any case, the result was excellent control of an experimental distillation column.

Luecke (L4) used the frequency domain methods of Newton Gould, and Kaiser (N1) to obtain an optimal composite controller. The resulting form of the optimal composite controller is a ratio of polynomials. Even with low order transfer functions, the controllers contained rather high order polynomials (in the frequency domain) in the numerator and denominator of the signal transfer function. A disadvantage of the Newton method is its limitation, at least for reasonable computational effort, to single-input, single output systems. The advantageous feature of the frequency domain control design is that the optimization is done completely in the frequency domain, making it more familiar to control engineers. Time domain formulations are a very recent phenomena.

## CHAPTER II

### MATHEMATICAL BACKGROUND

The optimal controller design equations developed in the upcoming chapters require the use of some mathematical ideas which are not yet a part of the general chemical engineering background. For this reason a brief discussion of some of these ideas are included here.

#### Review of Statistical Design Concepts

The system under consideration is assumed to be subject to random load disturbances. In order to use the statistical characterization of this disturbance signal in conjunction with the design procedure, several well-known concepts from the theory of random variables are presented.

The mean value of a random signal,  $x(t)$ , is its expected value which is defined by the following equation.

$$E\{x(t)\} = \int_{-\infty}^{+\infty} f(x,t) dx \quad (2.1)$$

where  $f(x,t)$  = the probability density

The mean value is, in general, a function of time.

The conditional mean value of a signal is a convenient function for the use in many physical situations. When a random signal is dependent on a deterministic signal, such as when the output of a plant is related to the input, more accurate estimates of the most probable future values of the random signal can be made if the deterministic signal is known at a particular instant. For example the output of a plant can be calculated at a particular moment if the transfer function and the value of the input signal are known. Then a more accurate estimate of the future values of the output can be made simply because its value at that one particular moment is known. In these situations a conditional probability is used because it is defined as the probability function of a random signal subject to a particular fixed value of some dependent parameter. Therefore the conditional mean of a random signal  $y$  subject to the fixed value  $x$  can be written as

$$E\{y|x\} = \int_{-\infty}^{+\infty} yf(y|x)dy \quad (2.2)$$

where  $f(y|x)$  is the conditional probability density.

The autocorrelation  $\theta_x(t_1, t_2)$  of a given signal,  $x(t)$  is defined as

$$\theta_x(t_1, t_2) = \int_{-\infty}^{+\infty} \int_{-\infty}^{+\infty} x_1(t_1)x_2(t_2)f(x_1, x_2; t_1, t_2)dx_1dx_2 \quad (2.3)$$

Another statistical function prevalent in the automatic control literature is the spectral density or power spectra of a signal which is the Fourier transform of its autocorrelation.

$$\Phi_{xx}(s) = \frac{1}{2\pi} \int_{-j\infty}^{+j\infty} e^{-sT}\theta_x(T)dT \quad (2.4)$$

We shall restrict the discussion of system disturbances to include only those signals which are stationary. Intuitively, a stationary signal has the property that its statistical characterization is not a function of time. Most disturbances of interest to the chemical engineer are stationary or can be approximated as stationary over the range of interest. For this limited class of signals, the autocorrelation is a function only of the time increment,  $t_1-t_2$ , i.e.

$$\theta(t_1-t_2) = \int_{-\infty}^{+\infty} \int_{-\infty}^{+\infty} x_1x_2f(x_1, x_2; t_1-t_2)dx_1dx_2 \quad (2.5)$$

The autocorrelation of a stationary signal can be written in a form similar to the mean.

$$\theta_x(T) = E\{x(t+T)x(t)\} \quad (2.6)$$

As will be shown later, an estimation problem is encountered in the feedforward portion of the controller design procedure. We are interested in predicting the signal at time  $t + T$  solely from its past history up to time  $t$ . By standard techniques (P3) the linear mean square estimate can be expressed as

$$x(t+\lambda) = \int_0^{\infty} x(\alpha)W(t-\alpha)d\alpha \quad t > 0 \quad (2.7)$$

The function,  $W(t-\alpha)$ , is the impulse response which is subject to the following condition.

$$W(t) = 0 \quad \text{for } t < 0 \quad (2.8)$$

Equation (2.7) is the famous Wiener-Hopf integral equation. The solution of this equation is not trivial but several methods (N1) of solution are available.

If we consider a system load disturbance signal which is corrupted by measurement noise, then we have a combined filter-prediction problem. However this again results in a Wiener-Hopf integral equation (N1).

If we consider normal or gaussian signals, our task is simplified considerably. It has been shown (P3) that the conditional mean can be used for mean square estimation. To facilitate discussion, the following notation for the conditional mean is introduced,

$$E\{x(u) | x(t), u > t\} = \overline{x(u)}^t \quad (2.9)$$

The conditional mean of a normal signal is easily calculated from the autocorrelation function and the mean.

$$\overline{x(u)}^t = E\{x\} + \frac{\theta(u-t)}{\theta(0)} x(t) \quad \text{for } u > t \quad (2.10)$$

In order to use this convenient equation, we have restricted ourselves to stationary, gaussian signals. This restriction is not devastating because most of the load disturbances of interest to chemical engineers can be included in this class. The Wiener-Hopf equation was presented to show how non-Gaussian signals can be handled. Since solving the Wiener-Hopf equation is a task in itself, it is not included in further discussions of the controller design method.

#### Mean Square Evaluation

As stated previously, we are interested in obtaining the mean square value of a signal in order to make a comparison of controller effectiveness. The mean square is a good indication of effective control when random disturbances are allowed (L1).

Consider the process (in the frequency domain)

$$X(s) = P(s)D(s) \quad (2.11)$$

A spectral density relationship for this process can be written.

$$\Phi_{xx}(s) = P(s)P(-s)\Phi_{DD}(s) \quad (2.12)$$



The above equation is a well known property of the spectral densities, so no attempt to derive it will be made. Many texts, including Laning and Battin (L1), provide detailed explanations.

The autocorrelation function is obtained from the spectral density by taking the inverse transform and multiplying by  $2\pi$ . Thus

$$\theta_x(T) = \frac{1}{j} \int_{-j\infty}^{j\infty} \Phi_{xx}(s) e^{sT} ds \quad (2.13)$$

Since integration is along the imaginary axis, we may write the inverse transform in terms of the real frequency,  $w$ .

$$\theta_x(T) = \int_{-\infty}^{+\infty} \theta_{xx}(jw) e^{wT} dw \quad (2.14)$$

The above equation leads to an easy way of evaluating the mean square value of a signal. The mean square, as can be seen by the definition in equation (2.14), is the value of the autocorrelation function at  $T = 0$ . Therefore

$$\text{mean square value} = \theta_x(0) = \int_{-\infty}^{+\infty} \Phi_{xx}(jw) dw \quad (2.15)$$

Appendix F shows how this equation can be computationally used to calculate the mean square value of a signal from the spectral density function.

Solution of Matrix Differential Equations

In the formulation and solution of multivariable control problems, linear matrix differential equations result. The method of solving such equations is well known and is given here only for reference. A text such as Coddington and Levinson (C4) should be consulted for rigorous discussion of this topic.

The differential equation of interest is

$$\frac{dx(t)}{dt} = Ax(t) + Bu(t) \quad 0 \leq t \leq T \quad (2.16)$$

$$x(0) = x_0$$

where A and B are constant matrices and x(t) and u(t) are vectors. Using the matrix exponential

$$\frac{d}{dt} \left[ e^{-At} x(t) \right] = e^{-At} Bu(t) \quad (2.17)$$

Integrating both sides of this equation from 0 to T

$$e^{-AT} x(T) = x_0 + \int_0^T e^{-At} Bu(t) dt \quad (2.18)$$

Rearranging this result gives the equation which is commonly called the impulse response solution.

$$x(T) = e^{AT}x_0 + \int_0^T e^{A(T-t)}Bu(t)dt \quad (2.19)$$

The matrix exponential used in the above derivation is also referred to as the matrizant, the fundamental matrix, and the transition matrix.

The above derivation holds only for time-invariant system dynamics, i.e., the matrices A and B are constant. For time-varying systems the matrix exponential is rather difficult to evaluate.

### Dynamic Programming

The technique used to optimize the control signal is called Dynamic Programming (B2). A brief discussion of this method is presented here for later reference.

The basic function to be minimized considered in this work can be written as

$$e(t) = \int_t^T h(x,m,t)dt \quad (2.20)$$

subject to the constraints

$$\dot{x} = f(x,m,t) ; m \in M \quad (2.21)$$

where M is a closed set.

The first step in applying the concept of dynamic programming is to imbed the minimization problem into a larger class

of problems. A dummy variable is introduced so that the present time can be treated as a constant during the minimization procedure.

$$e(\mu) = \int_{\mu}^T h(x, m, \mu) d\mu \quad (2.22)$$

where  $\mu \in [t, T]$

The state variable at time  $t$ ,  $x(t)$ , is treated as a constant or measured value.

Define the minimum cost function

$$E[x(\mu), \mu] = \min_m e(\mu) \quad (2.23)$$

Now the Principle of Optimality is used to obtain an equation for this minimum cost function. The Principle of Optimality (B2) can be stated as:

An Optimal policy has the property that whatever choice of initial state and control vector is made, the remaining choice of control vectors must constitute an optimal policy with respect to the state resulting from the initial choice of control vector.

Breaking the interval of integration into two parts and then using the above principle allows us to write the following equation.

$$E[x(\mu), \mu] = \min_m \min_{(\mu, \mu+\delta) \quad (\mu+\delta, T)} \left[ \int_{\mu}^{\mu+\delta} h(x, m, \sigma) d\sigma + \int_{\mu+\delta}^T h(x, m, \sigma) d\sigma \right] \quad (2.24)$$

or

$$E[x(\mu), \mu] = \min_m \left[ \int_{\mu}^{\mu+\delta} h(x, m, \sigma) d\sigma + \min_m \int_{\mu+\delta}^T h(x, m, \sigma) d\sigma \right] \quad (2.25)$$

From the definition of the minimum cost function

$$E[x(\mu+\delta), \mu+\delta] = \min_m \int_{\mu+\delta}^T h(x, m, \sigma) d\sigma \quad (2.26)$$

Using this result in the rearrangement of equation (2.25) gives

$$E[x(\mu), \mu] = \min_m \left\{ \int_{\mu}^{\mu+\delta} h(x, m, \sigma) d\sigma + E[x(\mu+\delta), \mu+\delta] \right\} \quad (2.27)$$

This solution is the familiar discrete recursive expression which is used in many digital computer solutions. The usual method of attack is to start at the terminal boundary condition and then calculate the optimal path using finite increments in the negative time direction (L2).

A continuous form of the dynamic programming algorithm can be found. Expand the minimum cost function in a Taylor series for a small increment,  $\delta$ .

$$\begin{aligned}
E[x(\mu+\delta), \mu+\delta] &= E[x(\mu), \mu] + \left( \frac{\partial E[x(\mu), \mu]}{\partial x(\mu)} \right)^T \dot{x}(\mu) \delta \\
&+ \frac{\partial E[x(\mu), \mu]}{\partial \mu} \delta + \dots
\end{aligned} \tag{2.28}$$

Substituting equation (2.28) into equation (2.27) results in

$$\begin{aligned}
E[x(\mu), \mu] &= \min_m \left\{ h(x(\mu), m(\mu), \mu) + E[x(\mu), \mu] \right. \\
&\quad \left. (\mu, \mu+\delta) \right\} \\
&+ \left( \frac{\partial E[x(\mu), \mu]}{\partial x(\mu)} \right)^T \dot{x}(\mu) \delta + \frac{\partial E[x(\mu), \mu]}{\partial \mu} \delta + \dots \tag{2.29}
\end{aligned}$$

Subtract the minimum error function from both sides of equation (2.29) and then divide the equation by  $\delta$ . In the limit as  $\delta$  approaches zero, the equation becomes

$$\min_{m(\mu)} \left[ h(x(\mu), m(\mu), \mu) + \left( \frac{\partial E[x(\mu), \mu]}{\partial x(\mu)} \right)^T \dot{x} + \frac{\partial E[x(\mu), \mu]}{\partial \mu} \right] = 0 \tag{2.30}$$

This partial differential equation is the continuous form of the dynamic programming algorithm which is used as the starting point in the optimal controller equation development.

For more rigorous discussions and various applications several basic texts which are listed in the bibliography should be consulted (B3, L2, B11).

## CHAPTER III

### OPTIMAL CONTROLLER DESIGN EQUATIONS

The object of this chapter is to present a method of calculating optimum controller designs for chemical processes. The method is limited to linear, time-varying systems. This restriction is not serious because a large number of control problems can be resolved with a linear approximation to the actual process dynamics. When deviations from steady-state operating conditions are not large, then the linear approximation is usually sufficient. With this restriction to linear models it is apparent that the controllers themselves will be linear functions. Using a linear approximation to a non-linear process in the optimal controller equation results in a linear-optimum controller. This name is usually given to the above mentioned optimal controllers to distinguish them from the optimal controllers calculated from the non-linear dynamic model. Since these latter controllers are not easily calculated, the linear-optimum controllers can be used as long as the assumptions involved in the model approximation are valid. The calculation of the linear-optimum controllers is the task of this work.

Another limitation of this method of finding optimum controllers is the mathematical formulation of the constraints. The constraints on the system must be expressed in terms of quadratic functions. This again is not a serious limitation because the chemical engineer frequently deals with variances so quadratic constraints can be formulated easily. System limitations resulting in variable "saturation" can not be directly included in the class of quadratic constraints. However, by putting a constraint on the square of the saturating variable, the fraction of time that the system violates the hard saturation barrier can be limited.

The matrix, time-domain representation of the process dynamics is used in this method. The more familiar transfer function representation can easily be changed into this form. Appendix A includes a discussion of the various ways to make this transformation.

#### Problem Formation

Consider the general matrix formulation of process dynamics.

$$\dot{\bar{x}}(t) = B\bar{x}(t) + C\bar{m}(t) + D\bar{u}(t) \quad (3.1)$$

$$\bar{q}(t) = A\bar{x}(t) \quad (3.2)$$

where

$\bar{x}(t)$  = state variable vector

$\bar{m}(t)$  = control variable vector



$\bar{u}(t)$  = load disturbance

$\bar{q}(t)$  = output vector

A,B,C,D = continuous time-varying matrices

The superbar is used to emphasize that the variables are vector quantities. In order to simplify notation, the super-script is not used in later discussions. A particular element of the vector,  $x_i$ , is recognized by subscript indices.

Since the system is linear, the perturbation form of the system dynamics can be used. The variables in the above equation are the deviations from steady state operating conditions. This technique of presentation is common in the control literature. It relieves the mathematics of unnecessary complications because the steady-state value of the perturbation variables is always zero.

The scalar performance index upon which the optimization is based is quadratic. A scalar function is used so that a multi-variable search, which would be extremely difficult, is not required. As in all variational mathematics, the scalar performance index function is formulated as an integral. Since random variables are included in this procedure the functions in the scalar performance index are conditional means which emphasizes the dependence of the procedure on the present time,  $t$ .

$$\frac{e(t)}{t} = \int_t^T \frac{\langle q(\sigma), \Phi q(\sigma) \rangle}{t} + \frac{\langle m(\sigma), \Psi m(\sigma) \rangle}{t} d\sigma \quad (3.3)$$

where

$T$  = terminal time boundary

$\Phi$  = diagonal non-negative definite weighting factor matrix

$\Psi$  = diagonal positive definite weighting factor matrix.

The weighting matrices can also be time-varying functions. However, as a result of the inability to formulate desirable time-varying functions, constant weighting factors are used. The limitation of only diagonal elements in these matrices is not necessary but practical. A cross product constraint is difficult to formulate and does not seem to have any particular advantage in the results which are obtained.

Positive definite weighting matrices are used in equation (3.3). The integrand of the scalar performance index is positive and strictly convex. The more restrictive condition on the control signal weighting factor is used so that an unrealistic unbounded optimum control signal will not be specified. Therefore the control signal is restricted to a closed set and the allowable control signal region is designated  $M$ . The minimization of the performance index with respect to the control signal is restricted to this allowable set  $M$ . This restriction is not explicitly noted in the minimization equation because of the complex notation, but

is inherent in the procedure.

The superbars in the preceding equation (3.3) indicate the conditional mean as introduced in equation (2.9). The notation is a reminder that the integrand is a function of real time  $t$ .

Following the same procedure developed in the dynamic programming section of Chapter II, an instantaneous minimum performance index is defined by

$$E[\overline{x(\mu)}, \mu] = \min_{m(\mu)} \overline{e(\mu)}^t \quad (3.4)$$

The index is defined in this manner because the real time  $t$  is treated as a fixed value in the minimization procedure. The fact that the minimum performance index has only the state variable and the time variable in its argument is a well known result (B2). Note that for each instant the minimization treats the real time  $t$  as the initial condition and it becomes very important in servomechanism problems to monitor the real time  $t$ . However, in regulator problems the interval of interest is the whole real time axis, making the particular fixed value of  $t$  arbitrary.

From the definition of the minimum performance index, it is apparent that the following boundary condition must hold.

$$E[\overline{x(T)}^t, T] = \min_{m(T)} \int_T^T \langle \overline{q(\sigma)}^t, \overline{\Phi q(\sigma)}^t \rangle + \langle \overline{m(\sigma)}^t, \overline{\Psi m(\sigma)}^t \rangle d\sigma \quad (3.5)$$

Since the integrand is bounded on the allowable region,  $M$ , the integral must be zero.

$$E[\overline{x(T)}^t, T] = 0 \quad (3.6)$$

The dynamic programming algorithm in the continuous form can be applied at this point. The dynamic programming algorithm was discussed in Chapter II.

$$\begin{aligned} \min_{m(\mu)} \left\{ \langle \overline{q(\mu)}^t, \overline{\Phi q(\mu)}^t \rangle + \langle \overline{m(\mu)}^t, \overline{\Psi m(\mu)}^t \rangle + \left( \frac{\partial E[\overline{x(\mu)}^t, \mu]}{\partial \overline{x(\mu)}^t} \right)^T \overline{x(\mu)}^t \right\} \\ = + \frac{\partial E[\overline{x(\mu)}^t, \mu]}{\partial \mu} \quad (3.7) \end{aligned}$$

The superscript  $T$  on the partial derivative of the minimum performance index with respect to the state variable denotes the transpose of that vector.

The above partial differential equation could be integrated by numerical techniques if the system order is limited to two or three dimensions. Larger dimensional problems can not be handled without a great deal of difficulty by present computer technology. The computer memory storage is not large enough. Computer storage limitation is a result of the famous "curse of dimensionality" (B2).

The Parametric Expansion Solution

One possible way of side-stepping this computational difficulty is to propose a mathematical form for the minimum performance index. Merriam (M3) suggested a Taylor series expansion with respect to the state variable which is truncated after the quadratic term. The coefficients in the expansion are then treated as unknown parameters.

$$E[\overline{x(\mu)}, \mu] = I(\mu) - 2 \left( \overline{x(\mu)}^t \right)^T J(\mu) + \left( \overline{x(\mu)}^t \right)^T K(\mu) \overline{x(\mu)}^t \quad (3.8)$$

where  $K(\mu)$  = symmetric  $n \times n$  matrix

$J(\mu)$  =  $n$ -element vector

$I(\mu)$  = scalar element

The partial derivatives needed in equation (3.7) are

$$\left( \frac{\partial E[\overline{x(\mu)}, \mu]}{\partial \overline{x(\mu)}^t} \right)^T = -2J(\mu)^T + 2 \left( \overline{x(\mu)}^t \right)^T K(\mu) \quad (3.9)$$

$$\frac{\partial E[\overline{x(\mu)}, \mu]}{\partial \mu} = \dot{I}(\mu) - 2 \left( \overline{x(\mu)}^t \right)^T \dot{J}(\mu) + \left( \overline{x(\mu)}^t \right)^T \dot{K}(\mu) \overline{x(\mu)}^t \quad (3.10)$$

Equation (3.9) is simply the gradient of the minimum performance index with respect to the components of the state variable vector. This derivative is in a tractable form because

of the symmetry of the matrix  $K(\mu)$  (B4).

In order to obtain the minimum of the right hand side of equation (3.7) the derivative of the terms within the braces are differentiated with respect to each element of the vector  $m(\mu)$  and then the result is set equal to zero. By rearranging this result the optimal control vector is obtained.

$$m^*(t) = \Psi^{-1} C^T J(t) - \Psi^{-1} C^T K(t) \overline{x(t)}^t \quad (3.11)$$

where  $m^* \in M$

Substituting this expression into equation (3.7) and performing some manipulations, the equations which allow for the evaluation of the parameters  $J(\mu)$  and  $K(\mu)$  can be found. These manipulations are tedious so they do not appear in this chapter. Appendix B contains the necessary algebraic detail.

The resulting matrix differential equations are

$$\dot{J}(\mu) = K(\mu) C \Psi^{-1} C^T J(\mu) - B^T J(\mu) + K D \overline{u(\mu)}^t \quad (3.12)$$

$$\dot{K}(\mu) = K(\mu) C \Psi^{-1} C^T K(\mu) - B^T K(\mu) - A^T \Phi A - K(\mu) B \quad (3.13)$$

The parameter,  $I(\mu)$  does not appear in the control equation and, therefore, does not add any information to the controller design, so it is not presented here. The boundary conditions for these equations follow directly from the boundary

condition of the minimum performance index which was stated in equation (3.6).

$$J(T) = 0; K(T) = 0 \quad (3.14)$$

The optimum control vector in the real time control system is found from equation (3.11) when the parameters are evaluated at  $\mu = t$  in conjunction with the solutions of equations (3.12) and (3.13).

These equations were first derived by Merriam (M3) but were made unduly complicated by his unfortunate use of summation notation. His general controller parameter equations, corresponding to equations (3.12) and (3.13), contained several typographical errors, thereby increasing the confusion. The development of the controller equations by matrix methods as presented in Appendix B is much simpler and far less confusing.

It can be seen that the parameter,  $J(\mu)$ , is a function of the load disturbance signal,  $u$ . This means that  $J$  is related to the feedforward portion of the controller. The other parameter,  $K(\mu)$  is the coefficient of the state variable in the optimal controller equation (3.11). Therefore,  $K(\mu)$  is related to the feedback gain of the controller.

The dynamic programming equation is a sufficiency condition because of the manner in which the minimum cost function,  $E$ , was defined. The important features are continuity and

convexity of this function. There are, of course, much weaker conditions under which this equation still remains sufficient to specify a unique optimum, but the above two properties are the most easily formulated.

Continuity is not restrictive because a discontinuous control implementation is not physically realizable in chemical processes. Convexity of the performance index is guaranteed by the quadratic forms in the integrand of equation (3.3).

In finding the equations for the optimal controllers, a solution was assumed. The question arises: Is this assumption valid? Peterson (P4) has shown that for linear systems, all terms of higher order than quadratic in the state variable are zero. Therefore, the parametric expansion is valid for linear systems. Since non-linear systems are not included in these conditions it seems better to search for other ways to solve non-linear problems. The familiar linearization about the steady-state is a popular one, especially in regulator control problems.

There are no worries concerning the stability of the controlled system. Merriam (M3) has shown that the minimum performance index is a Lyapunov function so the system is at least asymptotically stable in the large.



Separable Load Disturbance

If the load disturbance statistical characterization allows a separation of the conditional mean, equation (3.12) can be simplified. A separable signal can be represented as follows:

$$\overline{u(\mu)}^t = \overline{U(\mu)} + U(\mu, t) \overline{u(t)}^t \quad (3.15)$$

Since the conditional mean  $\overline{u(\mu)}^t$  is a linear factor in equation (3.12), it is immediately known that the solution  $J(\mu)$  can be written as the sum of the solutions for each additive component of the forcing term  $\overline{u(\mu)}^t$ . This linearity means that two parameters can be defined for  $J(t)$ .

$$J(t) = R(t) + \bar{S}(t) \quad (3.16)$$

Then the equations defining these two parameters are

$$\dot{R}(\mu) = [K(\mu)C\Psi^{-1}C^T - B^T] R(\mu) + K(\mu) D \overline{U(\mu)} \quad (3.17)$$

$$\dot{\bar{S}}(\mu) = [K(\mu)C\Psi^{-1}C^T - B^T] \bar{S}(\mu) + K(\mu) D U(\mu, t) \overline{u(t)}^t \quad (3.18)$$

$$\bar{S}(T) = 0; \quad R(T) = 0 \quad (3.19)$$

Since  $\overline{u(t)}^t$  is a non-zero constant with respect to this equation, equation (3.18) may be divided through by this factor. A new function is introduced which will prove to be more practical.

$$S(\mu) = \frac{\bar{S}(\mu)}{\overline{u(t)}^t} \quad (3.20)$$

With this new parameter, equation (3.16) is transformed into

$$J(t) = R(t) + S(t) \overline{u(t)}^t \quad (3.21)$$

where this redefined parameter is found by the following matrix differential equation:

$$\dot{S}(\mu) = [K(\mu) C \Psi^{-1} C^T - B^T] S(\mu) + K(\mu) DU(\mu, t) \quad (3.22)$$

An important point can be noted when equation (3.21) above is substituted into the optimal control signal equation (3.11).

$$m^*(t) = \Psi^{-1} C^T R(t) + \Psi^{-1} C^T S(t) \overline{u(t)}^t + \Psi^{-1} C^T K(t) \overline{x(t)}^t \quad (3.23)$$

$$m^* \in M$$

The three terms on the right hand side of this equation can be associated with physical controllers. The first term is the steady state correction, while the third term is the feedback controller. By the manipulation performed above, the second term has been shown to be a function multiplied by the input load disturbance signal and therefore is the feed-forward controller.

The requirement for this simplification is the separability of the conditional mean of the load disturbance signal.

It has been shown in equation (2.10) that stationary gaussian signals have this property. The terms involved in the separated signal are easily calculated from equation (2.10).

In the statement of the general problem in Chapter I, the restriction to stationary, gaussian signals with zero mean value was presented and discussed. It can be seen that these limitations are not inherent in the optimal controller equations, but their absence complicates the solution of the equations to the point that the only feasible control system would have to be connected to a digital computer for on-line controller calculations.

#### Time-Invariant Systems

To this point time-varying system matrices were included in the controller equations. The majority of chemical processes can be adequately represented by constant system matrices, i.e., time-invariant systems. Not only are the time-varying optimal controller equations more laborious to resolve but it is extremely difficult to even formulate the system dynamics. For this reason it is necessary to consider the previously derived equations from the standpoint of obtaining constant controller parameters.

For the time-invariant systems the terminal time boundary  $T$  in the performance index in equation (3.3) approaches infinity ( $T \rightarrow \infty$ ). Because of some mathematical difficulties

the standard method of treating this problem is by using some arbitrarily large (but still finite) terminal time boundary.

Consider the matrix Riccati equation (3.13) which defines the feedback controller.

$$\dot{K}(\mu) = K(\mu) C \Psi^{-1} C^T K(\mu) - B^T K(\mu) B - A^T \Phi A \quad (3.13)$$

$$K(T) = 0$$

The solution of interest is the "steady-state" value of  $K(\mu)$ .

$$\lim_{T \rightarrow \infty} K(\mu) = K \quad (3.24)$$

An illustration of the time behavior of the parameter  $K(\mu)$  is shown in Figure (3-11). The transient period of the variable  $K(\mu)$  is near the boundary condition ( $T \rightarrow \infty$ ). The usual explanation given in optimal control texts associates the terminal boundary condition with an initial time and then the response of  $K(\mu)$  would be in the negative time direction. This interpretation is intuitively acceptable to control engineers who are familiar with real time system response curves. One can see that as the terminal boundary  $T$  approaches infinity, the transient interval becomes less important in the description of the controller gain  $K$ . Therefore, it is this "steady-state" value which is desired in time-invariant controller design.

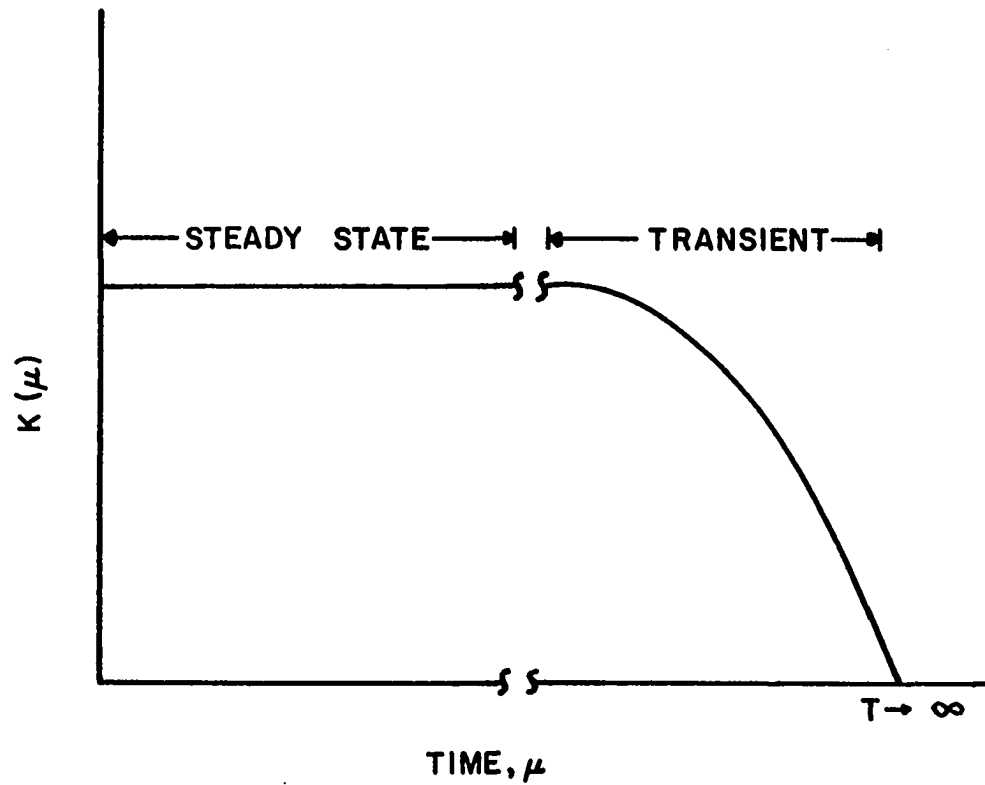


Figure 3-1. Response trajectory of the feedback parameter,  $K(\mu)$ .

The conditions on the system which guarantee that the parameter  $K(\mu)$  does have a unique finite value have been presented by Kalman (K1) in a concept known as controllability. A system is completely controllable if every allowable change of state can be made by an unconstrained control signal acting in a finite length of time. Kalman has shown that the cancellation of a system pole by a system zero (in the familiar transfer function nomenclature) is an example of a plant which is not completely controllable.

Some simplifications of the feedforward controller calculation can be made when time-invariant systems are the topic of interest. Consider the feedforward equation

$$\dot{S}(\mu) = [KC\Psi^{-1}C^T - B^T] S(\mu) + KD U(\mu, t) \quad (3.22)$$

$$S(T) = 0$$

The impulse response solution (equation 2.1) of equation (3.22) can be written as

$$S(t) = \varphi(t-T) S(T) + \int_T^t \varphi(t-\alpha) KD U(\alpha-t) d\alpha \quad (3.25)$$

where  $\varphi(t)$  = the fundamental matrix or matrizant of the homogeneous part of equation (3.22)

$$S(t) = - \int_0^{T-t} \varphi(-\epsilon) KD U(\epsilon) d\epsilon \quad (3.26)$$

Then with a similar argument as presented for the feedback parameter, the introduction of a very large terminal time boundary ( $T \rightarrow \infty$ ) results in the following expression:

$$S = - \int_0^{\infty} \phi(-\epsilon) KD U(\epsilon) d\epsilon \quad (3.27)$$

The above equation shows that a constant (not a function of time) feedforward controller can be evaluated.

The practical methods of calculating the feedforward and feedback controllers for time-invariant systems are discussed in Appendices D and C, respectively.

### Constraints

The constant weighting matrices in the performance index, equation (3.3), are energy constraints on the system. The weighting factors are actually Lagrange multipliers which imbed an integral energy constraint into the performance or cost function.

The saturation constraint is not in the proper mathematical form to be directly imbedded in the performance index. Newton, Gould, and Kaiser (N1) have presented a method by which quadratic energy constraints can be used to approximate saturation constraints. Given the statistical characterization of the saturating signal, the probability of finding the signal outside the linear range is plotted as a function of the ratio of the saturation signal value to the root

mean square response in the linear range. For example, if a saturation probability of 1% is acceptable, the above mentioned graph says that the root mean square response should be constrained to 40% of the saturation value. Fuller (F2) has also studied this problem. He states that the replacement of saturation constraints with energy constraints do not give the best possible results in simple analytic linear and non-linear systems, but the disadvantage is almost negligible when other limitations such as noise are incorporated in the actual physical systems.

#### Controller Specification

The optimal controller equation (3.11) is implicitly dependent on the values selected for the constant weighting matrices,  $\Phi$  and  $\Psi$ , which are used in the cost function (3.3). There is no general way of picking particular values to do a specific control job. The usual procedure in servomechanism work is to set up a systematic trial and error search until the desired trajectory is obtained. In the regulator problem, one could specify the desired response of the output variable to a unit step forcing and, in the same manner, search for a set of weighting values which specify a controlled output response trajectory corresponding to a desired one.

The disadvantage to this method of specifying a controller is that any change in the desired output forces a repeat



of all the calculations made previously. One of the major jobs of the design engineer is to calculate various alternatives for economic analysis. Therefore, it seems that a performance diagram of mean square control effort as a function of mean square controlled output would provide this versatility.

A set of weighting factors is used to calculate various optimal controller parameters and configurations. Then the performance diagram can be found with the aid of equation (2.15).

Consider the following frequency domain representation of system dynamics.

$$X(s) = P_M M(s) + P_D U(s) \quad (3.28)$$

The optimal controller equation can be written as

$$M(s) = Q_D U(s) - Q_C X(s) \quad (3.29)$$

Then substituting equation (3.29) into equation (3.28) and rearranging gives

$$X(s) = \frac{P_M Q_D + P_D}{1 + P_M Q_C} U(s) \quad (3.30)$$

The control effort can be found by substituting equation (3.30) into the optimal controller equation (3.29).

$$M(s) = \left[ Q_D - Q_C \frac{X(s)}{U(s)} \right] U(s) \quad (3.31)$$

Then from the spectral density of the input load disturbance, the mean square controlled output and mean square control effort can be calculated from equation (2.15), which was discussed in Chapter II. Appendix F explains the calculational procedure that can be used to evaluate this equation.

### Summary of Optimal Control Equations

The basic equations needed to obtain optimum feedforward and feedback controllers for linear time-invariant systems have been presented. It is convenient now to summarize these equations for easy reference.

(A) The system dynamics:

$$\dot{x}(t) = Bx(t) + Cm(t) + Du(t) \quad (3.1)$$

$$q(t) = Ax(t) \quad (3.2)$$

(B) The performance index:

$$\overline{e(t)}^t = \int_t^{T \rightarrow \infty} \langle q(\sigma), \Phi q(\sigma) \rangle + \langle m(\sigma), \Psi m(\sigma) \rangle d\sigma \quad (3.3)$$

(C) The optimal controller equation:

$$m^*(t) = \begin{cases} M^+ & ; \quad m^*(t) > M^+ & (3.23a) \\ \Psi^{-1} C^T [Su(t) - Kx(t)] & ; \quad m^*(t) \in M & (3.23b) \\ M^- & ; \quad m^*(t) < M^- & (3.23c) \end{cases}$$

(D) Control parameter equations:

$$S = - \int_0^{\infty} \varphi(-\epsilon) KD U(\epsilon) d\epsilon \quad (3.27)$$

$$K = \lim_{(T-\mu) \rightarrow \infty} K(\mu) \quad (3.24)$$

$$K(\mu) = KC \Psi^{-1} C^T K - B^T K - KB - A^T \Phi A \quad (3.13)$$

The above equations constitute the method by which the optimal controllers are calculated.

## CHAPTER IV

### FIRST ORDER SYSTEM ANALYSIS

It is worthwhile to examine the application of the optimal control design procedure to a first order system. The first order system was chosen because of its simplicity, since only in the single-pole first order system can the design equations be solved analytically. Higher order systems require digital computer solutions because of their complexity. With first order systems, the effects of various realistic factors such as time delays, measurement noise, and model misidentification are illustrated. The mean square control effort and mean square output are the indices upon which the effectiveness of the controllers are compared. Extensive digital computation was used to prepare the performance charts.

The system to be examined is a perfectly stirred tank which contains a heating coil. A diagram of the physical system is shown in Figure (4-1). The objective is to maintain the output temperature of the tank constant. The control variable is the temperature of the heating coils and the load disturbance is the input temperature. A process time delay occurs if the output is monitored at a point downstream from the tank outlet. A time delay in implementing a desired

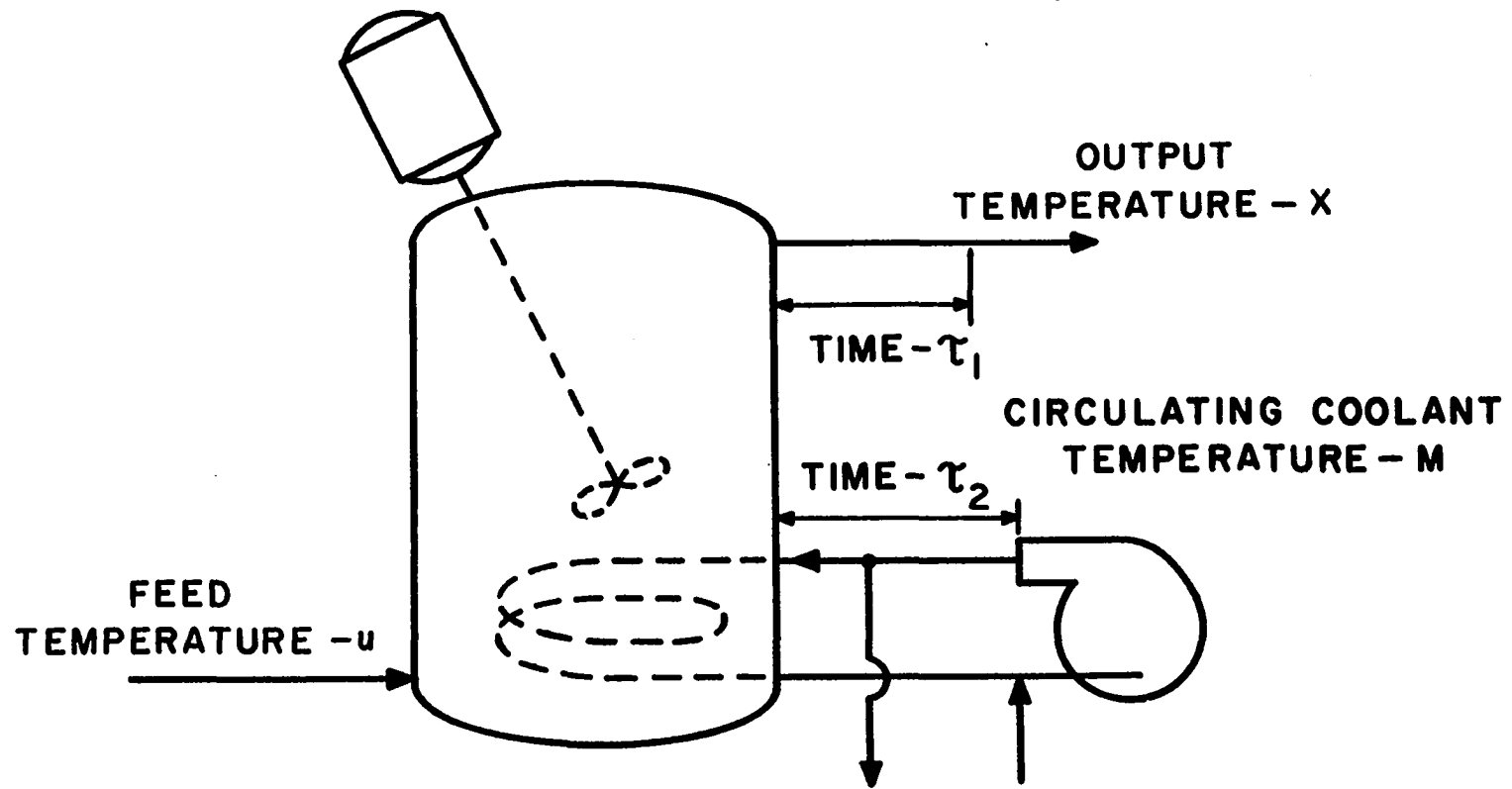


Figure 4-1. Perfectly stirred heating tank.

control action is conceivable in this system. The control variable, coil temperature, is changed by variation of the flow rate of the heating media. This system can be slowly responding if the heat transfer properties of the coil wall are not favorable. The slow response effect of heat transfer properties on the system dynamics is discussed later in the experimental description chapter. Noise is ever present in temperature measurements of flow systems. Physical properties such as heat transfer coefficients and heat capacities may change slowly over a period of time. For example, corrosion and scaling deposits change the heat transfer coefficient. We cannot monitor all the physical properties of the system continuously. Therefore these changes would cause an error in the process model. The effect of all these process problems on obtaining good control is examined.

#### The First Order Model

The process dynamics can be obtained by an energy balance around the unit. The resulting equations are

$$VC_p \frac{d\tilde{x}(t)}{dt} = FC_p \tilde{u}(t-\tau_1) - \tilde{x}(t) + U_H A_H \tilde{m}(t-\tau_2) - \tilde{x}(t) \quad (4.1)$$

where

$\tilde{x}(t)$  is the outlet temperature

$\tilde{u}(t-\tau_1)$  is the inlet temperature at a time  $\tau_1$  before its effect in the outlet is observed.

$\tilde{m}(t-\tau_2)$  is the coil temperature set by the controller at a time  $\tau_2$  before its effect in the outlet is observed.

$U_H$  is the overall heat transfer coefficient.

$A_H$  is the heat transfer area of the coil.

$F$  is the flow rate.

$\rho$  is the density of the fluid.

$C_P$  is the heat capacity of the fluid.

$V$  is the volume of the tank.

The above equation is a linear differential equation. The forcing terms,  $\tilde{m}(t-\tau_2)$  and  $\tilde{u}(t-\tau_1)$ , can have delayed arguments. This does not mean that we are dealing with the hard-to-solve delay differential equation. The latter type of differential equation occurs when the state variable  $x(t)$  appears in the equation with a delayed time argument.

Since the equation is linear, we can define a perturbation model. The perturbation form is very convenient because it translates all the initial conditions of the equation to zero.

$$\text{Define } x(t) = \tilde{x}(t) - x_{ss} \quad (4.2)$$

$$m(t) = \tilde{m}(t) - m_{ss} \quad (4.3)$$

$$u(t) = \tilde{u}(t) - u_{ss} \quad (4.4)$$

where

$x_{ss}$  = steady state outlet temperature

$m_{ss}$  = steady state coil temperature

$u_{ss}$  = steady state inlet temperature

By introducing the above definitions and then taking the Laplace Transform, equation (4.1) can be rewritten as:

$$x(s) = \frac{K_M e^{-\tau_2 s}}{s + \beta} m(s) + \frac{K_D e^{-\tau_1 s}}{s + \beta} u(s) \quad (4.5)$$

where

$$K_M = \frac{U_A}{H^2 H} ; K_D = \frac{F C_P}{V C_P} ; \beta = K_D + K_M$$

$m(s)$ ,  $x(s)$ , and  $u(s)$  are the Laplace transforms of  $m(t)$ ,  $x(t)$ , and  $u(t)$  respectively.

For ease in later manipulation, let us make the following definitions:

$$P_M = \frac{K_M}{s + \beta} e^{-\tau_2 s} \quad (4.6)$$

$$P_D = \frac{K_D}{s + \beta} e^{-\tau_2 s} \quad (4.7)$$

In order to make meaningful controller specifications, the statistical nature of the load disturbance is required. It is convenient to consider random disturbances with an auto-correlation function which can be represented as

$$\Theta_{\mu\mu}(T) = \mu^2 e^{-2\nu|T|} \quad (4.8)$$

where

$\mu^2$  = mean square amplitude

$\nu$  = frequency (radians per unit time)



This function is a good practical representation of physically observed random disturbances (L1,N1). The above autocorrelation functions limits the design procedure to stationary, gaussian load disturbances. Since equation (4.8) is an adequate description of many of the observed load disturbances, it does not seem worthwhile to cloud the analysis with the more complex nongaussian, nonstationary representations. The power spectral density of this function is more commonly used in the control literature.

$$\Phi_{\mu\mu}(s) = \frac{2\mu^2\nu}{4\nu^2 - s^2} \quad (4.9)$$

Another incentive for using this type of load disturbance is that it is readily generated by available equipment in the Process Control Laboratory. Analog simulation tests of the resulting controller designs are an important part of the total design effort.

The preceding transform domain representation of the system dynamics was made because of its familiarity to control engineers. However, the starting point for the design procedure requires the time-domain representation. For higher order systems, the time-domain equivalent of a given transfer function is not unique. There are several methods available to define the state (A1) variable. A discussion of the various methods is presented in Appendix A. The first order system

process equations are

$$\dot{x}(t) = -\beta x(t) + K_M m(t-\tau_2) + K_D u(t-\tau_1) \quad (4.10)$$

The scalar performance index chosen as the basis for the optimization is

$$e = \int_t^T \Phi x^2 + \Psi m^2 dt \quad (4.11)$$

where

$$\Phi \geq 0 ; \Psi > 0 ; T \rightarrow \infty$$

Let us now take the simple case of no time delays, i.e.  $\tau_1 = \tau_2 = 0$ . This is an unrealistic problem, but it will serve as a basis for comparison because of its position as the limiting case. Remember that negative values for  $\tau_1$  and  $\tau_2$  are physically unrealizable, so the case of zero time delay is a limiting one.

The optimal control law obtained in Chapter III has the following form for this example.

$$m^*(t) = \frac{K_M J(t)}{\Psi} - \frac{K_M K x(t)}{\Psi} \quad (4.12)$$

where  $K$ ,  $J$  are defined by the equations

$$\frac{K^2 K_M^2}{\Psi} + 2\beta K - \Phi = 0 \quad (4.13)$$

$$J(t) = S u(t) \quad (4.14)$$

The parameter,  $S$ , is the steady state value obtained from the following boundary-value ordinary differential equation. This simplification in solving for the  $J(t)$  function arises from the separable nature of the statistical characterization of the load disturbance.

$$\dot{S}(\mu) = \left[ \frac{K K_M^2}{\Psi} + \beta \right] S(\mu) + K K_D U(\mu-t) \quad (4.15)$$

with the boundary condition

$$S(T) = 0 \quad (4.16)$$

where

$$U(\mu-t) = e^{-\nu(\mu-t)}$$

The solution of this equation is

$$S = \frac{K K_D}{\nu + \beta + K K_M^2} \quad (4.17)$$

The solution for the  $K$  parameter is

$$K = \frac{\Psi}{K_M^2} \left[ -\beta + \sqrt{\beta^2 + K_M^2 \frac{\Phi}{\Psi}} \right] \quad (4.18)$$

By rearranging the equations into a more useful form, it can be seen that the optimal control law consists of a feed-forward component and a feedback component.

$$m(t) = Q_D u(t) - Q_C x(t) \quad (4.19)$$

The feedforward controller is

$$Q_D = -\frac{K_D}{K_M} \cdot \frac{-\beta + \sqrt{\beta^2 + K_M^2 \frac{\Phi}{\Psi}}}{\nu + \sqrt{\beta^2 + K_M^2 \frac{\Phi}{\Psi}}} \quad (4.20)$$

The feedback controller is

$$Q_C = \frac{-\beta + \sqrt{\beta^2 + K_M^2 \frac{\Phi}{\Psi}}}{K_M} \quad (4.21)$$

The controllers are functions of the ratio of the two weighting functions. It is of interest to examine the effect of limiting values of the weighting functions on the value of the controllers.

Let  $\Phi \rightarrow \infty$ . This corresponds to placing a very heavy penalty on the deviations of the state variable,  $x$ . Therefore the allowable range of the state variable approaches zero as the weighting function  $\Phi$ , approaches  $\infty$ . Notice the effect on  $Q_D$ .

$$\lim_{\Phi \rightarrow \infty} Q_D = -\frac{K_D}{K_M} \quad (4.22)$$

The result is the "ideal" feedforward controller. This limiting value is obtained by setting  $X = 0$  and solving for perfect invariant control. From equation (4.5) we can get the same result.

$$X(s) = 0 = \frac{K_M}{s + \beta} M(s) + \frac{K_D}{s + \beta} U(s) \quad (4.23)$$

rearranging gives

$$M(s) = - \frac{K_D}{K_M} U(s) \quad (4.24)$$

Therefore, "ideal" feedforward is the limiting case for this portion of the optimal controller.

Consider the case when  $\Psi$  approaches zero. This corresponds to very little concern for the magnitude of the control signal in the scalar performance index. The resulting effect on the feedback controller is

$$\lim_{\Psi \rightarrow 0} Q_C = \infty \quad (4.25)$$

This is the classical result obtained by Newton, Gould, and Kaiser (N1) which requires an infinite feedback gain for perfect attenuation.

For a first order system the ideal feedforward controller does the same job as an infinite feedback gain. However, the manner in which they attain the goal of perfect control is entirely different.

$$X(s) = \frac{P_M Q_D + P_D}{1 + P_M Q_C} U(s) \quad (4.26)$$

Feedforward control attempts to cancel the gain of the system, while the feedback controller increases the stability of the system. Stability increase can be thought of as a system desensitizing action, i.e., the system does not react to load disturbances. One, however, must be careful to point out that large feedback gains will not always increase the system stability. For systems of higher order, large feedback gains can actually move the system to instability (C5).

One noticeable result in equations (4.20) and (4.21) is that both control functions are dependent upon the ratio of the performance index weighting factors. The problem does not contain adequate degrees of freedom to allow different controllers for changes in both weighting factors. However, this result is to be expected. In most optimal control problems found in the literature, the weighting factor,  $\Phi$ , is assumed to be one (unity). The weighting factor,  $\Psi$ , corresponds to a Lagrangian multiplier which imbeds an integral (energy) constraint on the control effort into the performance index. Bellman has presented a rigorous justification of this technique (B2) and also points out that in some cases there is no multiplier that will minimize the performance index. These abnormal problems should not be worried about until a problem at hand exhibits this behavior. The steps involved in solving abnormal problems are complex and time-consuming (B2).

With the above comments in mind, it seems convenient to specify the weighting factor,  $\Phi$ , to be unity. Then, varying the weighting factor,  $\Psi$ , corresponds to varying the energy constraint on the control effort.

A saturation constraint on the control effort,  $m$ , can not be directly imbedded into the performance index. A common procedure is to replace the saturation constraint ( $m(t) \leq \text{constant}$ ) by the energy constraint ( $\int_0^{\infty} m(t) dt \leq \text{constant}$ ). The difficulty is that it is not clear how to assign a value to the energy constraint corresponding to a specific saturation constraint. In servomechanism problems the transient control effort trajectory is calculated. Then the energy constraint is adjusted until the control signal trajectory does not violate the saturation constraint. However, trajectories are not useful in regulator problems. In the case of linear systems with gaussian disturbances, Newton, Gould and Kaiser (N1) have proposed a method of replacing saturation with energy constraints. This constraint replacement problem is one of the major difficulties in optimal control theory.

#### A Particular System

For purposes of illustration, several numerical values were chosen for the parameters in the system transfer function.

$$K_M = K_D = 1$$

$$\beta = 2$$

mean square disturbance amplitude,  $\mu^2 = 25$ .

state variable weighting factor,  $\Phi_s = 1.0$

Figure (4-2) is the performance diagram for this system. The cross-plotted values of  $\Phi/\Psi$  show where the various optimal controllers lie on the performance loci. For a particular disturbance frequency every combination of feedback and feedforward gains lie on a single line on the performance diagram as can be seen from Figure (4-3).

From the general shape of the performance loci, it seems that a large amount of control effort is required to cause any noticeable reduction of the mean square output. This is deceiving. The performance diagram is plotted on the logarithmic scale which squeezes the range of interest. In terms of quality of performance, Figure (4-4) will give the reader another representation of the ability of these controllers to perform their tasks. In all upcoming work, the performance diagram is used because of its larger range.

With the results of Figure (4-4) in mind, we can more fully understand the performance chart, Figure (4-2). As the performance loci flattens out, indicating that small changes in the mean square control effort produce significant changes in the mean square output we must always keep in mind that this occurs at the 99% output efficiency level. Although a large portion of the mean square output range on the diagram



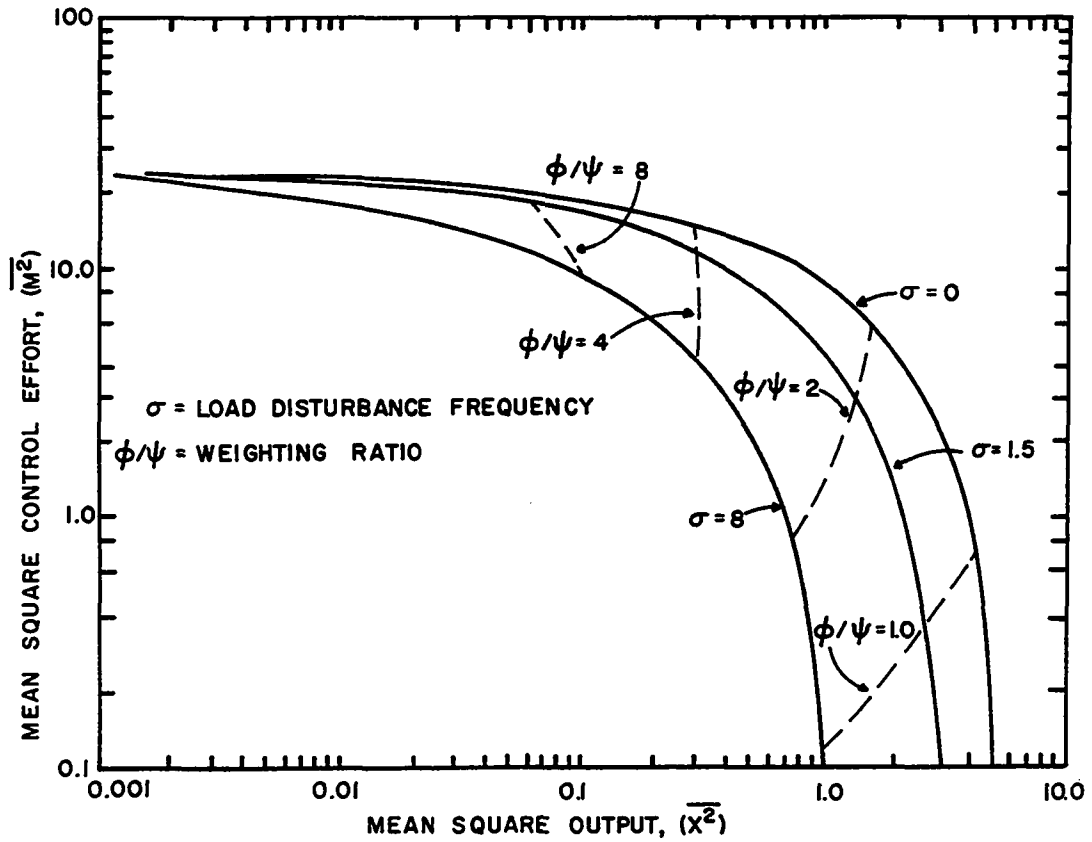


Figure 4-2. Response characteristics of optimally controlled system for various disturbance frequencies.

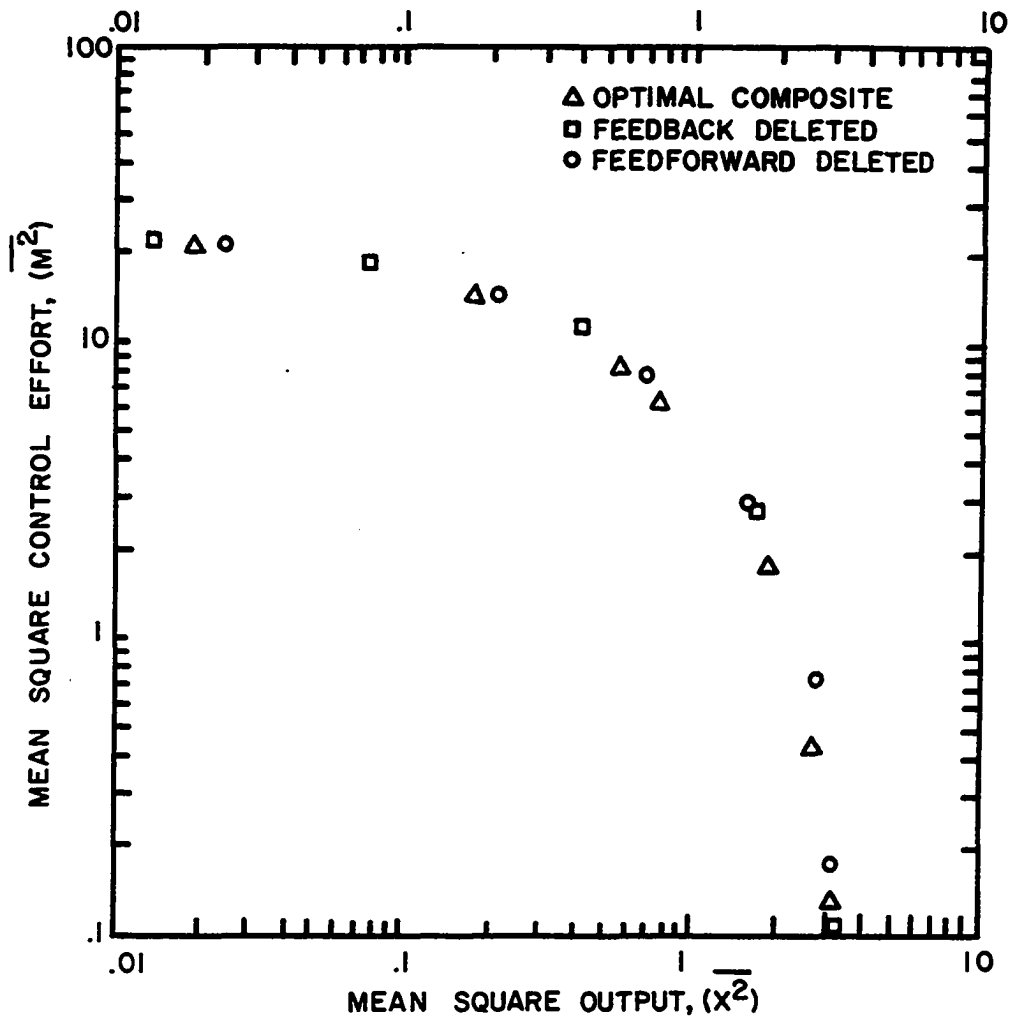


Figure 4-3.

Performance diagram with various portions of the optimal controller deleted.

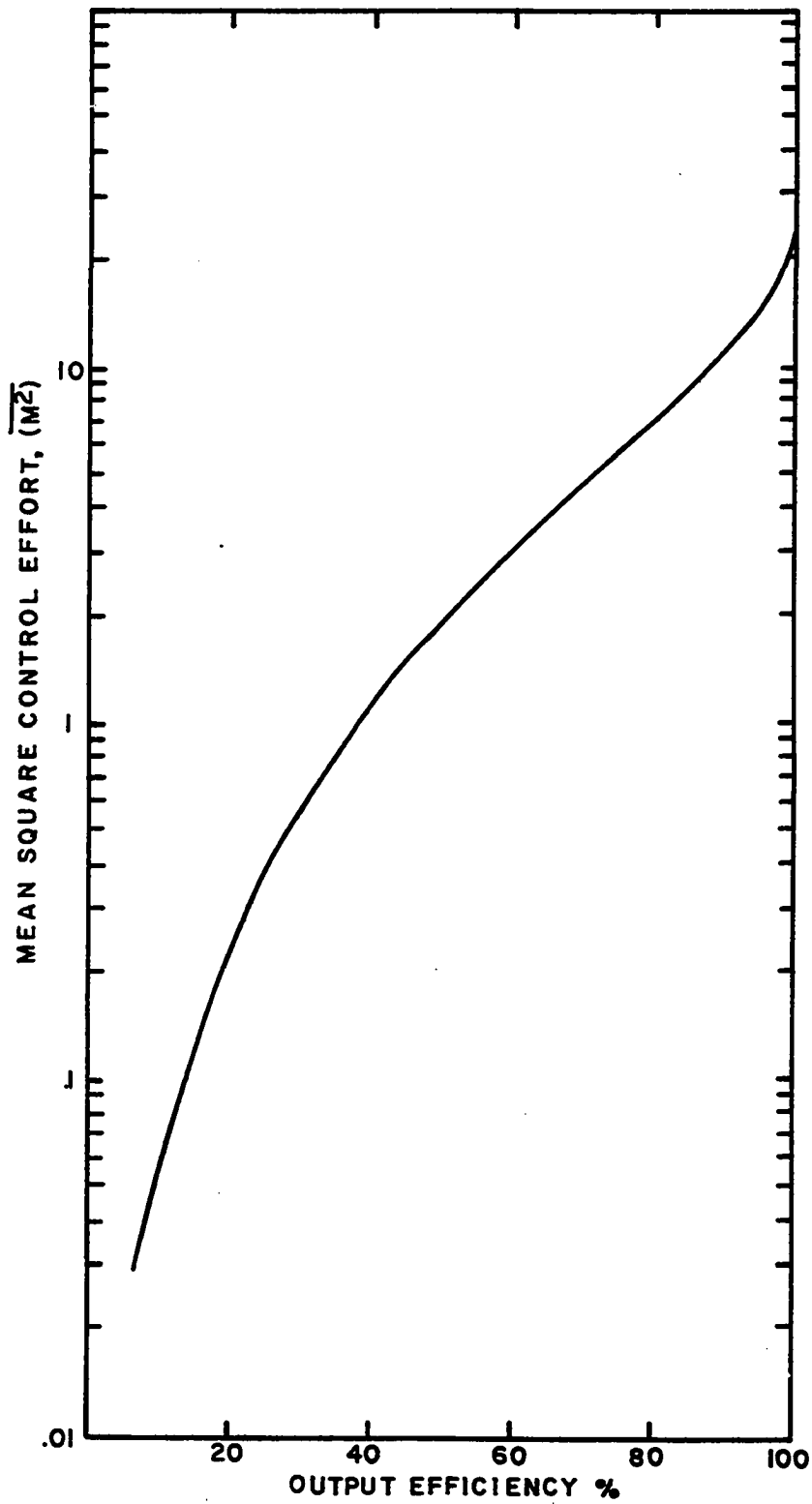


Figure 4-4. Output efficiency in relation to the amount of control effort expended.

is involved, it is only in the small number range which does not appreciably affect the output efficiency.

In terms of the control parameters, the decrease in mean square control specifies larger and larger feedback gains. There is, of course, a practical limit on the size of the feedback gain, but this limit has not been introduced in the optimization procedure. In fact, it is almost impossible to imbed a constraint on the feedback gain into the optimization equations. There are some indirect methods of accomplishing this, but they all are only rough estimates. The reason that it is difficult to consider feedback gain constraints is that we are minimizing with respect to the control signal,  $m(t)$ , not the gain portion of this signal. While a limit on the feedback gain is common, the constraint on the total control signal is more important. As the gain increases, it causes the output signal to decrease. The control signal, which is the product of these two functions, is approaching a limit. For example, the analog computer which is widely used to construct controllers has an operating range of  $\pm 100$  volts. Therefore the output of the feedback amplifier should not exceed 100 volts. There is not an explicit limit to the size of the feedback gain that can be used with this amplifier, but because of noise limitations of the analog equipment, it is not wise to use a gain larger than 100. This would mean that the input voltage to the amplifier

would be restricted to a range less than  $\pm 1$  volt which is only 1% of the computer range. With this low signal, noise becomes a major limitation.

An important point to notice is that the mean square control effort for ideal feedforward control is the upper bound on control effort. Therefore, a constraint on the control effort hinders the operation of ideal feedforward as well as feedback controllers. This point has not been discussed in previous studies on ideal feedforward control. A probable reason for this is that the particular process under consideration does not have a strong constraint on control effort.

It is interesting to note the separate effects of each control action. In Figure (4-5), the weighting function ratio is plotted against the mean square output for three different control configurations; feedback control, feedforward control, and the combination of the two. These cases represent the extremes in the ability to measure the load or output signal. If, for example, the load variable can not be measured, this situation corresponds to the case of no feedforward available. The feedback controller is more efficient than the feedforward controller throughout the whole range for the same weighting function. At the same value of the weighting function, it can be seen that the composite controller is much better than either controller acting alone. Of course the value of

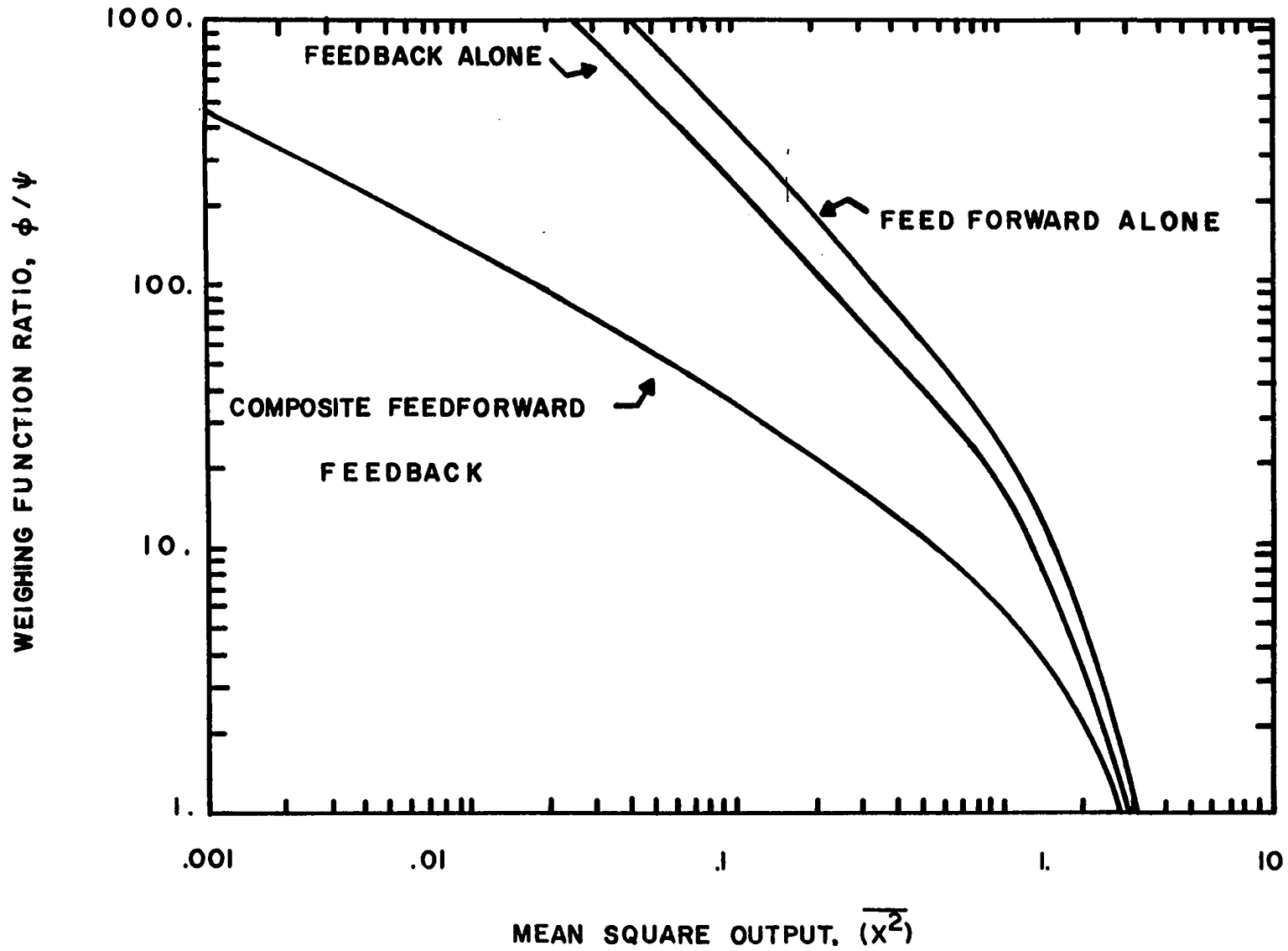


Figure 4-5. Contribution of each portion of the optimal controller to overall system attenuation.

the  $Q_C$  gain needed to produce a given mean square output is much larger for the  $Q_D = 0$  case than the composite case. In the composite case we have two gains  $Q_C$  and  $Q_D$  which contribute to the control action, while in the other cases the  $Q_C$  and  $Q_D$  which contribute to the control action, while in the other cases the  $Q_C$  or  $Q_D$  have to make up in effort for the deleted member. In Figure (4-6) the same three cases are shown on the weighting factor versus mean square control effort diagram. (From this graph it can be seen that the feedback takes more control effort than the feedforward.) The reason for this unequal division of control effort is that we have chosen to work with a load disturbance frequency of 1.5. Since only the feedforward controller is sensitive to load frequency, it is this controller whose efficiency is affected. When the frequency is zero, the optimal controller splits the work evenly between feedforward and feedback. The work of the composite controller is split about evenly in this case because the ratio of the control gain to disturbance gain is unity.

#### Constraint on the Integral of the State Variable

Consider the effect of adding another constraint to the optimization problem. This new constraint specifies proportional and integral feedback control action. Without introducing the integral constraint in the weighting matrix coupled

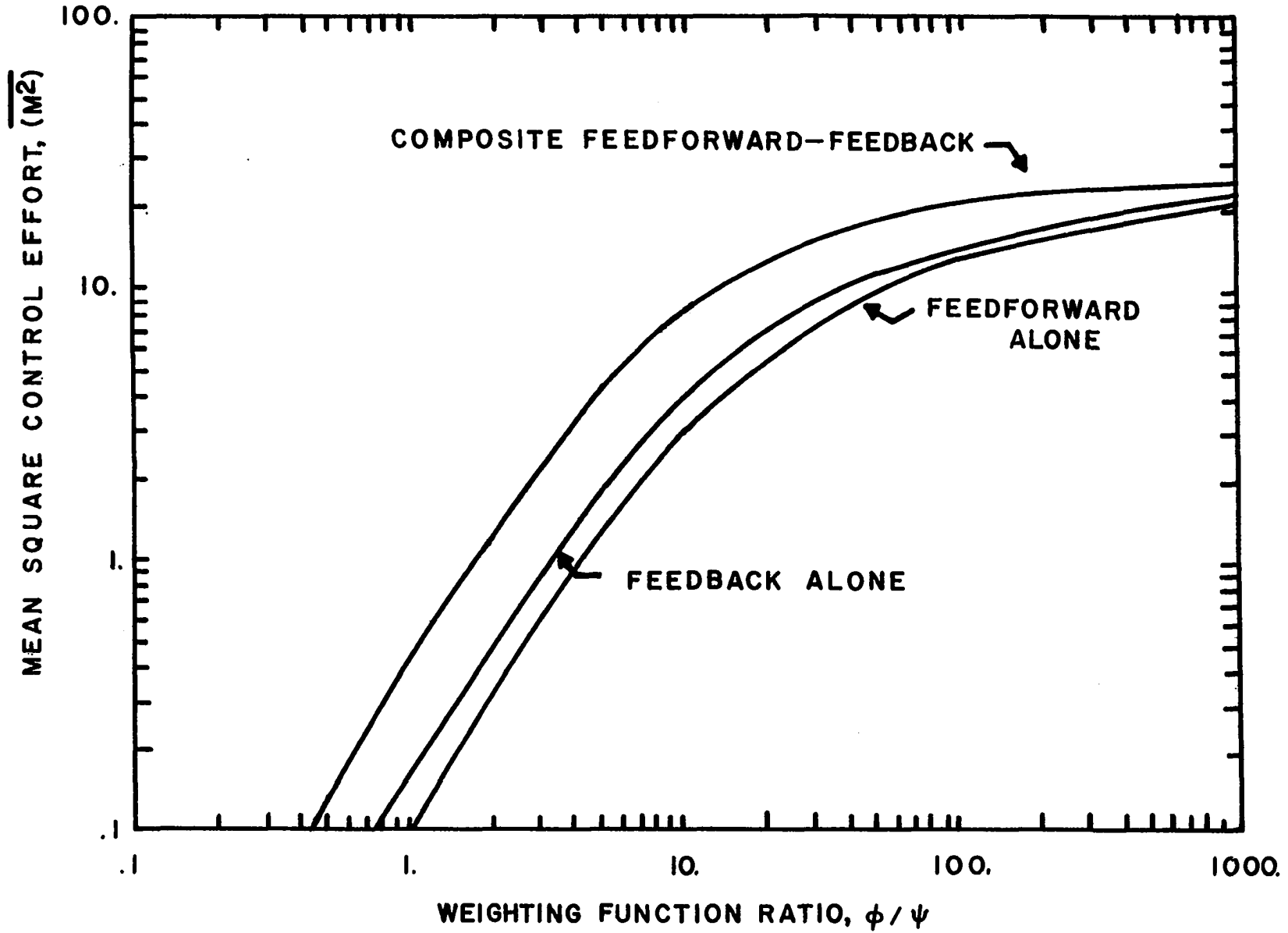


Figure 4-6. Contribution of each portion of the optimal controller to overall control effort.



with the fact that the integral output does not appear in the system dynamics, there is no possibility of obtaining integral control. The reason is that all of the possible coefficients of the integral output are zero. However, by adding a finite constraint on the integral output, the mathematical manipulation of the various system matrices carries along a finite coefficient for the integral output.

Figure (4-7) shows the difference between mean square output and mean square integral output on the performance diagram. Notice that the mean square integral goes to infinity as control effort goes to zero. If the integral output is used as the only output criterion in the scalar performance index (by setting the normal output weighting factor equal to zero), both proportional and integral control action are specified by the optimization technique. However, if the integral output is neglected, then only a proportional controller is specified. Without an integral controller the mean square integral output is always infinite. This result points out the importance of including all the significant variables in the scalar performance index.

Figure (4.8) shows the effect of mean square integral output on the mean square output. By increasing the integral weighting factor, the mean square integral output corresponding to a given mean square output is reduced. Furthermore a reduction in value of the proportional feedback gain needed

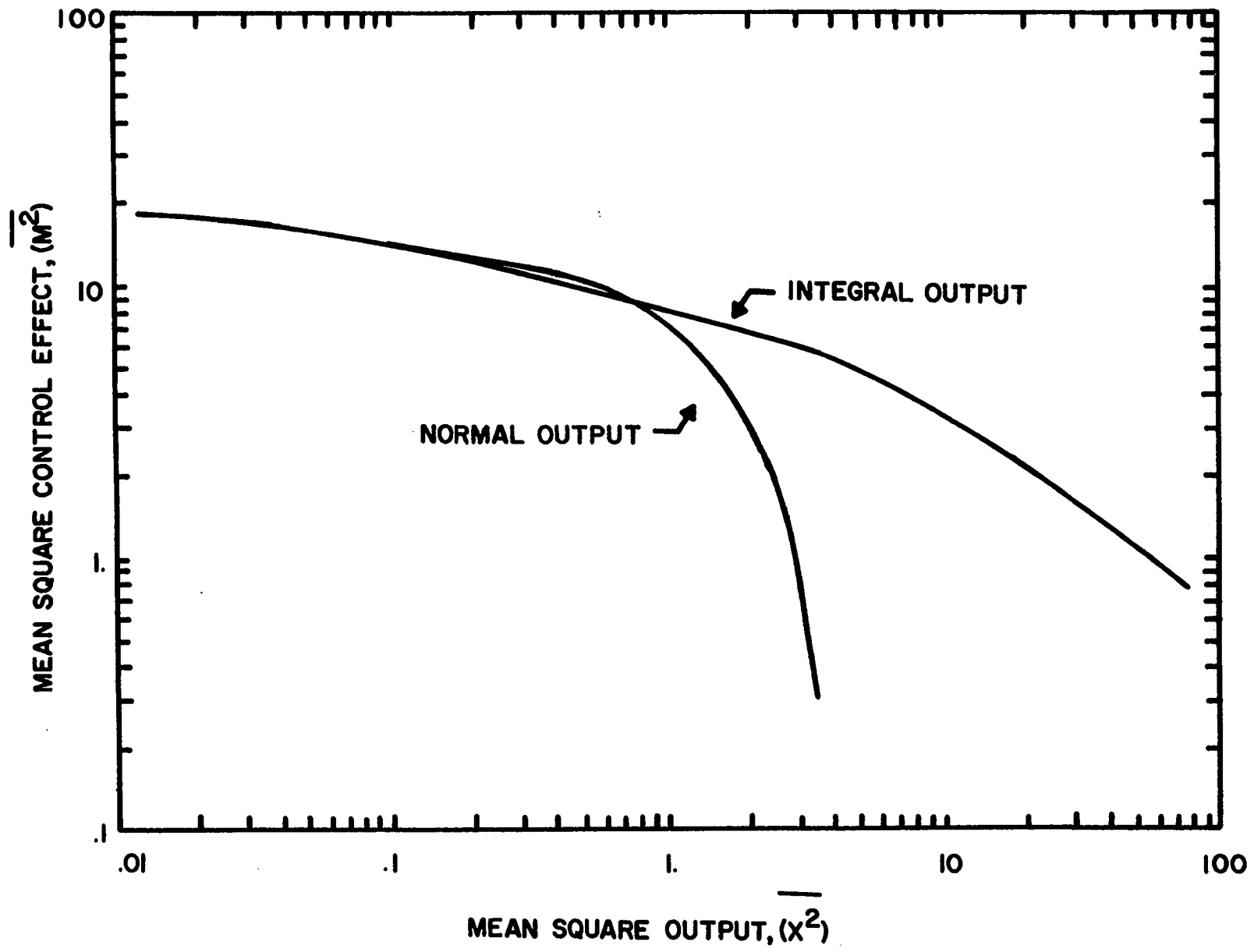


Figure 4-7. Performance diagram for both the output and the integral output.

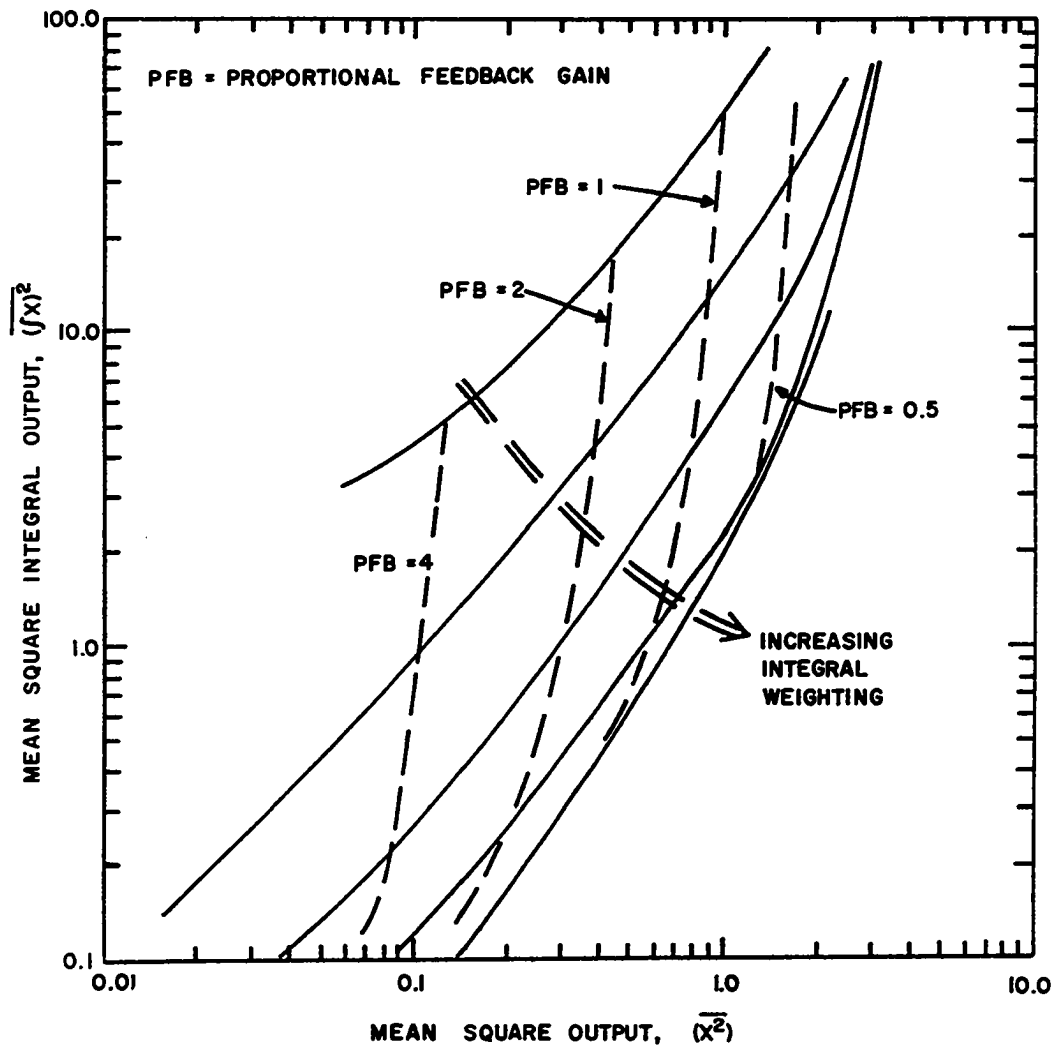


Figure 4-8. Effect of integral constraints on the mean square output.

to produce a given mean square output also results as seen from the cross-plotted values on Figure (4-8). This point can be illustrated by using the same value of mean square output for various combinations of integral and proportional gains.

<u>MSQ Integral Output</u>	<u>Prop. Feedback</u>
$\infty$	3.38
1.8	3.14
0.16	1.55

The first value corresponds to the case when no integral constraint (integral weighting is zero) is considered. A lower mean square integral output uses less proportional feedback and more integral feedback to achieve the desired level of output attenuation.

The cross-plotted feedback proportional gains are approaching a particular value as the mean square integral output approaches infinity. This limiting value is the proportional gain when no integral constraints are included in the performance index.

By including the integral output in the design, we should be aware of its effect on the controlled process. The transient response of the controlled first order system to a step disturbance is a familiar example for explanation of these effects. Proportional control is subject to a phenomena called "offset". Increasing the weighting factor on the output

variables just reduces the offset. Integral action relieves "offset". Whereas the proportional controller alone will never bring the system back to the desired state, adding integral control will allow attaining the desired value of the state variable. Varying the weighting factor of the integral output causes a difference in the manner in which the system tries to reach the desired state. As the integral controller gain increases, the system response becomes more oscillatory as shown in Figure (4-9). For a fixed proportional gain, increases in integral gain cause the system to approach a small oscillatory response. Remember that the performance index is quadratic, so it does not discriminate against systems with a small highly oscillatory response.

When we increase the weighting factors, both proportional and integral gains are affected. Figure (4-9) shows the effect of proportional gain on a system with PI controllers. It can be seen that an increase in the proportional gain of a PI controller reduces the over-shoot of the response trajectory.

When the output integral was included in the scalar performance index, the integral weighting factor is considered to be another degree of freedom. Since there was one degree of freedom in choosing the weighting factors for the case of proportional control only, the present system will have two degrees of freedom. One specifies a relative weight between

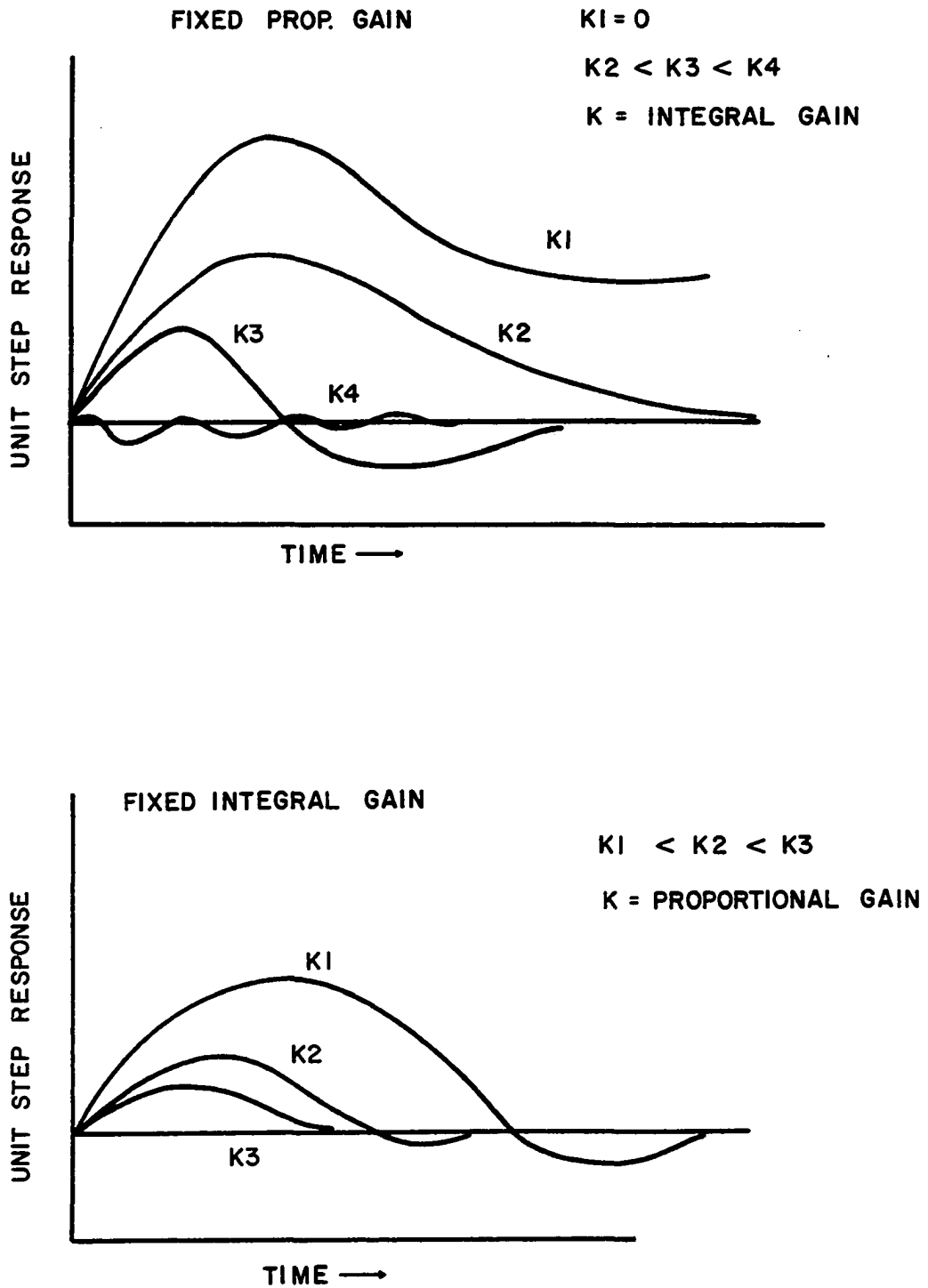


Figure 4-9. Unit step response of a first order system with proportional-integral controllers.

feedforward and feedback, while the other specifies a relative weighting between proportional and integral action. In any case an increase in the weighting factors causes a decrease in system mean square output. Notice that an increase in weighting factor causes both proportional and integral gains to increase. Since these two parameters individually have opposite effects on the oscillatory nature of the system, our optimal control specifications combine both faster response with quicker damping. As the load disturbance appears in the system dynamics without any transfer function zeros, the integral constraint does not affect the feedforward controller.

#### The Effect of Feedback Noise

In actual control equipment there is usually a dead band, i.e., a certain finite signal must be obtained before the control and measurement equipment can detect it. It is this dead band that limits the size of the feedback gain which can be physically realized since the optimal control law states that larger and larger feedback gains are required in order to make the output variable smaller and smaller.

In the previous mathematical formulation, we restricted the control variable,  $m(t)$ , to be in the closed set;

$$M^- \leq m(t) \leq M^+$$

This type of set would include the case of control signal saturation. The optimal control law is

$$m(t) = \begin{cases} M^- & \text{for } m^*(t) < M^- \\ m^* & \text{for } M^- \leq m^*(t) \leq M^+ \\ M^+ & \text{for } m^*(t) > M^+ \end{cases}$$

If the dead band region is included, the allowable set of control signals must be changed. The following set would be desirable.

$$m(t) = \begin{cases} M_1^- & \text{for } m^*(t) < M_1^- \\ m^*(t) & \text{for } M_1^- \leq m^*(t) \leq M_1^+ \\ 0 & \text{for } M_1^+ \leq m^*(t) \leq M_2^- \\ m^*(t) & \text{for } M_2^- \leq m^*(t) \leq M_2^+ \\ M_2^+ & \text{for } m^*(t) > M_2^+(t) \end{cases} \quad (4.28)$$

This new formulation restricts the control signal to a set which is made up of the sum of two closed sets. Figure (4-10) shows a typical allowable control signal.

The problem in solution of the optimal control equations arises because of the discontinuities at points "a" and "b". This set of allowable control signals is not suitable for the previously developed theory.

One way to get around this difficulty is to consider noise in the feedback circuitry. The level of the feedback noise will allow us to pick reasonable weighting factors for the



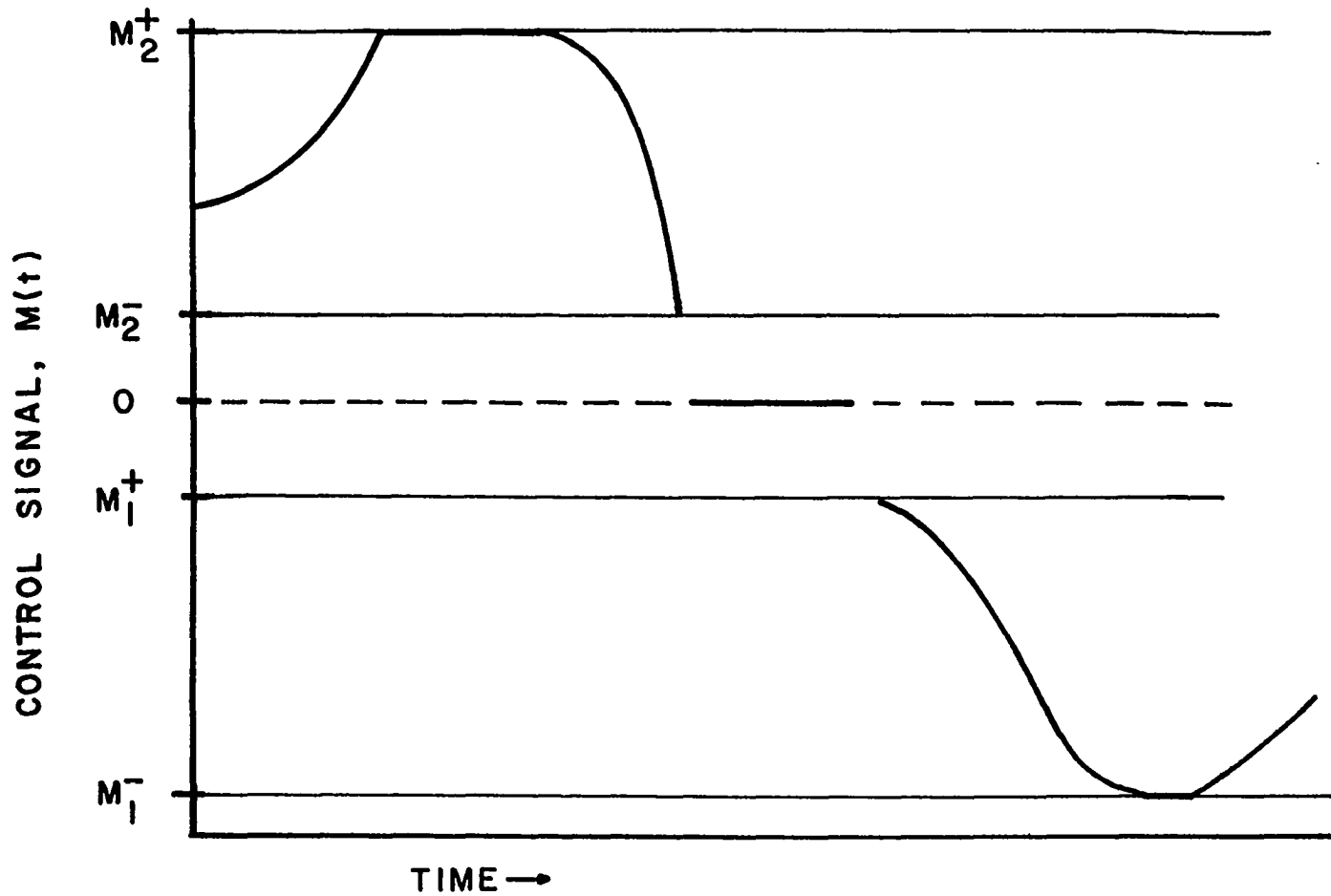


Figure 4-10 A Typical control signal trajectory for a system containing a dead band.

the performance indices. The basic idea of entering the new independent parameter, feedback noise, is to reduce the number of degrees of freedom of the whole design procedure. In Figure (4-11) the block diagram shows how feedback noise is related to the overall process.

The control equation for this system with noise in the feedback is

$$M(s) = Q_D U(s) - Q_C (X(s) + \delta(s)) \quad (4.29)$$

Using this control equation in the first order process previously mentioned

$$X(s) = \frac{P_M Q_D + P_D}{1 + P_M Q_C} - \frac{P_M Q_C}{1 + P_M Q_C} \delta(s) \quad (4.30)$$

It can be seen that as  $Q_C$  is made larger, the output variable  $X(s)$  approaches the negative value of the noise,  $\delta(s)$ . The performance diagram, Figure (4-12), shows this very clearly. The important point is that there is a set of weighting factors which will give a physically realizable feedback gain. For example, when the mean square amplitude of the noise in the physical equipment is 0.01, the performance diagram shows this value to be the best possible control of the output that can be obtained. Further increases in the mean square control effort do not produce any reductions in the mean square output. This is intuitively reasonable because the controller can not act upon something it can not see. Therefore

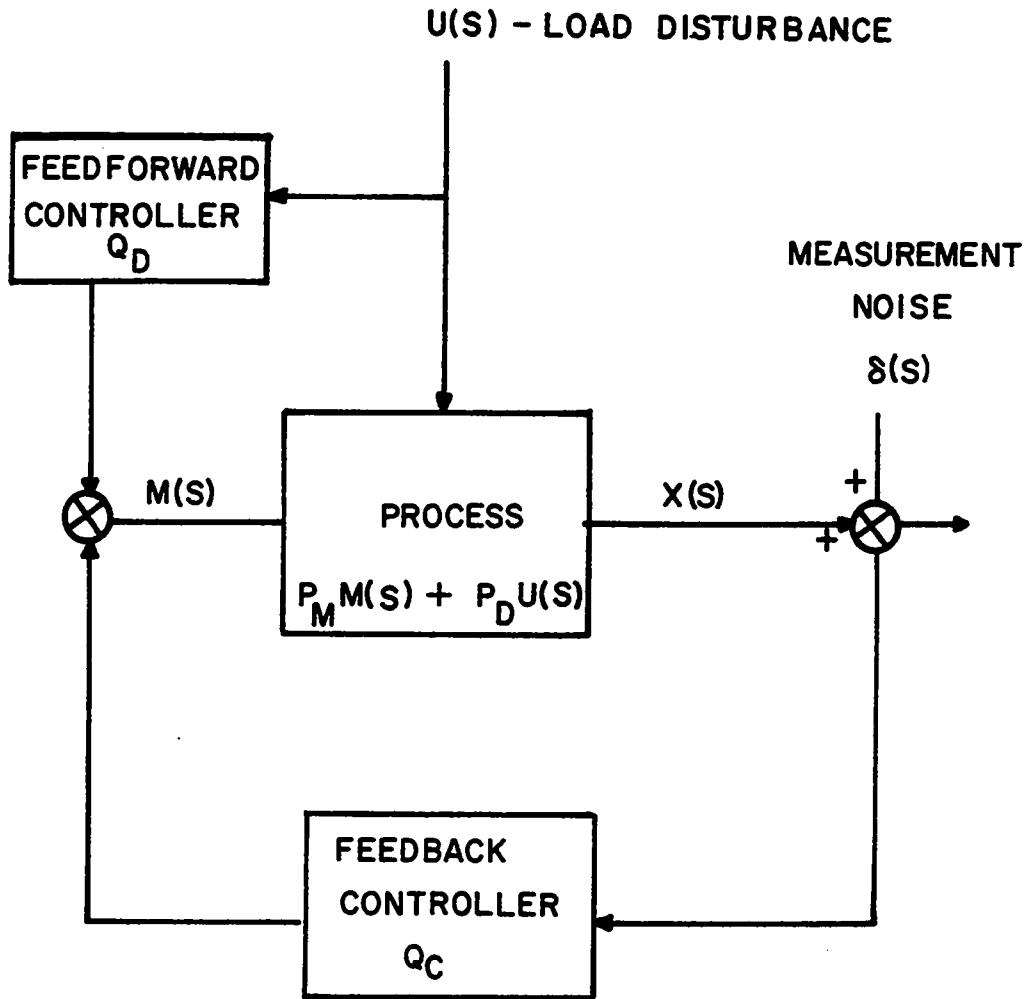


Figure 4-11. Block diagram of a controlled system with measurement noise in feedback.

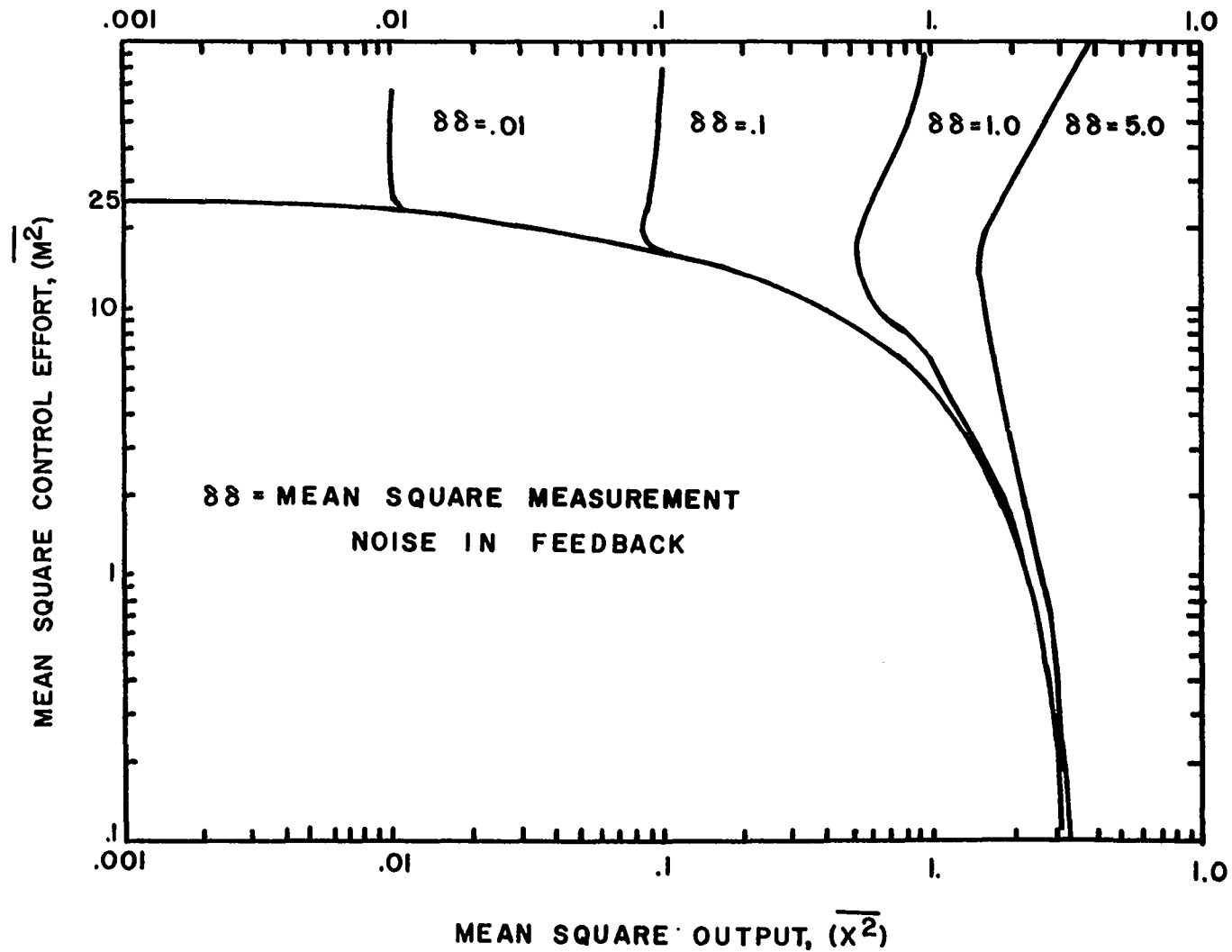


Figure 4-12. The performance diagram of a first order system with various levels of feedback noise present.

the introduction of feedback noise serves the purpose of approximating the dead band phenomena of actual equipment. In the control equipment literature the feedback noise level is usually referred to in terms of the signal-to-noise ratio (NI). However, most of the control literature is concerned with relatively low signal-to-noise ratios such as is common in radar and communications networks. This equipment requires filters to estimate the true signal value.

We are only concerned with rather high signal-to-noise ratios. Furthermore, it is difficult to filter the noise in a measurement of a chemical process. The time constants prevalent in most heat transfer systems are so large that the filter would affect the system dynamics. The performance diagram, Figure (4-12), show that when the signal-to-noise ratio approaches unity, the system will not be subject to control. However, at a feedback mean square noise level of 1.0 we can still reduce the output mean square to a value of 0.5 which is 50% lower than the noise level. Notice that this is still an 86% reduction in the level of the output variable. But, normally when the noise level is too high, it is best to reconsider the measurement and control equipment to be used. However in the situations where there is no way to get around a high signal-to-noise ratio, the performance diagram shows that some attenuation below the noise level is still possible with the right selection of feedback gain.

Effect of Model Error

In empirical mathematical process models the system gains and time constants are not known precisely and one can usually associate error bounds with each parameter. These error bounds can be thought of as limits of the fluctuation of system parameter. These fluctuations are ever present and can be a result of small non-linearities of the system. In order to grasp the importance of these uncertainties, a sensitivity study can be made.

Consider the following functional form of the system dynamics

$$\dot{x}(t) = f(x, t, p) \quad (4.31)$$

where  $x$  = state variable

$t$  = time

$p$  = a system parameter

The parameter,  $p$ , can be any of the system gains or time constant of interest. If we need to observe the effect of variations in the parameter, we can solve the above equation successively for various parameter values.

$$\dot{x} = f(x, t, p + \Delta p) \quad (4.32)$$

By comparing solutions we can obtain an indication of the sensitivity of the system. A more quantitative measure of this sensitivity can be defined

$$\tilde{Z}(t,p) = \lim_{\Delta p \rightarrow 0} \frac{x(t,p + \Delta p) - x(t,p)}{\Delta p} \quad (4.33)$$

or

$$\tilde{Z}(t,p) = \frac{\partial x(t,p)}{\partial p} \quad (4.34)$$

This function  $\tilde{Z}(t,p)$  is called the sensitivity coefficient. This type of function has been used in recent years by control engineers to study stability, most notably the study of airplane stability (D2,K3,P2,T1).

In order to qualify the above sensitivity definition, we must recognize the two classes of sensitivity coefficients which are commonly used today. If the actual initial or steady state is not the nominal one used in the design stage, the difference acts as a static disturbance. This static sensitivity is not considered here. On the other hand, if varying parameters appear explicitly in the state transition equation, they are labeled dynamic disturbances. It is this latter class of variations which are of interest here. The reason for this interest is a result of several observations made during the experimental phase of this work and are explained in detail in the experimental chapter.

The sensitivity coefficient can be redefined for convenience in the following manner.

$$Z(t,p) = \lim_{\Delta p \rightarrow 0} \frac{x(t,p + \Delta p) - x(t,p)}{\Delta p/p} \quad (4.35)$$

or

$$Z(t,p) = \frac{\partial x(t,p)}{\partial \ln p} \quad (4.36)$$

This definition gives an indication of the change in the state variable corresponding to a relative variation in the parameter.

A transform domain definition follows directly from the differentiation property of the Laplace integral.

$$Z(s) = \frac{\partial X(s)}{\partial \ln p} \quad (4.37)$$

Then we can use a mean square sensitivity coefficient in later discussions.

$$\Theta_{ZZ}(0) = \frac{1}{j} \int_{-j\infty}^{j\infty} Z(s) Z(-s) ds \quad (4.38)$$

This mean square evaluation has been discussed earlier in the preliminary mathematical background presented in Chapter II.

The sensitivity coefficient is calculated from the error bound estimate of the parameter in question. This gives a "worst" value sensitivity. Then the sum of the mean square



output of the model and the mean square sensitivities calculated from all parameters subject to variation provides an estimate of the actual mean square output of the physical process.

$$(\Theta_{xx})_{\text{actual}} = (\Theta_{xx})_{\text{model}} + \Theta_{zz} \epsilon^2 \quad (4.39)$$

where  $\epsilon$  is the parameter error bound.

Figure (4-13) shows the effect of error in the system gains upon the mean square output. Error in the system pole is negligible in comparison to the gain errors. It can be seen that the control signal gain,  $K_M$ , is the most sensitive parameter when the composite controller is used. However, if only the feedforward portion of the controller is available, a variation in the disturbance gain causes a larger deviation. This points out the necessity of using a feedback controller whenever possible because of its ability to de-sensitize the system model errors as a safeguard in actual physical process control systems.

In Figure (4-13) each point on the forty-five degree line represents a value of mean square control effort. The actual mean square output is higher due to inclusion of the error bounds than the model mean square output. Notice that the actual output still goes to zero as the control effort increases but at a slower rate than the model output. When a feedforward controller alone is considered, the actual mean

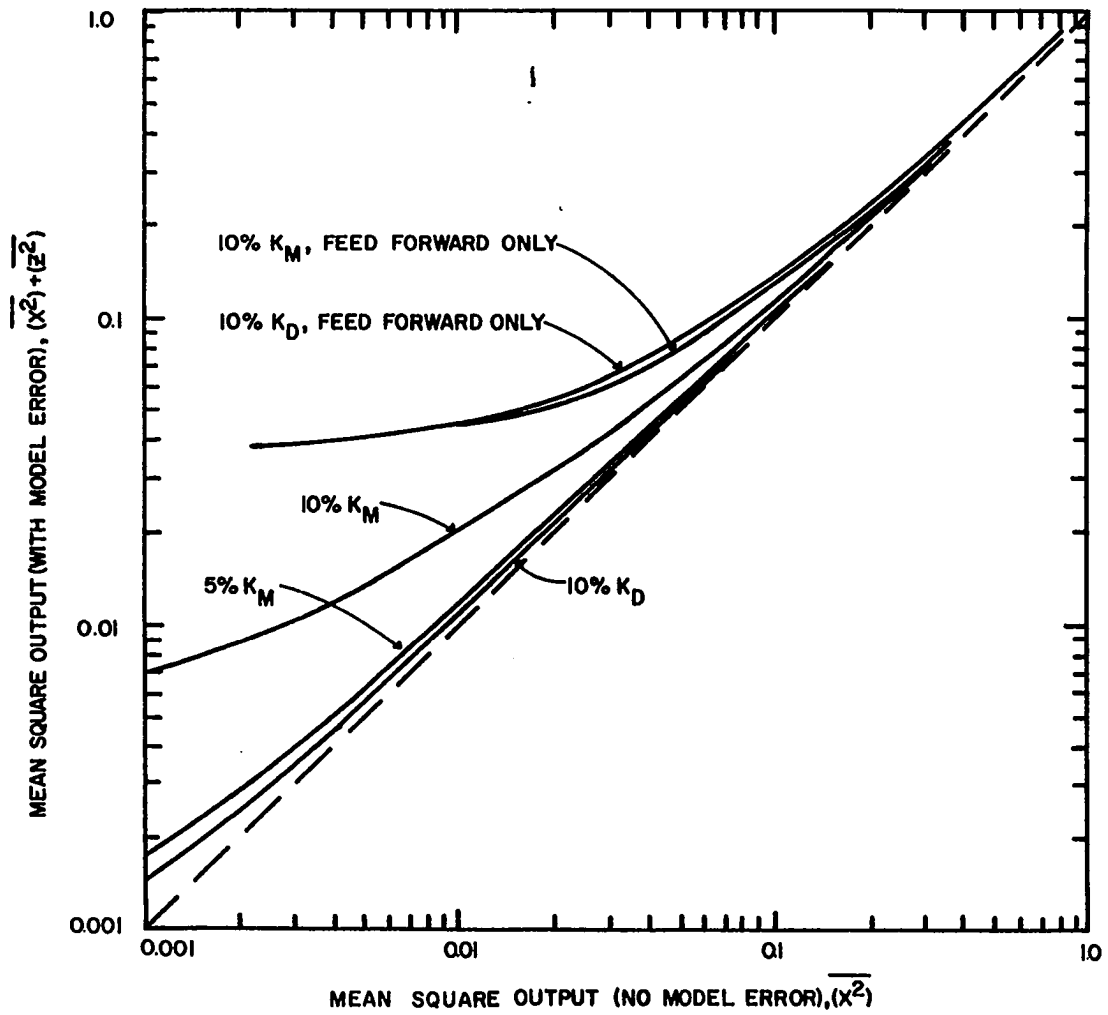


Figure 4-13. The effect of model error on the mean square output of an optimally controlled first order system.

square output does not tend to zero, but rather it approaches some finite value.

This emphasizes the effect of model error on the optimum composite feedback-feedforward controller. It is the feedforward portion which is the cause of the higher mean square output.

#### Process Time Delay

Consider a first order process with a time delay. This model is extremely useful as a representation for many industrial processes. Ziegler and Nichols (Z1) used this representation as a guideline in formulating their highly successful empirical design procedures for selecting controller parameters.

An example of the type of processes under consideration is shown in Figure (4-1). For simplification, but with no loss of generality, the time delay  $\tau_2$  is assumed to be zero. The case of non-zero delay  $\tau_2$  is discussed later. The transfer function for this model is

$$X(s) = P_M e^{-Ts} M(s) + P_D e^{-Ts} U(s) \quad (4.40)$$

The constants and variables are the same as in the previous discussion. The parameter,  $\tau$ , in the exponential factor is the time delay. Time delays of this type are common in the chemical industry because of the nature of the flowing system

in that it takes time for an upset in the input stream to be detected in the outlet. This time interval is the delay time,  $\tau$ . Using equation (3.23) to get the controller

$$m^*(t) = Q_D u(t) - Q_C x(t + \tau) \quad (4.41)$$

The feedforward controller,  $Q_D$ , and the feedback controller,  $Q_C$ , have been defined previously in equations (4.20) and (4.21). Since the argument of the state variable is  $t + \tau$ , this means that we must know the value of state variable,  $x$ ,  $\tau$  time units in the future. Although this is physically unrealizable, we do have an alternative. Rewriting the state variable in terms of the impulse response

$$x(t+\tau) = \varphi(\tau) x(t) + \int_{t-\tau}^t \varphi(t-\eta) K_M m(\eta) d\eta + \int_{t-\tau}^t \varphi(t-\eta) K_D u(\eta) d\eta \quad (4.42)$$

where  $\varphi(\tau)$  = matrizant or fundamental matrix of the homogeneous state variable equation.

Notice that  $x(t + \tau)$  is a function of the measurable quantities:  $x(t)$ ,  $m(t)$ ,  $u(t)$ , and the control and load signal in the past. This gives a completely measurable result. Since the inlet stream variables will not affect the outlet until  $\tau$  time units later, the inlet variable at time,  $t$ , and their recent past values will determine the outlet at time,  $t + \tau$ . In practical applications, problems exist because we usually

do not have a complete mathematical model which will include all the disturbances but a good approximation can be generated. The above equation can be rearranged into the following form.

$$\begin{aligned} x(t+\tau) = & e^{-\beta\tau} x(t) + K_M \{e^{-\beta\tau} \times m(t) - e^{-\beta\tau} e^{-\beta(t-\tau)} \times m(t-\tau)\} \\ & + K_D \{e^{-\beta\tau} \times u(t) - e^{-\beta\tau} e^{-\beta(t-\tau)} \times u(t-\tau)\} \quad (4.43) \end{aligned}$$

The symbol,  $\times$ , denotes the convolution product.

Using equation (4.41) and (4.43) and taking the Laplace transform results in

$$\begin{aligned} M^*(s) = & Q_D U(s) - Q_C e^{-\beta\tau} X(s) \\ & - P_M Q_C (1 - e^{-\tau s} e^{-\beta\tau}) M(s) \\ & - P_D Q_C (1 - e^{-\tau s} e^{-\beta\tau}) U(s) \end{aligned} \quad (4.44)$$

Simplifying

$$M^*(s) = Q_D^*(s) U(s) - Q_D^* X(s) \quad (4.45)$$

where

$$Q_D^* = \frac{Q_D - P_D Q_C (1 - e^{-\tau s} e^{-\beta\tau})}{1 + P_M Q_C (1 - e^{-\tau s} e^{-\beta\tau})} \quad (4.46)$$

$$Q_C^* = \frac{Q_C e^{-\beta\tau}}{1 + P_M Q_C (1 - e^{-\tau s} e^{-\beta\tau})} \quad (4.47)$$

Here the new functions,  $Q_D^*$  and  $Q_C^*$  are the feedforward and feedback controllers. It is interesting to consider the physical interpretation of these new functions. Although these functions appear complicated, they can be easily simulated using block diagram algebra (C5). Figure (4-14) shows the block diagram of this system. Notice that the optimal control equations specify a minor loop around the feedback gain. This configuration is similar to the Smith linear prediction investigated by Buckley (B12,S2). However, Buckley considered a pure dead time process which does not contain any other dynamic elements. This minor loop tries to "tune out" the process dead time. This apparatus is not commercially available. However, it can be approximated with analog and/or digital components. Buckley has reported some successful applications of this type of configuration (B12).

The performance diagram for this system with the minor feedback loop is exactly the same as the system with no dead time. If the minor loop is neglected, a point of instability can be reached. The instability is a direct result of the exponential term in the denominator of the overall system transfer function, i.e.

$$X(s) = P_M e^{-Ts} M(s) + P_D e^{-Ts} U(s) \quad (4.40)$$

But for the controller without the minor feedback loop

$$M(s) = Q_D U(s) - Q_C e^{-\beta T} X(s) \quad (4.49)$$

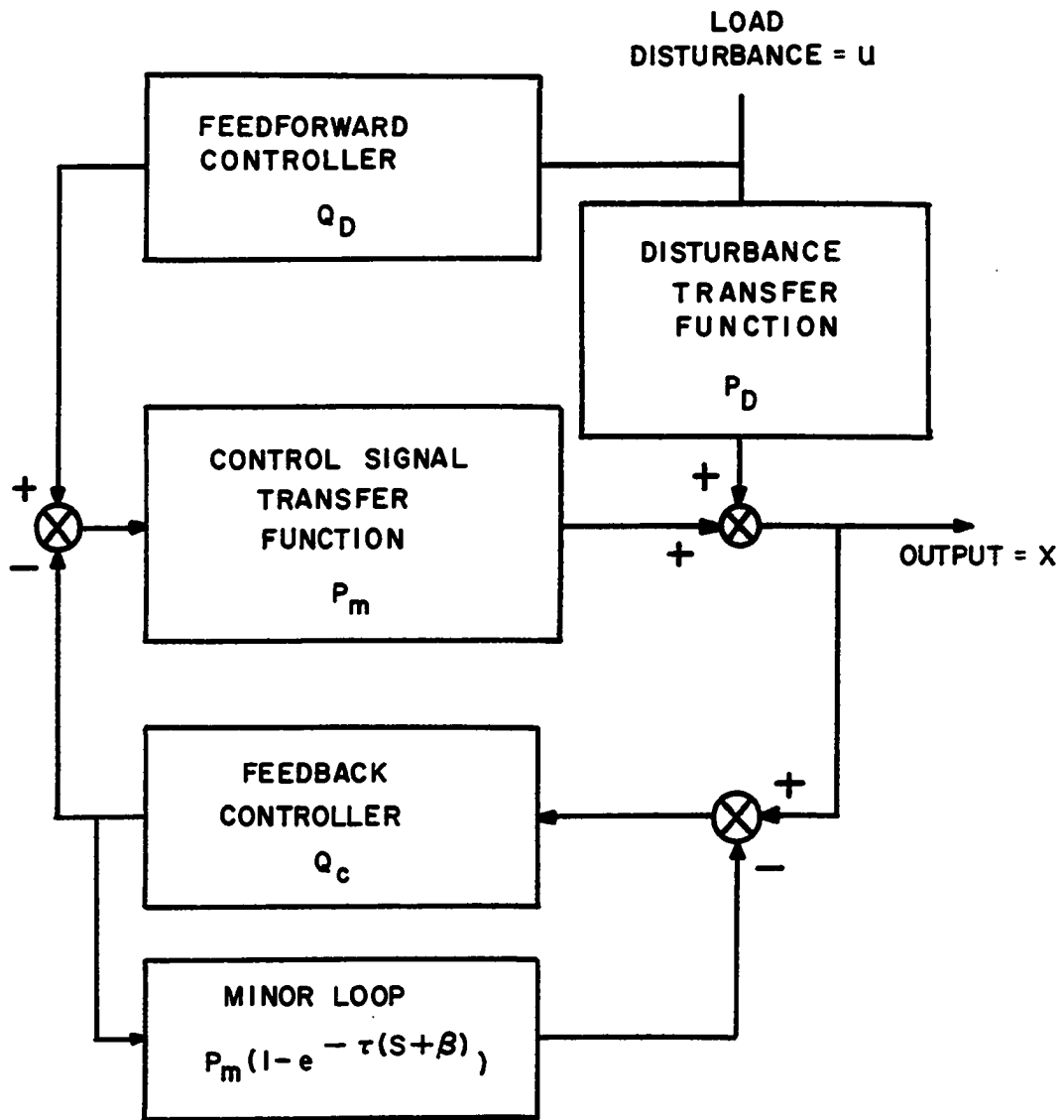


Figure 4-14. Block diagram of a first order time delay system.

Combining these two equations gives the overall controlled system transfer function.

$$\frac{X(s)}{U(s)} = \frac{P_{M^2D} + P_D}{e^{+\tau s} + P_{M^2C} e^{-\beta\tau}} \quad (4.50)$$

To evaluate the behavior analytically, substitute the first order Pade expansions (B12) for the denominator exponential and rearrange so that

$$\frac{X(s)}{U(s)} = \frac{(K_{M^2D} + K_D) ((-\tau/2) s + 1)}{((\tau/2)s + 1) (s + \beta) + K_{M^2C} e^{-\beta\tau} ((-\tau/2)s + 1)} \quad (4.51)$$

and

$$\frac{X(s)}{U(s)} = \frac{(K_{M^2D} K_D) \left( \frac{\tau}{2} s - 1 \right)}{\frac{\tau s^2}{2} + \left( 1 + \frac{\tau\beta}{2} - \frac{\tau K_{M^2C} e^{-\beta\tau}}{2} \right) s + \beta + K_{M^2C} e^{-\beta\tau}} \quad (4.52)$$

From this simple approximation to the exponential, it can be seen that as the feedback gain increases, a point can be reached where the roots of the transfer function denominator move into the right-half plane. This result implies that the system becomes unstable, and the controller reinforces the disturbance at this point with the natural result of causing the system to become oscillatory.

Figure (4.15) shows the effect of deleting the minor feedback loop at various values of time delay. The larger time delays cause the system to go unstable at higher values of



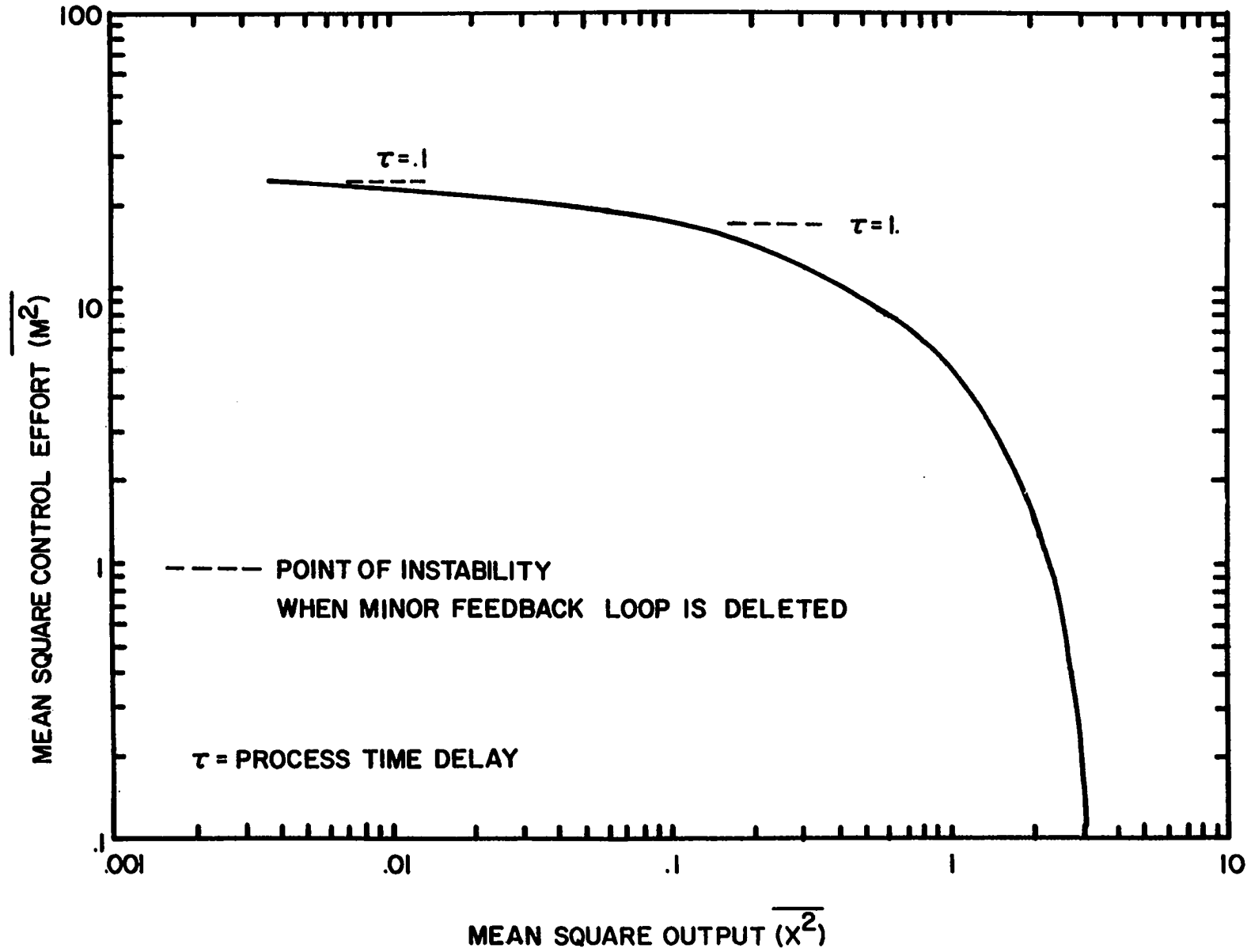


Figure 4-15. The performance diagram of a first order system showing the points of instability.

mean square output. The advantage of the performance chart over the root locus or Nyquist stability charts lies in the ability to show the degrees of attenuation that are possible before instability occurs. By adding the minor loop or at least a fractional part of the minor loop, increased attenuation for the same time delay is apparent.

It is interesting to investigate the effect of integral control action in the case of a process delay. The integral or floating controller is popular in the chemical process industry (B12). As in the previous case, the optimal controller specifies a minor feedback loop. This loop again causes the system to act like process with proportional and integral action with no delay time.

Without the minor loop the system can be unstable as discussed before. In fact, the point of instability on the mean square control versus mean square output occurs at the same point for each time delay. Therefore integral action does not provide any increased stability to the controlled system. The major function of integral control is to reduce the amount of control effort expended by the proportional controller.

Figure (4-16) shows the effect of various time delays on the mean square integral output. It is intuitive that the larger time delays should cause a decrease in the output attenuation. In order to maintain a given level of mean

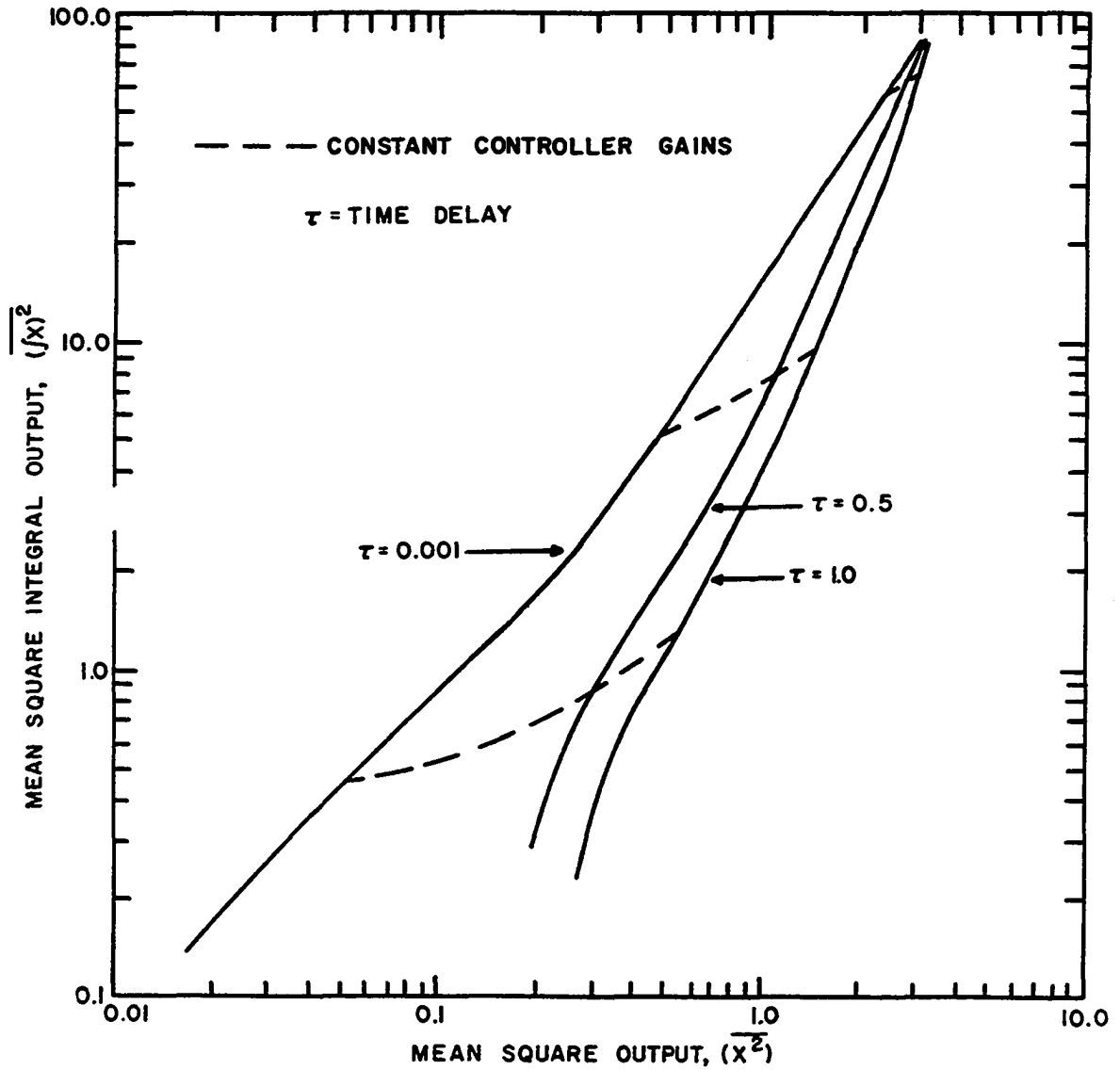


Figure 4-16.

The effect of time delay on the mean square output of a first order system using the same integral weighting factor.

square integral output for larger time delays, Figure (4-16) shows that larger controller gains are required. The spread in the curves as lower mean square integral outputs are derived shows that the larger delay times cause a more oscillatory behavior.

Model errors due to time delay fluctuations do not affect the controlled mean square output to the same extent as does error in the system gains. Figure (4-17) shows that the time delay sensitivity is not as important when the optimum controller containing the minor loop is used. However, if the minor loop is deleted then changes in the value of time delay can be vital, especially when the system is being operated close to the point of instability. Figure (4-18) shows how the point of instability is affected by time delay fluctuations. This chart can be used in a design procedure to estimate the attainable controlled output when an approximate error bound on the time delay is known. Time delay is a function of the vessel volume and flow rates, so any fluctuation or gradual change in these quantities will cause a change in the identified model time delay.

#### Effect of Control Delay

There are many instances in the operation of a process when a delay in the actuation of the control signal may occur. For example, a delay in implementation of the control signal

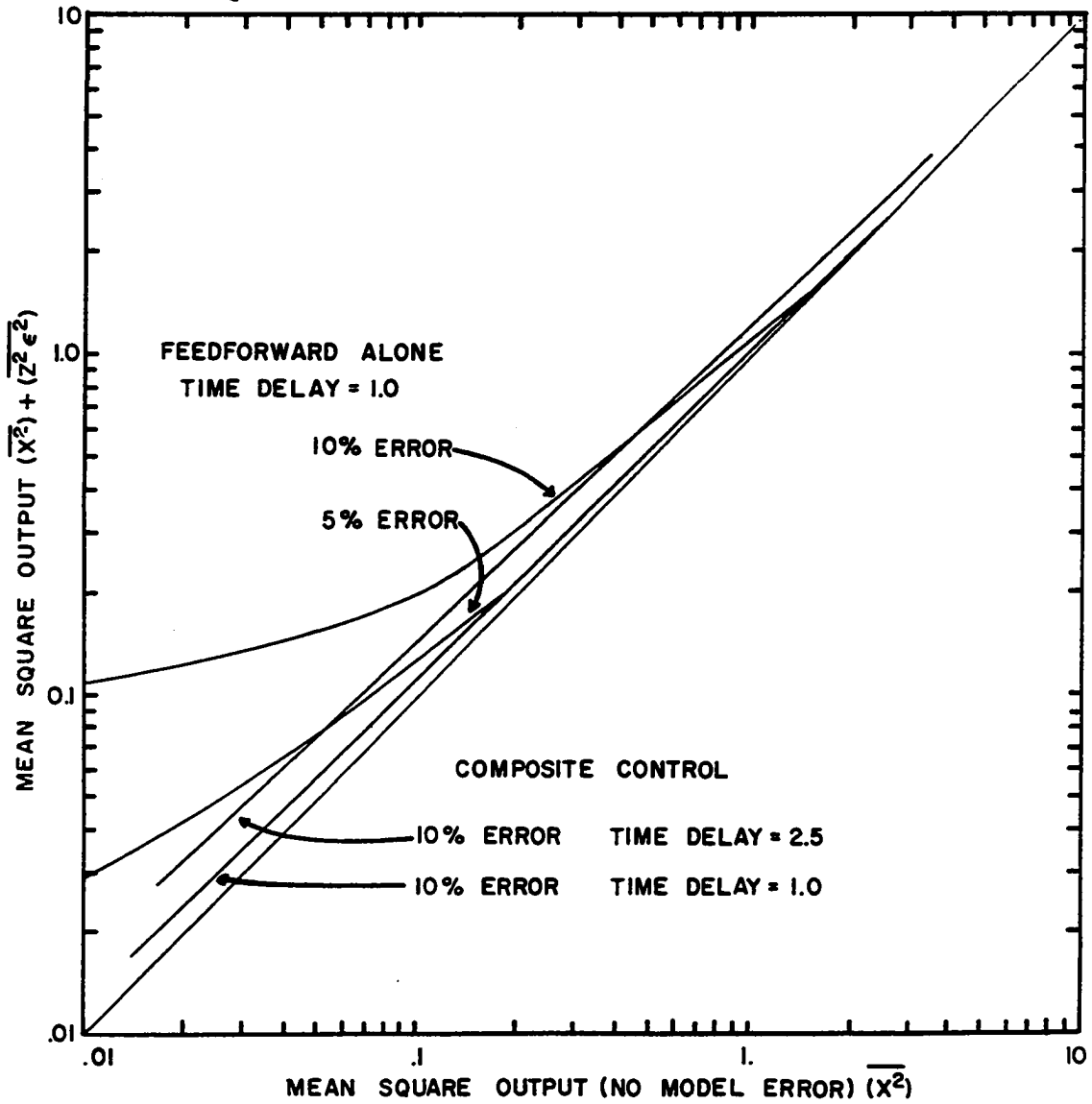


Figure 4-17. Sensitivity of a first order time delay system to errors in the value of the model time lag.

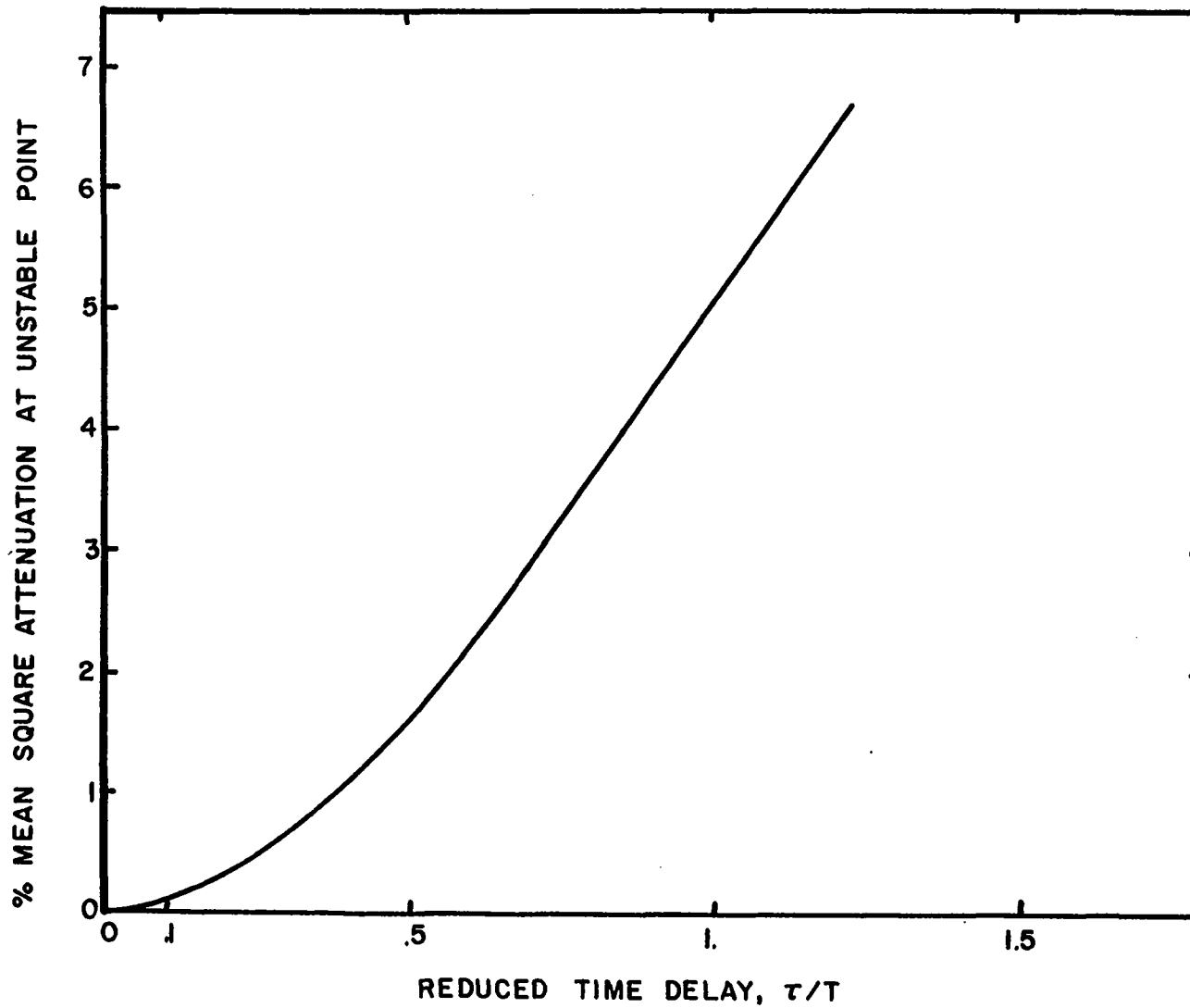


Figure 4-18. The influence of time delay on the point of instability which occurs when the minor feedback is deleted.

occurs in system where the manipulative variable is temperature. A finite time is usually required to furnish the desired amount of thermal energy and there is also a finite time required to heat the control fluid to the desired temperature. The underlying limitation is due to a finite maximum heating rate.

When some of the physical limitations of a process cause the control actuation to be noticeably delayed, then it becomes necessary to consider this delay in the model equations. Referring to Figure (4-1), the system under discussion occurs when  $\tau_1$  is negligible but  $\tau_2$  cannot be ignored. The transform representation of this system is

$$X(s) = P_M e^{-Ts} M(s) + P_D U(s) \quad (4.53)$$

The optimal control signal for this system is found from equation (3.23)

$$m^*(t) = Q_D u(t+\tau) - Q_C x(t+\tau) \quad (4.54)$$

This signal can never be obtained because it is physically impossible to measure the future value of the disturbance,  $u(t+\tau)$ . However, the statistical characterization of the disturbance is known, so an estimate of the probable future values of the disturbance can be made.

Solving the feedforward equation (3.22) for this system gives:

$$Q_D = - \frac{K_D}{K_M} \frac{\beta + \sqrt{\beta^2 + K_M^2 \Phi/\Psi}}{\alpha + \sqrt{\beta^2 + K_M^2 \Phi/\Psi}} e^{-\alpha\tau} \quad (4.55)$$

This equation is very similar to the feedforward function derived for the no time delay case which was expressed in equation (4.20).

The feedback term  $Q_C$  can be evaluated as previously shown from the matrix riccati equation (3.13)

$$Q_C = \frac{-\beta + \sqrt{\beta^2 + K_M^2 \Phi/\Psi}}{K_M} \quad (4.21)$$

The future value  $x(t+\tau)$  can be expressed as a function of the load and control variables with an impulse response relation, i.e. equation (2.19)

$$x(t+\tau) = \varphi(\tau) x(t) + \int_{t-\tau}^t \varphi(t-\mu) K_M m(\mu) d\mu + \int_t^{t+\tau} \varphi(t-\mu) K_D u(\mu) d\mu \quad (4.56)$$

Using the conditional mean expression, equation (2.10), an estimate of the future values of the load disturbance can be made.

$$x(t+\tau) = e^{-\beta\tau} x(t) + K_M \{e^{-\beta\tau} \bar{x}_m(t) - e^{-\beta\tau} e^{-(t-\tau)} \bar{x}_m(t-\tau)\} + K_D \frac{\{e^{(\beta-\alpha)\tau} - 1\}}{\beta-\alpha} u(t) \quad (4.57)$$



where  $\alpha$  = frequency of the load disturbance noise.

The symbol  $\star$ , denotes the convolution product of two functions

(N1). Combining equations (4.57) and (4.54),

$$\begin{aligned} m^*(t) = & Q_D u(t) - Q_C e^{-\beta\tau} x(t) - K_M Q_C \{e^{-\beta\tau} \star m(t) \\ & - e^{-\beta\tau} e^{-\beta(t-\tau)} \star m(t-\tau)\} - K_D Q_C \left\{ \frac{e^{(\beta-\alpha)\tau} - 1}{(\beta-\alpha)} \right\} u(t) \end{aligned} \quad (4.58)$$

Transforming this equation into the frequency domain and re-arranging

$$\vec{M}(s) = \vec{Q}_D U(s) - \vec{Q}_C X(s) \quad (4.59)$$

$$\vec{Q}_D = \frac{Q_D - K_D Q_C \left\{ \frac{e^{(\beta-\alpha)\tau} - 1}{\beta-\alpha} \right\}}{1 + P_M Q_C \{1 - e^{-\tau s} e^{-\beta\tau}\}} \quad (4.60)$$

$$\vec{Q}_C = \frac{Q_C e^{-\beta\tau}}{1 + P_M Q_C (1 - e^{-\tau s} e^{-\beta\tau})} \quad (4.61)$$

Figure (4-14) shows how these equations can be simulated with the aid of block diagram algebra. In Figure (4-19), the performance diagram for this system is shown for various values of delay time. Notice that the size of the time delay limits the amount of output attenuation that can be obtained. Intuitively, this result is reasonable, since processes can not be controlled if the control action takes place too late to compensate for the disturbance.

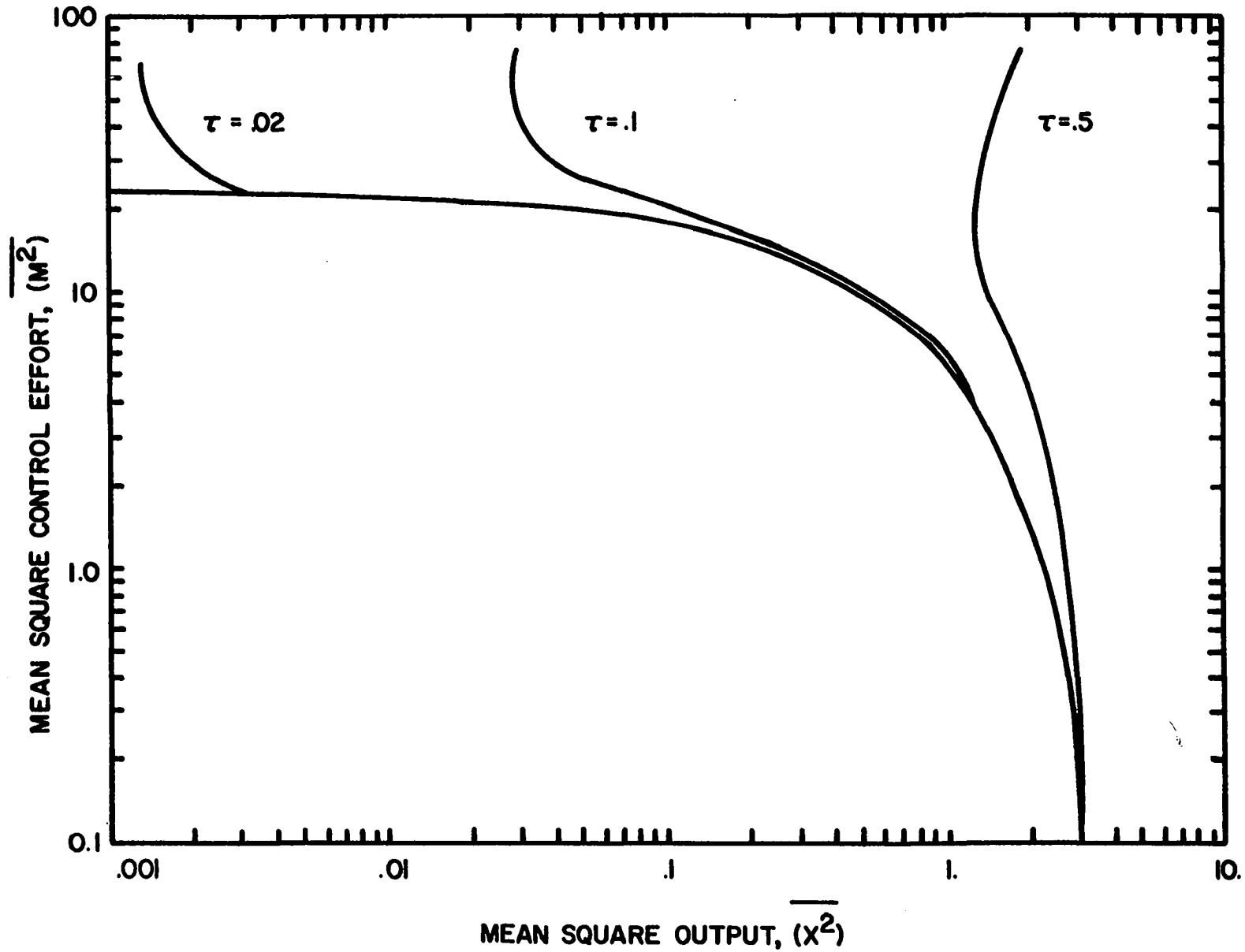


Figure 4-19. The effect of control time delay on the performance diagram of a first order system.

It is interesting to note the form of the feedforward controller. In order to reduce the algebraic detail, consider the case where the time delay is rather large. By rearranging equation (4.58) and using the definition of  $P_M$  presented in equation (4.6), a one-pole, one-zero controller results.

$$\bar{Q}_D = \frac{Q_D - K_D Q_C \left\{ \frac{e^{(\beta-\alpha)\tau} - 1}{\beta - \alpha} \right\}}{\beta + K_M Q_C} \cdot \frac{s + \beta}{\left\{ \frac{1}{\beta + K_M Q_C} \right\} s + 1} \quad (4.62)$$

As a higher penalty (increased weighting factor) is placed in the output variable, it has been previously shown in equation (4.25) that  $Q_C$  approaches infinity. Therefore, the feedforward controller shown above approaches a differentiating predictor of the form:

$$\bar{Q}_D = K(s + \beta) \quad (4.63)$$

Then the overall controlled system transfer function would be zero order rather than first order. The mean square value of this system would increase without bound in the attempt to achieve control (F1).

This same type of differentiating predictor controller was observed by Luecke (L4), but his frequency domain approach does not allow the prediction of the controller parameters from the weighting function and system parameters. Therefore,

Luecke was only able to observe the overall predictor feed-forward controller by repeating his calculational procedure for various values of the weighting factor.

## CHAPTER V

### EXPERIMENTAL STUDIES

The purpose of this chapter is to show how the previous optimal controller design procedures can be applied to a physical system. Although the physical apparatus used is not a familiar piece of chemical plant equipment, it possesses a number of features common to process equipment.

The laboratory process is a stirred tank jacketed vessel with hot and cold fluids entering the center and the annulus respectively. This process serves as a good test because it contains many of the little unknown disturbances of process equipment. Steady state drift, heat loss, measurement error and noise, instrumentation dead band, valve hysteresis, and controller delay due to pneumatic air lines are among the problems beset a plant engineer in his quest to obtain control over actual chemical processes. These effects were reduced as much as possible but certainly not entirely. In fact, if all these problems did not arise, then our objective to show how the controller design can be applied to a physical process would not be valid.

### Experimental Description

The physical apparatus described herein is located in the Process Control Laboratory in the Engineering Center of the University of Oklahoma. It was originally assembled in the late 1950's. Several previous doctoral dissertations were concerned with various aspects of this equipment. Both identification (B6,F1,S1,S4) and control (H2,L4) were investigated. Though many changes evolved over the years, the last two investigators (L4,S1) used the same configuration. In particular, the most recent investigator gives an exhaustive equipment description. For this reason only the basic equipment and recent modifications are discussed here. The overall process flow chart is shown in Figure 5-1.

The heart of the process is the simulated reactor or heat exchanger shown in Figure (5-2). Type metal was used for the wall for its heat transfer properties. Seven thermocouples were located at 3/4 inch spacing and were imbedded in the metal wall. These thermocouples were connected in parallel to give an average wall temperature. Hot oil (approximately 175°) entered the reactor through the bottom and was stirred by a 1/10 horsepower 1800 rpm motor. The coolant, Dow Chemical's industrial grade ethylene glycol, entered the bottom of the reactor through a series of perforations in the lucite and plates.

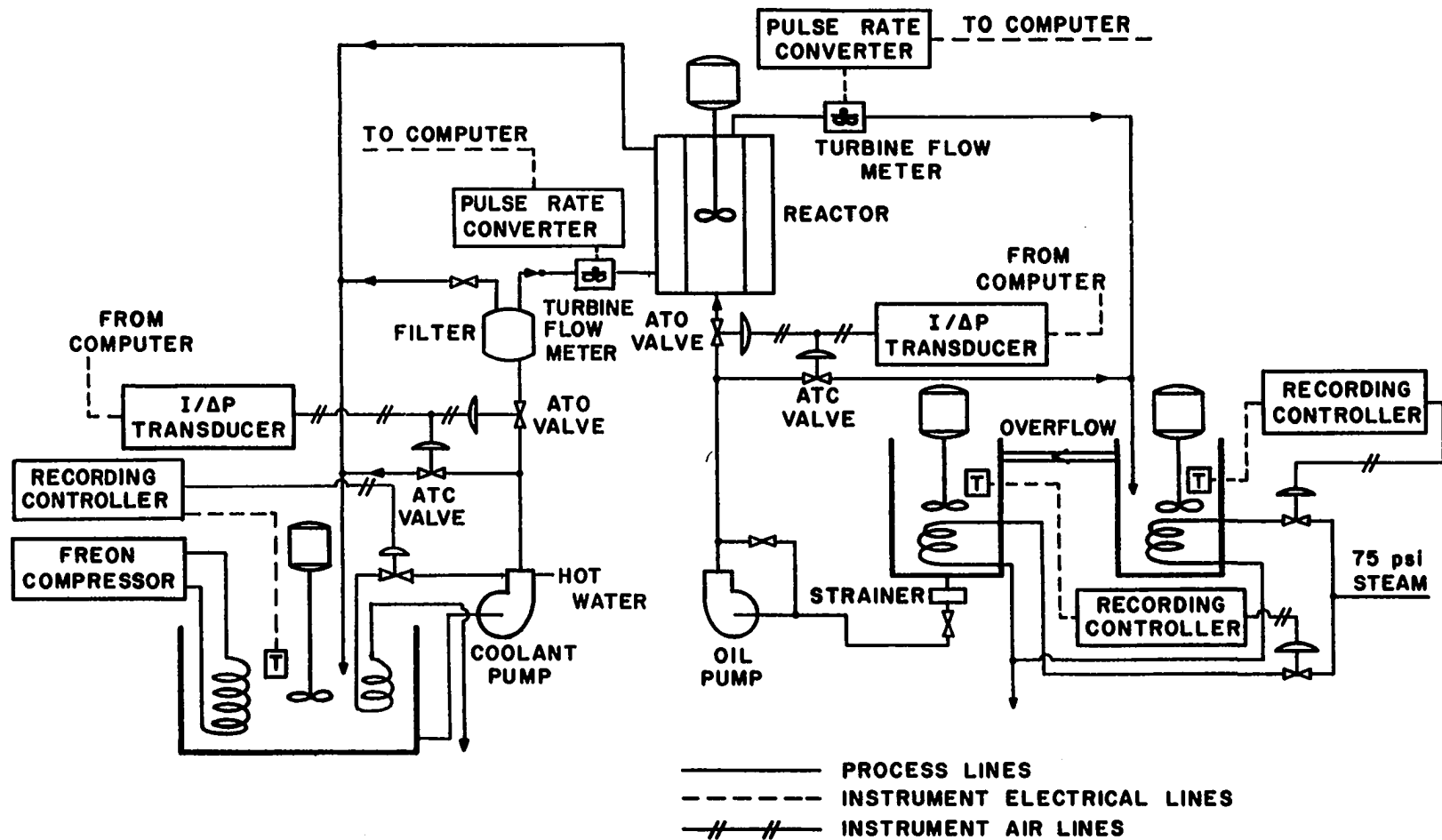


Figure 5-1. Schematic flow sheet of experimental system.

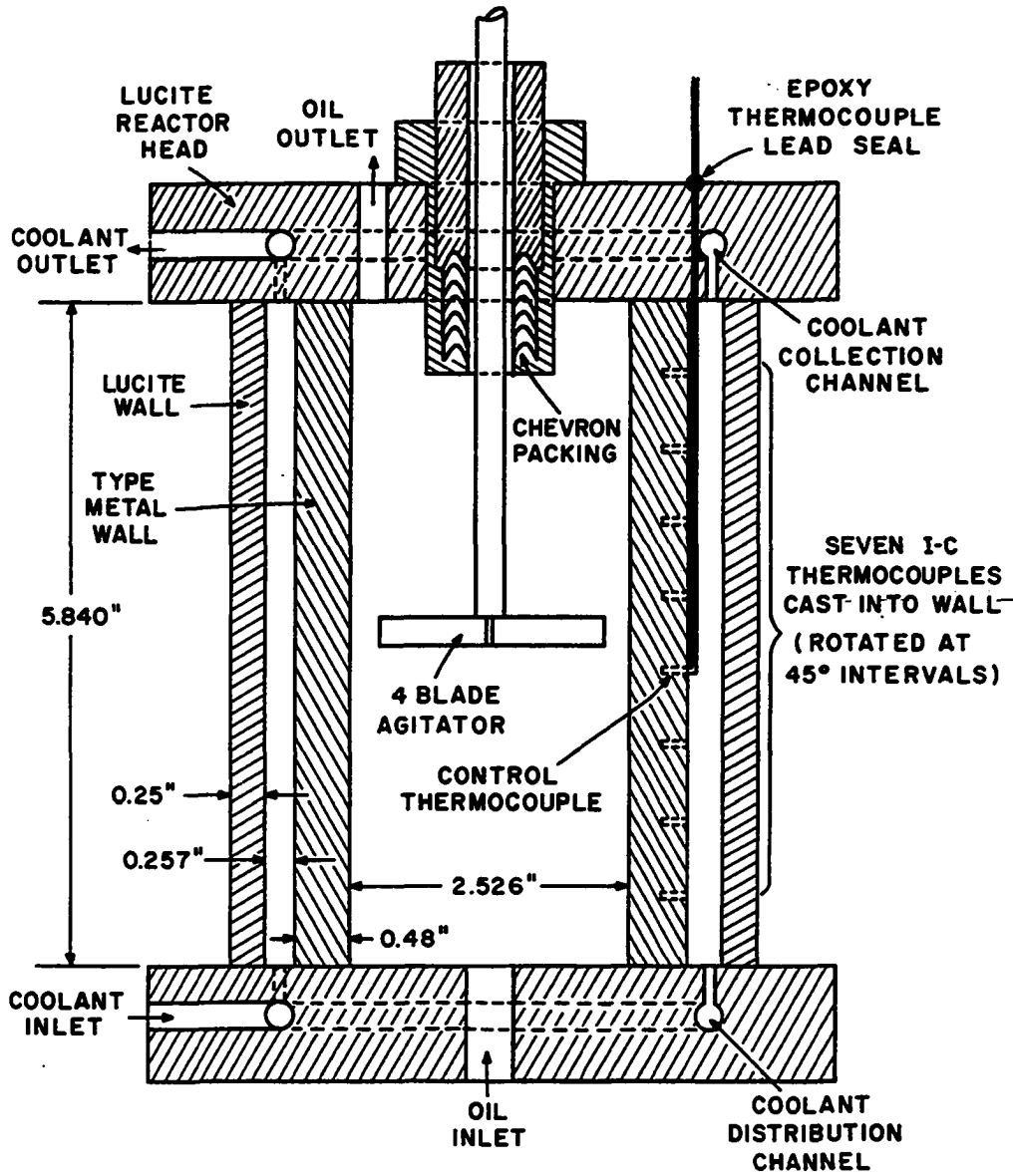


Figure 5-2. Detail of reactor.



### Temperature Baths

The temperature of the turbine oil was maintained at a given level in two 30 gallon tanks, each independently controlled. High pressure steam was used as the controlling heat source. Control was provided by Brown Electronic recording-controlling pyrometers. These instruments operated pneumatic Research Control valves on the steam lines. By using the tanks in series the oil temperature was maintained within  $\pm 0.25^{\circ}\text{F}$ .

The ethylene glycol was maintained at a specified temperature in a 25 gallon plexiglass tank. A  $1\frac{1}{2}$  ton Freon-12 compressor with evaporator coil in the tank provided the cooling. Another Brown Electronic controller was used to control the temperature. The controlling media was hot water flowing through a set of heat exchange coils within the coolant bath.

### Flow System

Both the coolant and oil were circulated by Gould  $\frac{1}{2}$  inch helical gear pumps driven by  $\frac{3}{4}$  horsepower electric motors. The operating pressures at the pump outlets were the same at approximately 30 psi.

The flow through the pumps had to remain nearly constant so that the control valves would operate in the linear range. This was accomplished through the use of a reactor bypass arrangement. The flow in each stream was divided so

that the fluid passed through a control valve back into the temperature bath. All four valves were Research Controls, type 75B, with G trims. The pneumatic signal to these valves was generated by Taylor Transet electro-pneumatic controllers with an output range of 3-15 psi and an input range of  $\pm 100$  volts. The electrical signals were transmitted through coaxial cable from their origination on the Donner analog computer.

The oil flow rate was measured by a Waugh, type GFLS, turbine meter and its corresponding Waugh pulse rate converter. The output of the pulse rate converter was 0-200 millivolts which made it necessary to provide amplification on the analog computer. A proportional-integral controller was constructed on the analog computer to control the flow rate (Figure 5-3). This was necessary primarily to overcome the very noticeable hysteresis in the control valves.

The coolant flow rate was measured with a Fisher-Porter type 10CI505 turbine meter. The AC signal from the meter was introduced into a custom made pulse rate converter. This converter was made by Dr. R. A. Sims in the Process Dynamics and Control Laboratory at the University of Oklahoma, and has an output range of 0-1 volts. A similar controller, shown in Figure (5-4), was constructed for the coolant flow system.

#### Temperature Measurement

The output voltage of the thermocouples in the reactor were amplified with a Sanborn, Model 350-1500, low level DC

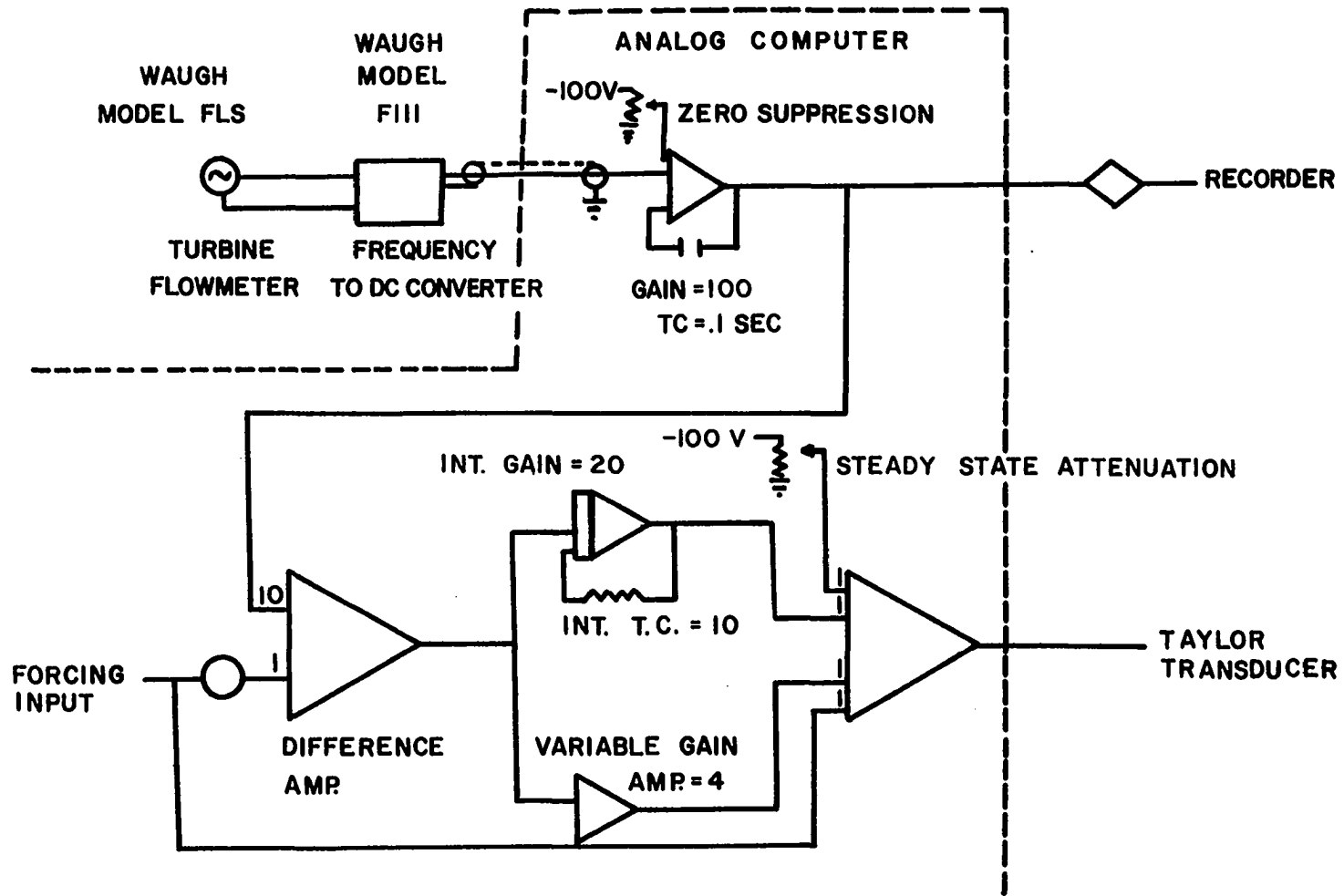


Figure 5-3. Oil flow control system.

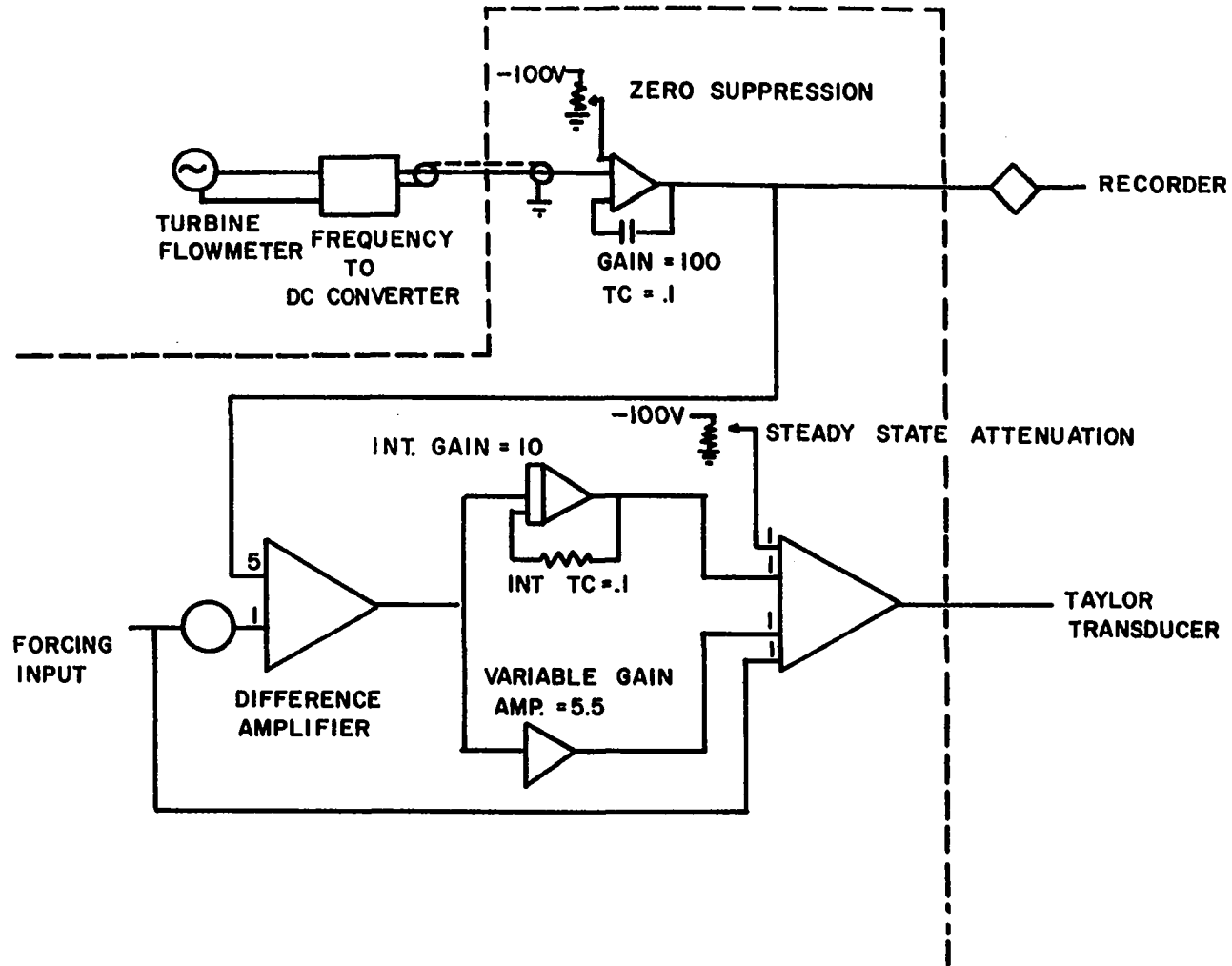


Figure 5-4. Coolant flow control system.

preamplifier with a Model 350-2 plug-in unit. A gain of 500 and input suppression of 5 millivolts were used. Figure (5-5) shows the configuration of temperature measuring equipment.

#### Analog Equipment

The overall process controllers were constructed on the Donner, Model 3400, analog computer (B6). Model identification data was recorded on the analog to digital converter which consisted mainly of a Dymec digital voltmeter and scanner coupled with a Hewlett Packard line printer.

The system load disturbance was generated by a custom built signal generator. At intervals, as determined by an adjustable time base, the output voltage was electronically switched. The resulting output was a constant square wave signal with random sign changes. The desired spectral density of the load disturbance was obtained by filtering the noise generator output. The final filtered noise had a frequency of about 1.5 radians per minute (14). This was chosen because the system time constants are in this range.

#### Dynamic Mathematical Model

Appendix G presents a derivation of the theoretical linear mathematical model of this system. This model is not accurate because of its inherent limitation as an approximation to a nonlinear model. Inaccurate or changing parameters, such as, heat transfer coefficients and physical

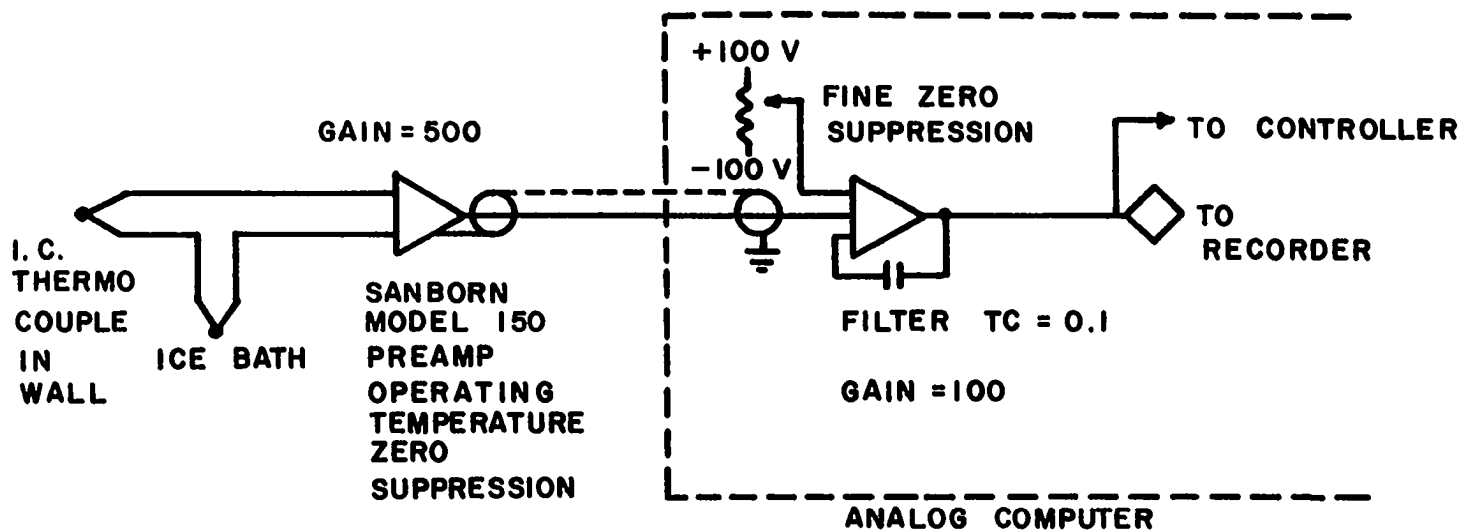


Figure 5-5. Wall temperature measuring system.

properties, are the probable causes of the model deficiencies.

An experimental identification technique developed by Heymann (H5) and Sims (S1) at the University of Oklahoma Process Dynamics and Control Laboratory was used to obtain a system transfer function. Simulation tests of the model on the analog computer were carried out to make adjustments to some of the parameters of this model. The final transfer function model of the experimental system is

$$X(s) = \frac{1.87 U(s) - 0.418(s + 2.76) M(s)}{(s + 1.41 + 1.24i)(s + 1.41 - 1.24i)} \quad (5.1)$$

where  $s$  = frequency in radians per minute

$X(s)$  = wall temperature in volts (frequency domain)

$U(s)$  = oil flow rate in volts (frequency domain)

$M(s)$  = coolant flow rate in volts (frequency domain)

The model is shown in the form which is most useful for control purposes. Various scale factors within the system must be used if one wishes a transfer function in units more common to the variables (temperature in degrees, flow rates in lbs/min.). This transfer function includes the dynamics of the value control system and the measure devices, so these factors do not have to be considered in arriving at an overall transfer function.

Figure (5-6) shows the responses of the system and the model to a unit step in coolant flow rate. Notice that there

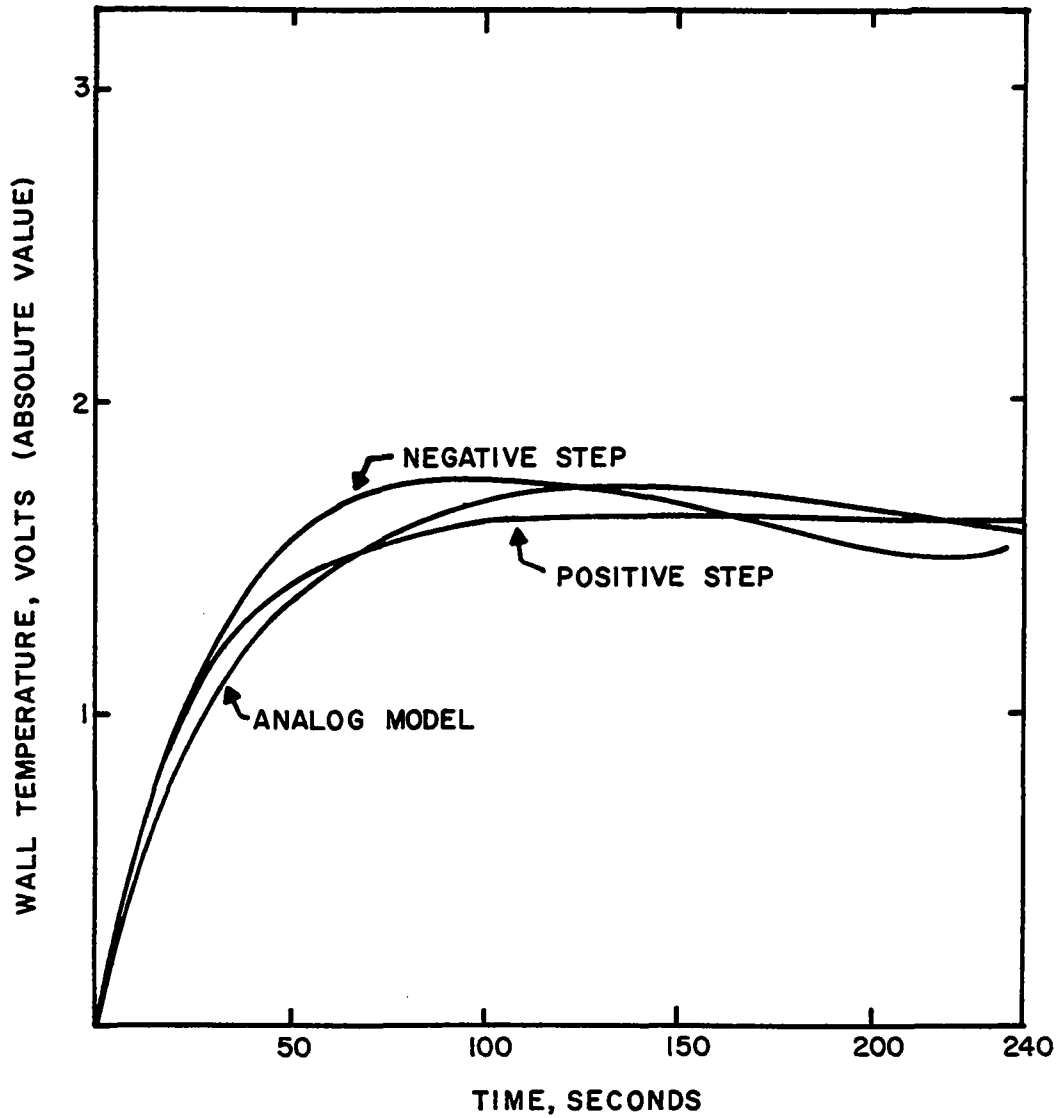


Figure 5-6. Response of the wall temperature of the experimental system and the model to a step change in coolant flow rate.



is a difference in the system response to a unit step of equal magnitude but opposite sign. This is due to the non-linear product term in the dynamic model which can not be included in a transfer function representation. Figure (5-7) shows the responses to a unit step in oil flow rate. The product non-linearity exerts much more influence on the dynamic response of the oil side.

The initial slope of the model response is slightly smaller than the system responses. The system was given a unit step forcing on the analog computer, but the valves do not follow a forcing signal. The slightly underdamped flow control system responded to give an initially higher flow before it settled down to the steady state value of the imposed unit step input.

#### Controller Results

Figure (5-8) shows the control effort-system output relationship for the transfer function given in equation (5.1) as calculated from the computer programs listed in Appendix I. The stars on the diagram indicate controllers which were constructed to test their performance under process conditions. A transfer function representation of these controllers is given in Table (5.1). These functions were the controller as programmed on the Donner analog computer.

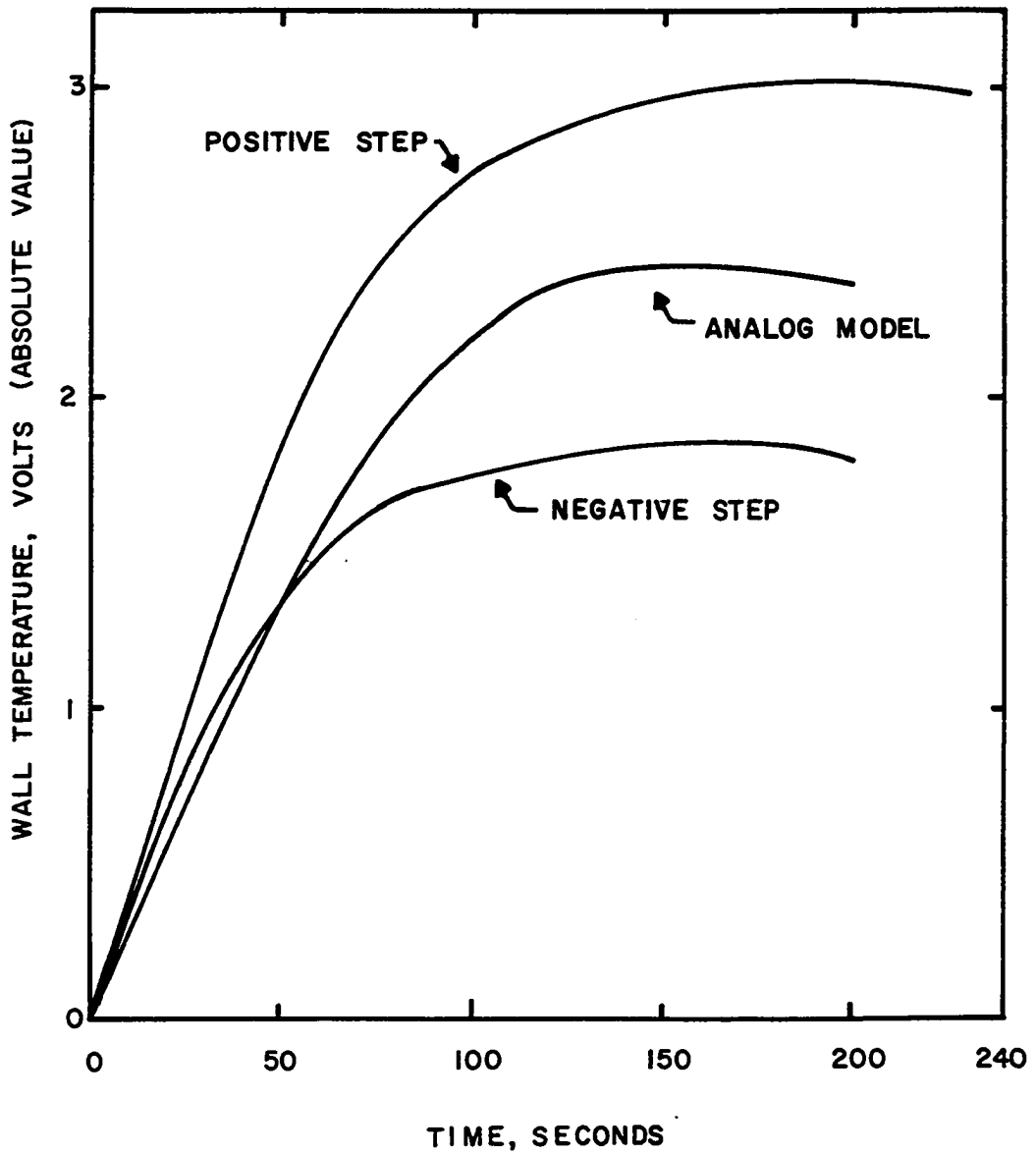


Figure 5-7. Response of the wall temperature of the experimental system and the model to a step change oil flow rate.

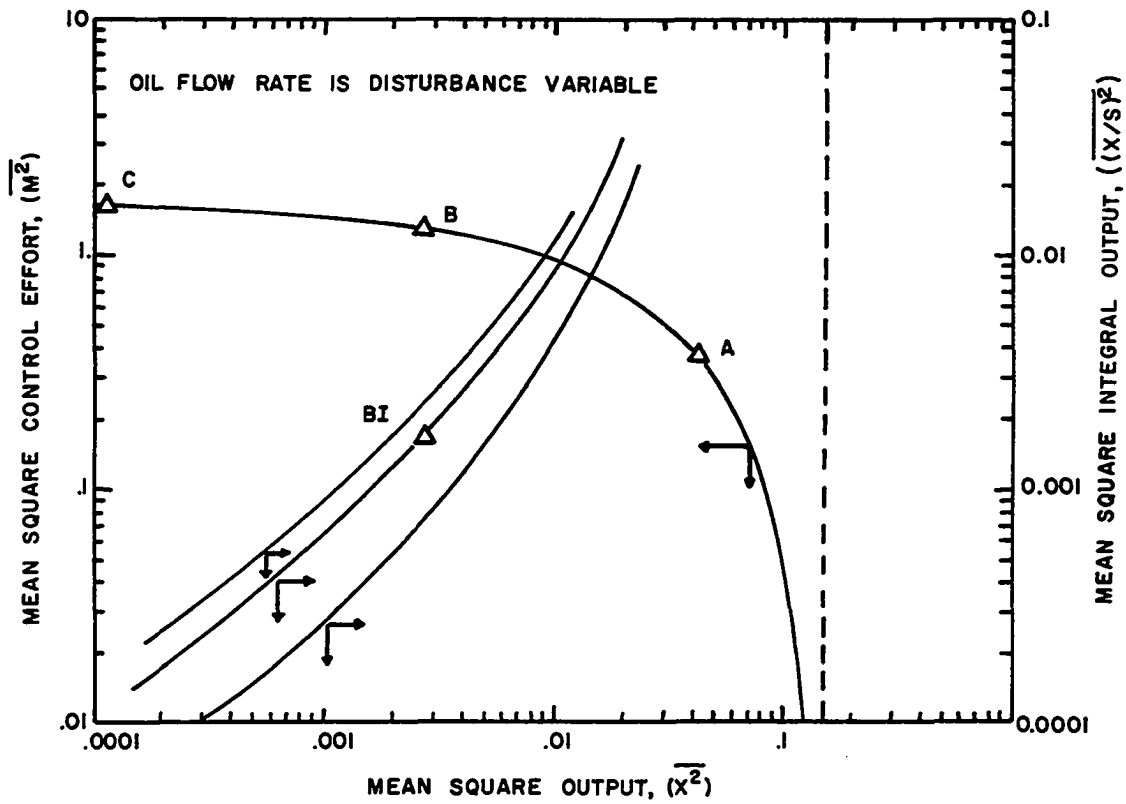


Figure 5-8. Performance diagram of the experimental system model with coolant flowrate as manipulative variable

Table 5.1

Controller	Feedforward	Feedback
A	$Q_D = \frac{0.947}{s+2.76}$	$Q_C = \frac{1.31 (s+3.39)}{s+2.76}$
B	$Q_D = \frac{2.55}{s+2.76}$	$Q_C = \frac{(5.41) (s+4.40)}{s + 2.76}$
BI	$Q_D = \frac{2.55}{s+2.76}$	$Q_C = \frac{4.04 (s+4.3 + 7.3/s)}{s + 2.76}$
C	$Q_D = \frac{3.68}{s+2.76}$	$Q_C = \frac{13.9 (s + 6.54)}{s + 2.76}$
Ideal Feedforward	$Q_D = \frac{4.47}{s+2.76}$	_____

Time base is in minutes

The uncontrolled open loop system output without the random forcing is shown in Figure (5-9). This system is rather stable with small steady-state fluctuations. Imposing the random disturbance causes a slow fluctuation in wall temperature. The third section of Figure (5-9) shows the response after application of the ideal feedforward controller. This response is to be used as a standard of comparison with the calculated optimal controllers. Notice that when coolant saturation occurs there is a loss of ability to control the system with the ideal feedforward controller. This loss of control is expected since ideal feedforward requires maximum control effort which thereby increases the chances of control signal saturation.

Figure (5-10) shows the typical response trajectories of the experimental system when the optimal controllers are applied. Optimal controller "A" is not particularly effective because it was chosen close to the point of no control on the performance diagram. As optimal "B" specified more control effort, further attenuation of the output response results. However, the control signal, coolant flow rate, is operating at its saturation level in some instances. This saturation again causes a reduction in ability to control.

By adding an integral constraint, integral control action is specified. The optimal controller labeled "BI" is better than its proportional counterpart, controller "B", because of the absence of control signal saturation. This reduction in

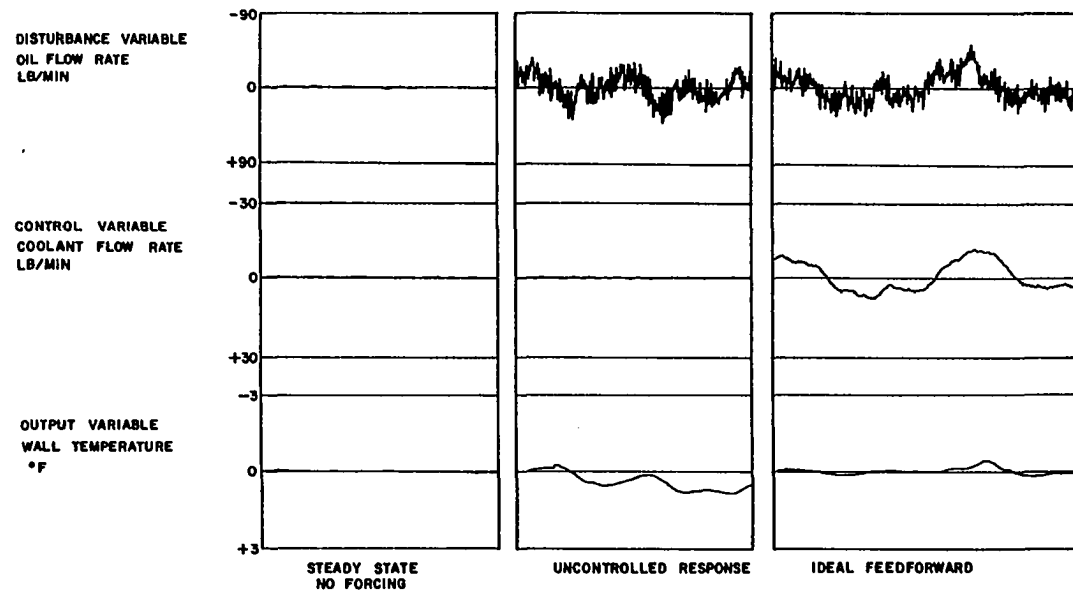


Figure 5-9. Response of experimental system to disturbances in oil flowrate.

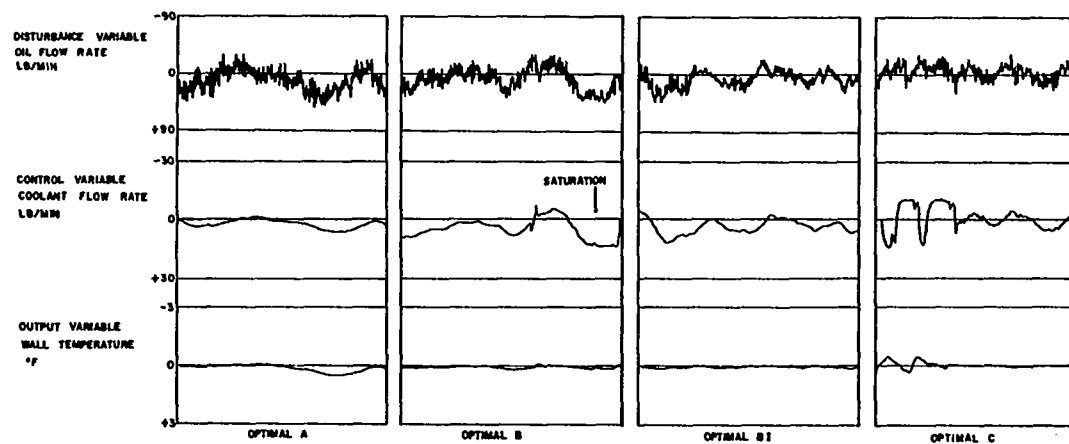


Figure 5-10. Response of optimally controlled experimental system to disturbances in oil flow rate.

saturation is a direct result of the fact that the proportional integral controller specifies less proportional gain to attain the same level of attenuation.

Optimal "C" was selected from the performance diagram to use the most control effort. Some saturation of the control caused this controller to be only slightly better than the proportional-integral controller, "BI". Part of this output response shows the effect of controller start-up. Initiation of control action to an uncontrolled system is a servomechanism problem and was not the subject of this investigation. However, the result shows vividly that the optimal regulator controllers would not do a good job in start-up operations. Therefore, one must be careful in the distinction between servo and regulator problems--the same type of controllers are not used for both types of control.

It would be valuable to calculate the mean square output of these controlled systems and compare the results with the calculated values on the performance diagram. Unfortunately a mean square calculation on the analog computer is very difficult to obtain. Multiplication and division of signals over a rather long period of time are required to calculate a mean square value. These operations coupled with the long sampling period usually cause amplifier voltage saturation. This type of calculation can only be successfully applied to high frequency signals where the sample period is rather short.



A technique of comparing controller performance on the analog computer is to use the integrated absolute value ratio.

$$\text{controller efficiency} = 1 - \frac{\left( \int \frac{|x| dt}{|u| dt} \right) \text{ controlled}}{\left( \int \frac{|x| dt}{|u| dt} \right) \text{ uncontrolled}}$$

Table (5-2) presents the controller efficiency comparison of the previously discussed controller configurations. Included in this table is the result for the ideal feedforward controller.

The system was also investigated with the opposite configuration where the disturbance was the coolant flow rate and the manipulative variable was the oil flow rate. This system reacts differently to the former oil-disturbed experiment. Figure (5-11) shows the performance chart for this configuration. The points on the diagram marked with triangles were investigated by simulation of their corresponding optimal controllers. The controller transfer functions are listed in Table (5.3).

Notice that all of the optimal controllers are predictive in that the numerator is of higher order than the denominator. This results from the system reaction to coolant disturbances. Since the coolant flow rate has a quicker effect on the value of the output variable, the oil flow rate must have some prediction included in the control equation in order to have any chance to counteract the coolant disturbance.

Table 5.2

Type of Controller	Controller Efficiency $1 - \frac{\left( \frac{\int  x  dt}{\int  u  dt} \right) \text{ (controlled)}}{\left( \frac{\int  x  dt}{\int  u  dt} \right) \text{ (uncontrolled)}}$
optimal A	0.66
optimal B	0.85
optimal BI	0.91
optimal C	0.94
Ideal Feedforward	0.89

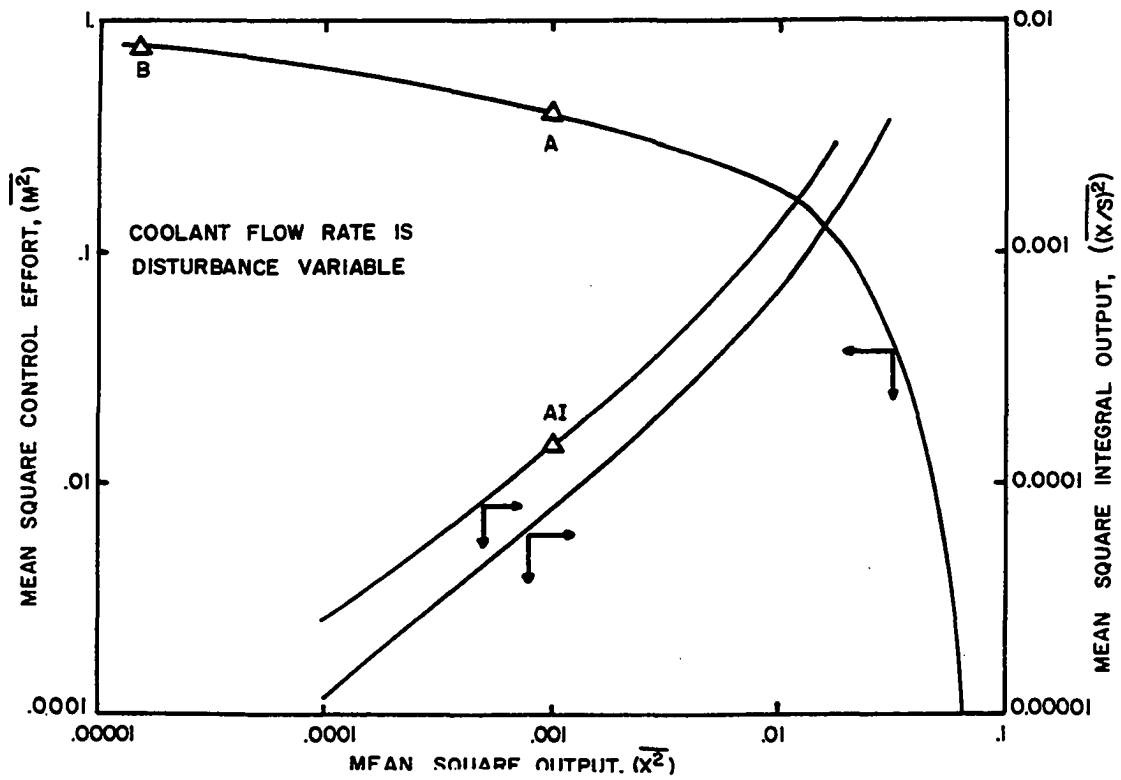


Figure 5-11. Performance diagram of the experimental system model with oil flow rate as manipulative variable.

Table 5.3

Controller	Feedforward	Feedback
A	$Q_D = 0.124s + 0.849$	$Q_C = 0.796s + 5.4$
AI	$Q_D = 0.124s + 0.849$	$Q_C = 0.71s + 412 + \frac{6.4}{s}$
B	$Q_D = 0.194s + 0.715$	$Q_C = 3.8s + 29.2$
Ideal Feedforward	$Q_D = 0.224s + 0.618$	_____

Figure (5-12) shows the typical output response trajectories of this system. Optimal controller "A" provides some output attenuation but the control variable, oil flow rate, operated almost as a bang-bang controller. The proportional-integral controller, labeled "AI", does a similar job of output attenuation. However, the big advantage in this controller is its specification of lower predictive and proportional gains. Then the control signal from the oil flow rate does not change as rapidly as before. Optimal controller "B" causes further attenuation but at the expense of wildly varying control signals. Ideal feedforward could not be simulated on the analog because the gains caused amplifier saturation.

None of these controllers seem to perform as well as they should. The main reason for reduced performance is the well-known (B.12) velocity-limitation of control valves. The valve stems do not travel fast enough in response to a rapidly changing signal. Therefore a constraint not included in the optimization equations limits the amount of attenuation that can be attained.

In order to put a constraint on the velocity (first derivative) of the control signal, the first derivative must appear in the transfer function. Equation (5.1) shows that the system output is not a function of the first derivative of the oil flow rate. The absence of this derivative term does not mean that this dependence does not exist. A zero

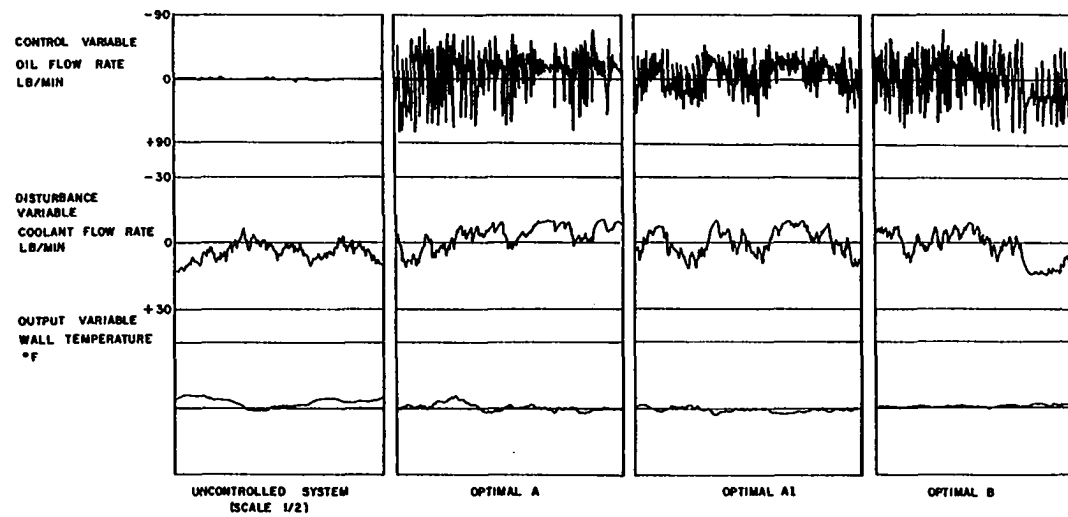


Figure 5-12. Response of experimental system to disturbances in coolant flow rate.

of the complete transfer function may have been cancelled by a comparable system pole. Kalman (K1) has shown that a system which contains a pole and zero which cancel each other is not completely controllable. If the cancelled pole and zero were known, they could not be used in the optimal control design procedure. Kalman (K1) has shown that the matrix riccati equation used to calculate the feedback gain matrix is asymptotically stable and approaches a unique steady-state if the system is completely controllable. If the system is not controllable, the infinite-interval approximation used in Chapter III is no longer valid and the inclusion of cancelling poles and zeros would render the optimal control equations unsolvable.

If a process design engineer is confronted with the problem of absence of complete controllability, the most practical solution is to redesign the process. Physical characteristics of the process, such as flow rates, heat transfer area, and steady state operating level could be modified so that the system dynamics become more favorable for the application of practical controllers.

The controller equations from this time domain method of formulating optimal control are much simpler than those specified by frequency methods. The following control equation was obtained by Luecke (L5) for a similar transfer function. Only the feedforward portion is reproduced here.

$$Q_D = \frac{Q_{DN} \frac{T_D Q_C}{Q_{DN}} - T_C}{1 - T_C Q_{CN}}$$

where

$$Q_{DN} = \frac{(1 + 0.33S)}{(1 + 1.33S)}$$

$$T_D = -0.991 \frac{(1 + 0.035S)(1 + 0.120S)(1 + 0.33S)}{(1 + 0.029S)(1 + 0.083S)(S + 1.68)(1 + 1.38S)}$$

$$T_C = \frac{0.558(1 + 0.76S + 0.158S^2)}{(1 + 0.033S)(1 + 0.496S)(1 + 0.366S + 0.0375S^2)}$$

$$Q_{CN} = \frac{(1 + 1.38S)(1.68 + S)}{(1 + 1.33S)}$$

One can see that this optimal controller would not be easy to simulate. Therefore, the simple controller equations listed in Tables (5.1) and (5.3) are far superior for practical realization. The time domain approach for optimal controllers can be calculated once a completely general program is available. This program would be useful in selecting the range of practical controllability at the design stage of plant development.



## CHAPTER VI

### ANALOG COMPUTER SIMULATIONS

Many chemical process units, such as distillation columns and double pipe heat exchangers, exhibit third order dynamics. A theoretical energy balance of the experimental apparatus discussed in Chapter V shows the dynamics to contain three poles for both the oil side and the coolant side. However the model identification technique (H5,S1) shows that a second order transfer function is an adequate representation.

One of the initial objections was to examine the effect on control objectives by using a first order transfer function with a time lag to approximate third order dynamics. Figure (6.1) shows typical unit step response trajectories for first and third order systems. In most physical apparatus there is a finite level at which the response is first detected. Measurement equipment has a lower sensitivity bound below which no signal is detected or the process itself may be noisy. In any case, it can be seen from this graph that the approximation of the third order by a first order plus a time lag function may be within the limits of required accuracy.

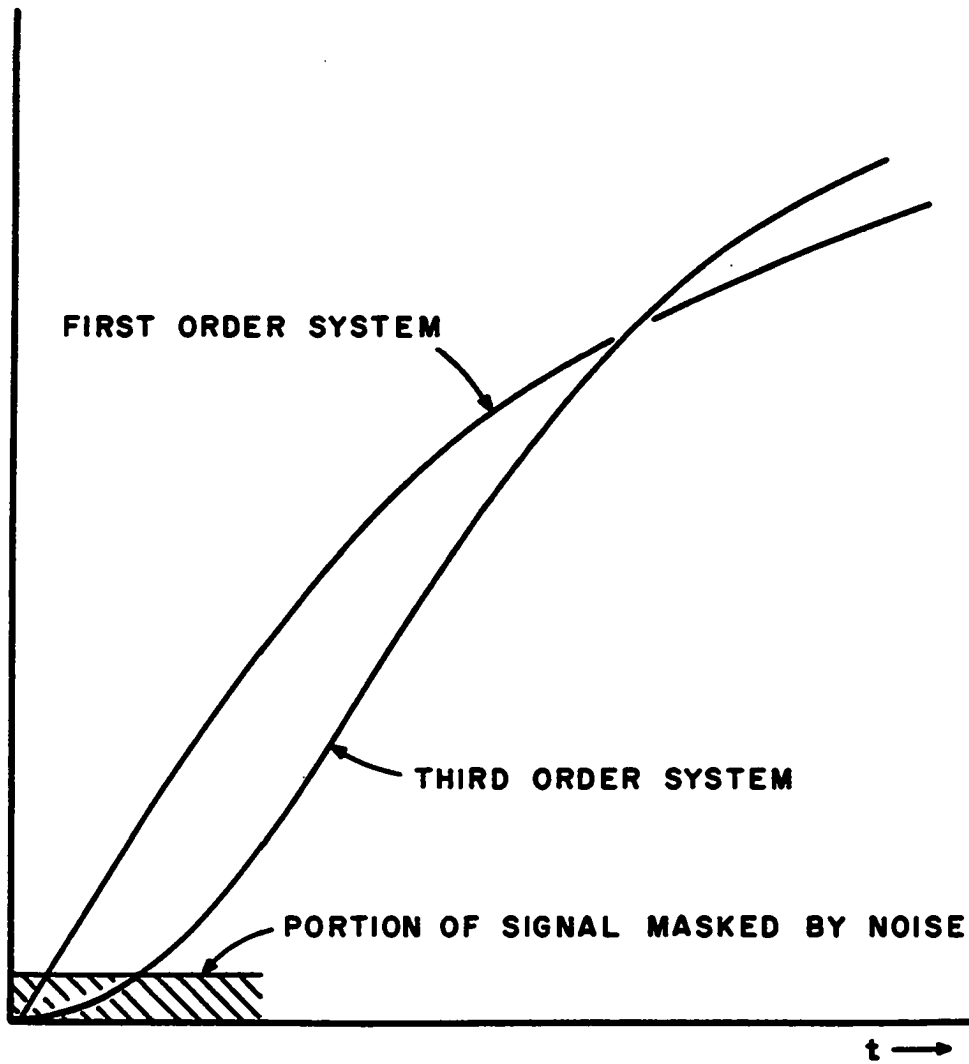


Figure 6-1.

A comparison of the unit step response trajectories of 1st and 3rd order systems.

Third Order Model

The theoretical transfer function of the experimental heat exchange process was modeled on the analog computer. The analog flow diagram is shown in Figure (6.2). The transfer function is

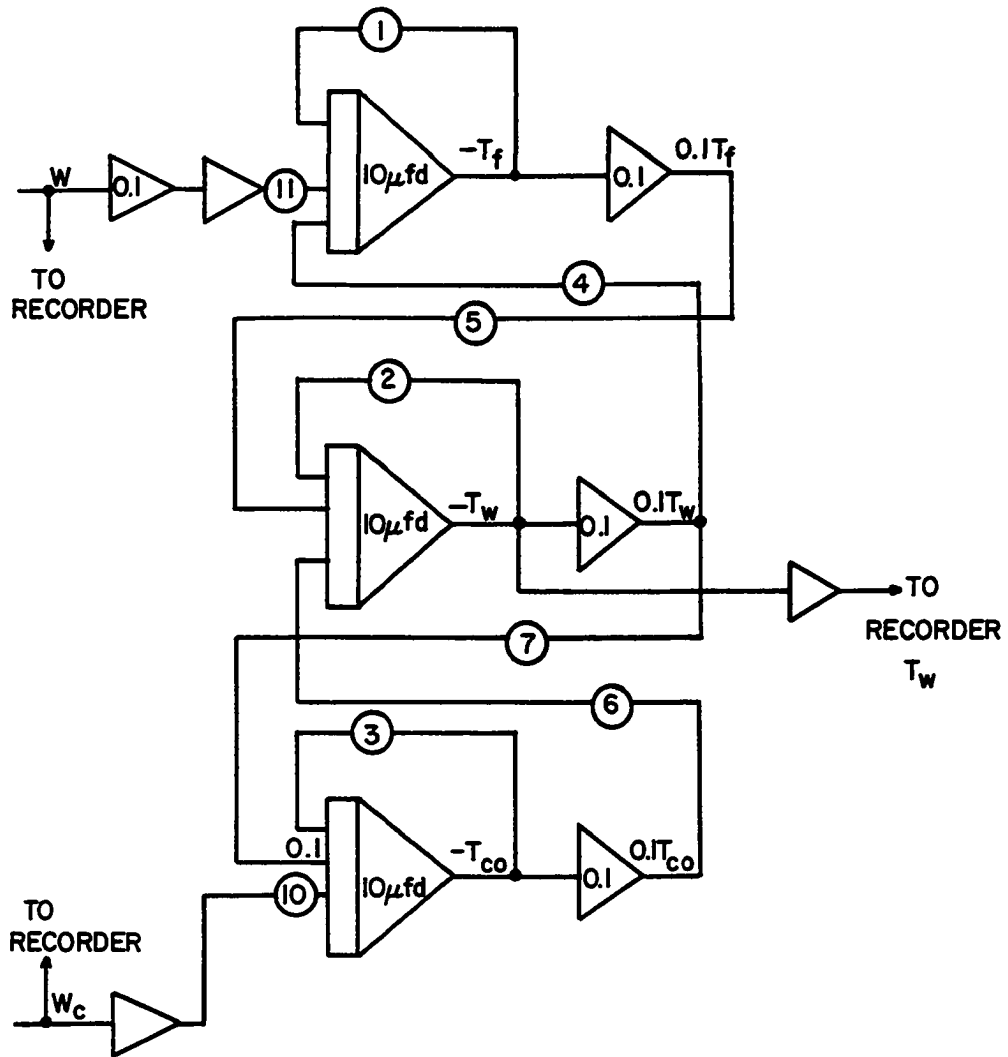
$$X(s) = \frac{(0.156)(s + 0.329)W - 0.207(s + 0.569)W_c}{(s + 0.117)(s + 0.45)(s + 0.583)} \quad (6.1)$$

Using the cancellation methods of Luecke, McGuire, and Crosser (L5), the following approximation was made.

$$X(s) = \frac{0.195 e^{1.0s} W - 0.449 e^{1.5s} W_c}{(s + 0.117)} \quad (6.2)$$

A performance diagram was calculated for each of these transfer functions and they are shown in Figure (6.3). The breakaway line indicates the point of instability when the minor loop is deleted. For this discussion the coolant flow rate,  $W_c$ , was chosen as the load disturbance.

Table (6.1) shows the controller transfer functions corresponding to the indicated stars on the performance chart. These controllers were constructed on the analog computer. The exponential in the minor feedback loop of the first order model was approximated by a third order Pade expansion. Although the first order controller equations appear complex, they are readily simulated if a block diagram, such as Figure (4.16), is formulated.



## COEFFICIENT POTENTIOMETERS

1. 0.569	4. 0.6	7. 0.273
2. 0.252	5. 0.532	8. 0.208
3. 0.329	6. 0.994	9. 0.293

Figure 6-2.

Analog computer circuit for simulation of the experimental transfer function.

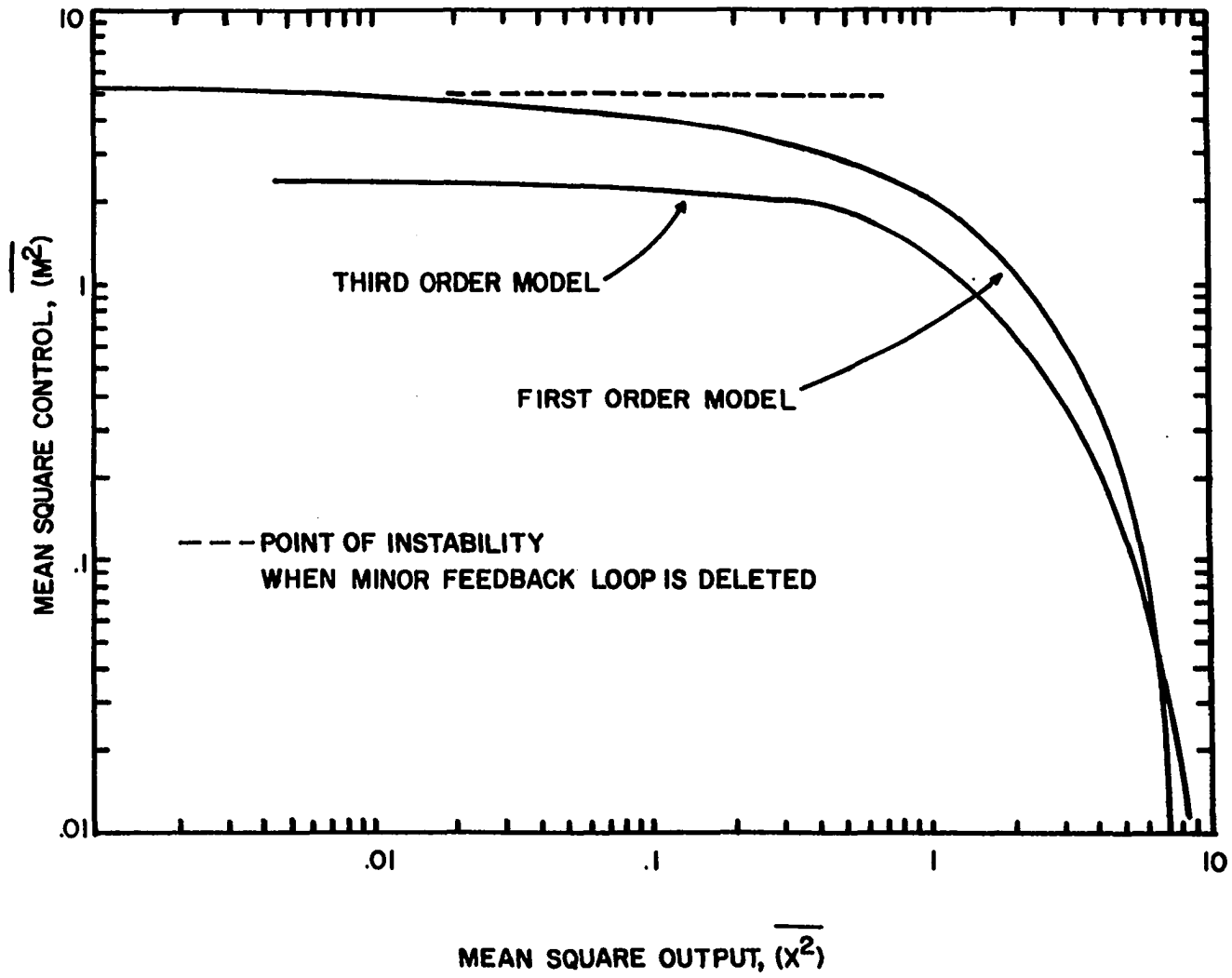


Figure 6-3. Performance diagram for third order model.

Table 6.1

Model Order	Feedforward Controller	Feedback Controller
1st	$Q_D = - \frac{1.84 (s+0.117) + 1.99 (1 - e^{-1.5s-0.175})}{s + 0.117 + 0.866 (1 - e^{-s-0.117})}$	$Q_D = - \frac{4.44 (s + 0.117) e^{-0.117}}{s + 0.117 + 0.866 (1 - e^{-s-0.117})}$
3rd	$Q_C = \frac{0.166s + 0.0948}{0.156s + 0.0513}$	$Q_C = \frac{0.458 s^2 + 0.632 s + 0.266}{0.156 + 0.0513}$

The response curves for these controllers are shown in Figures (6.4) and (6.5). The manner in which the controlled systems were actually simulated on the analog computer did not allow recording of the control signal as was done in the experimental work. The reason for this method of simulation was to avoid the possibility of controller saturation, which was discussed in the chapter on experimental work. Furthermore, analog simulation allows amplitude and time scaling of the functions to allow for smoother operations. These simulation techniques allow the points in question to be emphasized without the background noise and unknown system upsets encountered in physical processes.

The optimal controllers calculated from the third order model are definitely superior. However, the controllers calculated from the first order approximation do a reasonable job of attenuating the system output. They might even do a better job if an accurate simulation of the minor loop delay time were available. The Pade approximation used in most analog devices does not provide the required accuracy. Figure (6.6) shows the unit step response of the transportation delay generator used with the Donner Analog computer. This dead time simulation has a frequency limitation which might cause further inaccuracies when used with faster reacting systems (B6).

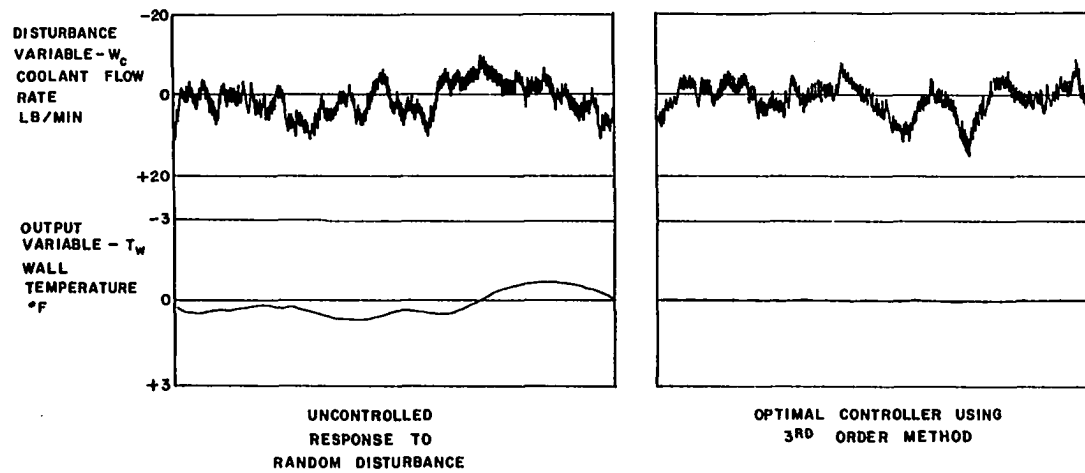


Figure 6-4. Response of the third order analog model to disturbances.



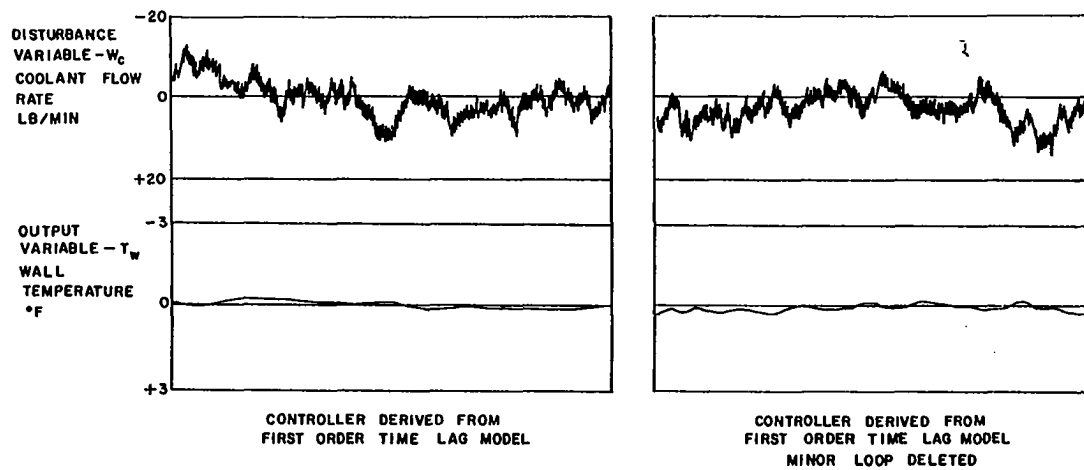


Figure 6-5. Response of the third order analog model to disturbances.

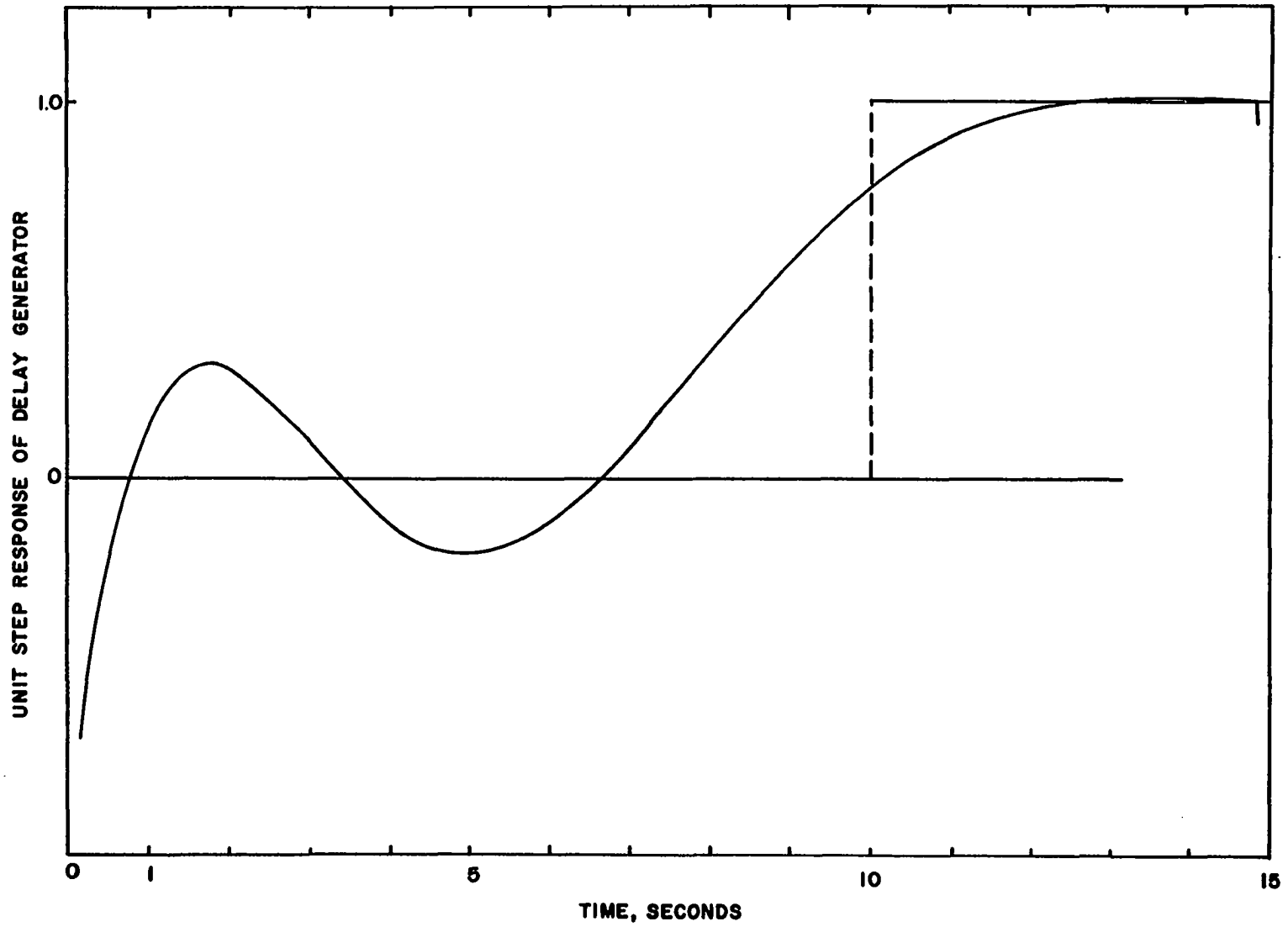


Figure 6-6. Unit step response of the transport delay generator.

It should be noted that no instability was observed when the minor feedback loop is neglected even though the controller used in the example was past the instability point. One reason for this observation is that it may be caused by the cascading of approximations. The delay time can only be approximated on the analog computer and the model itself is an approximation of the third order system

Actually the approximation of delay time by the Pade Expansion may be more effective than the true exponential. When obtaining the first order approximation of higher order models, zeros and poles of the transfer function are cancelled against each other with the remainder being placed in the exponential term. Therefore, in the original analysis, the exponential was used as an approximate function for a ratio of polynomials. Then the Pade approximation, which is a net zero order ratio of polynomials, would be closer to the actual system. The overall effect is to replace several characteristic parameters from the original system transfer function with one parameter  $-\tau$ , the delay time.

Although this dead time approximation may be useful in some cases, large distillation columns and double-pipe heat exchanges exhibit a definite dead time which is about the magnitude of the fluid residence time. In these situations the exponential should be simulated in the best possible way, generally with an on-line digital computer.

In general, more effort must be expended to obtain a third order mathematical model than a first order time lag model. The increase in controller effectiveness with the use of the high order model does not seem sufficient to warrant the expanded identification technique required for the relatively slow responding chemical and thermal systems.

## CHAPTER VII

### CONCLUSIONS AND RECOMMENDATIONS

The optimal controllers derived from the Dynamic Programming optimization technique are easily simulated for practical control jobs. This time domain formulation specifies both feedforward and feedback controllers which carry an almost equal share of the control effort. It has been shown that the limiting cases of these controllers are the ideal feedforward and infinite feedback controllers.

The problems associated with these limiting cases cause the control engineer to "back down" the performance chart to obtain realistic controller configurations. It is well-known that a very large feedback gain is undesirable when control signal saturation occurs. However the less known fact that ideal feedforward also contributes to controller saturation is apparent from the performance chart of the optimally controlled system.

If a system output in which the disturbance reacts faster than the manipulative signal is to be controlled, the optimal control equations specify predictive controllers. This is a fact of life from which there is no reprieve. Because of the difficulties involved in the practical simulation of predictive

controllers, it is worthwhile to consider ways of redesigning the system to relieve the necessity of using predictive control. The modifications would not be in the realm of optimal control, but they would be pointed out from the unsuitable controllers specified by optimal control theory. This aspect of specification of unsuitable but still realizable controllers is one of the unfortunate results of optimal control theory. It is not mathematically feasible to exclude certain controller configuration because of the simulation difficulties.

Optimal controllers for time delay systems can be specified with this method. It has been shown that optimal control of systems with process dead time can be obtained with the use of a Smith linear predictor. Furthermore the exact parameters of this minor feedback loop are specified. Previous investigators (Bl2) have used the cut-and-try method of selecting minor loop parameters. Some of the difficulties involved in the practical use of the minor feedback loop were pointed out in the analog simulation tests.

#### Recommendations

Optimal control theory seems to be of more value in servomechanism problems. In these situations a trajectory of the state variable is specified. It is much harder to obtain a good trajectory by trial and error methods for a servo problem than it is to find by the same methods a reasonably good controller for a regulatory situation. The same equations need

to be solved for both servo and regulator problems. Furthermore, the equipment in the Process Dynamics Laboratory could be modified to study start-up and shut-down operations. There is no work reported in the literature of composite controlled servomechanism problems.

Because of the increased use of digital computers in chemical process control, the sampled-data formulation of the optimization problem should be studied. Fast response systems, such as chemical reactors sensitive to temperature variations, would provide the best test for the discrete sampled-data controllers.

The optimal controller equations developed in this work are valid for multivariable systems without resorting to uncoupling techniques. It would be valuable to compare controller configurations obtained by uncoupling (non-interaction) techniques with those obtained by the equations presented in Chapter III. The basis of comparison should be ease of simulation of the specified controllers.

## BIBLIOGRAPHY

- A1. Athans, M. and Falb, P. L. Optimal Control. New York: McGraw-Hill Inc., 1966.
- B1. Balakrishnan, A. V. and Neustadt, L. W. (ed.), Computing Methods in Optimization Problems. New York: Academic Press, 1964.
- B2. Bellman, R. E. Adaptive Control. Princeton, N. J.: Princeton University Press, 1961.
- B3. Bellman, R. Mathematical Theory of Control Processes, Vol. 1, New York: Academic Press, 1967.
- B4. Bellman, R. E. Introduction to Matrix Analysis. New York: McGraw-Hill Inc., 1960.
- B5. Bendat, J. S. Principles and Application of Random Noise Theory. New York: John Wiley and Sons, Inc., 1958.
- B6. Bishop, K. A. and Sims, R. A. Analog Computation Using the Modified Donner Model 3100-D. Internal Report at the University of Oklahoma Process Dynamics and Control Laboratory, 1963.
- B7. Bishop, K. A. and Sims, R. A. "Electronic Instrumentation for Research in Process Control," Paper presented at the 1962 Mid-American Electronics Conference, Kansas City, Mo., 1962.
- B8. Blackburn, T. R. "Solution of the Algebraic Matrix Riccati: Equation VIA Newton-Raphsen Iteration," Proc. Joint Auto. Control Conf., pp. 940-944, 1968.
- B9. Bollinger, R. E. and Lamb, D. E. "Multivariable Systems: Analysis and Feedforward Control," I. & E.C. Fundamentals, Vol. 1, No. 4, p. 245, 1962.
- B10. Bollinger, R. and Lamb, D. E. "1963 Joint Automatic Control Conference," Preprint XVIII-4, University of Minn., Minneapolis, 1963.



- B11. Boltyanskii, V. G. "Sufficient Conditions for Optimality and the Justification of the Dynamic Programming Method," J. Siam Control, Vol. 4, p. 326.
- B12. Buckley, P. Techniques of Process Control. New York: John Wiley and Sons, Inc., 1964.
- C1. Cadman, T. W., Rothfus, R. R. and Kermode, R. I. "Estimation of the Nonlinear Dynamic Effectiveness of Feed-forward Control for Multicomponent Distillation by Linear Methods," A. I. Ch. E. National Meeting, Houston, Texas, Feb. 1967.
- C2. Chan, S. Y. and Chuang, K. "A Study of Effects on Optimal Control Systems Due to Variations in Plant Parameters," Int. J. Control, Vol. 7, No. 3, pp. 281-299, 1968.
- C3. Chang, S. S. L. Synthesis of Optimum Control Systems. New York: McGraw-Hill, Inc., 1961.
- C4. Coddington, E. A. and Levinson N. Theory of Ordinary Differential Equations. New York: McGraw-Hill, Inc., 1955.
- C5. Coughanowr, D. R. and Koppel, L. B. Process Systems Analysis and Control. New York: McGraw-Hill, Inc., 1955.
- D1. Derusso, P. M. and Roy, R. J. and Close, C. M. State Variables for Engineers. New York: John Wiley & Sons, Inc., 1965.
- D2. Dorato, P. "On Sensitivity in Optimal Control Systems," I.E.E.E. translation on Automation Control, Vol. 5, No. 2, p. 1074, 1959.
- E1. Ellert, F. J. Ph.D. Thesis, Rensselaer Polytechnic Institute., Troy, New York, 1963.
- E2. Eveleigh, V. W. Adaptive Control and Optimization Techniques. New York: McGraw-Hill, Inc., 1967.
- F1. Fanning, R. J. and Sliepcevich, C. M. "The Dynamics of Heat Removal from a Continuous Agitated-Tank Reactor," A. I. Ch. E. Journal, Vol. 5, No. 2, p. 1074, 1959.
- F2. Fuller, A. T. "The Replacement of Saturation Constraints by Energy Constraints in Control Optimization Theory," Int. J. Control, Vol. 6, No. 3, pp. 201-227, 1967.

- H1. Harris, J. T. and Schechter, R. S. "Feedforward Control of a Chemical Reactor," I & E C Fundamentals, Vol. 2, No. 3, p. 245, 1963.
- H2. Haskins, D. E. and Slipevich, C. M. "The Invariance Principle of Control for Chemical Processes," I & E C Fundamentals, Vol. 4, No. 3, p. 241, 1965.
- H3. Hazelbroek, P. and Van der Waerden, B. L. "Theoretical Considerations on the Optimum Adjustment of Regulators," Trans. ASME, 72, p. 309, 1950.
- H4. Heidemann, R. A. "Optimal Control of a Distillation Column Using an Empirical Mathematical Model," Doctoral Dissertation, Washington University, St. Louis, Missouri, 1966.
- H5. Heymann, M. "A Time Domain Technique for Linear System Identification," Ph.D. Thesis, University of Oklahoma, 1965.
- H6. Horowitz, I. M. Synthesis of Feedback Systems. New York: Academic Press, 1963.
- J1. Jackson, S. J. Analog Computation. New York: McGraw-Hill, Inc., 1960.
- K1. Kalman, R. E. "Contributions to the Theory of Optimal Control," Bo. Soc. Mat. Mex., Vol. 5, pp. 102-119, 1960.
- K2. Kalman, R. E. and Englar, T. S., Tech. Rpt. 62-18 R. I. A. S., Baltimore, Maryland, 1962.
- K3. Koivo, A. J. "Performance Sensitivity of Dynamical Systems," Proceedings J.A.C.C., pp. 444-453, June, 1968.
- L1. Laning, J. H. and Battin, R. H. Random Processes in Automatic Control. New York: McGraw-Hill, Inc., 1956.
- L2. Lapidus, L. and Luus, R. Optimal Control of Engineering Processes, Waltham, Mass.: Blaisdell Co., 1967.
- L3. Leondes, C. T. Advances in Control Systems. Vol. 4, New York: Academic Press, 1966.
- L4. Luecke, R. L. "Optimal Composite Feedforward-Feedback Control," Ph.D. Thesis, University of Oklahoma, 1966.

- L5. Luecke, R. L. and McGuire, M. L. and Crosser, O. K. "Dynamic Flowsheeting," Chem. Eng. Prog., Vol. 63, No. 2, pp. 60-66, 1967.
- L6. Luecke, R. L. and McGuire, M. L. A. I. Ch. E. Journal Vol. 14, No. 1, p. 181, 1968.
- L7. Lupfer, D. E. and Oflesby, M. W. "The Application of Dead Time Compensation to a Chemical Reactor for Automatic Control of Production Rate," ISA Trans., Vol. 1, No. 1, p. 72, 1962.
- L8. Luyben, W. L. and Gerster, J. A. "Feedforward Control of Distillation Columns," I & E C Fundamentals, Vol. 3, No. 4, p. 106, 1964.
- L9. Luyben, W. L. "Nonlinear Feedforward Control of Chemical Reactors," A I. Ch. E. Journal, Vol. 14, No. 1, p. 37, 1968.
- M1. MacFarlane, A. G. "An Eigenvector Solution of the Optimal Linear Regulator Problem," Jl. Elec. Cont., Vol. 14, No. 6, 1963.
- M2. MacMullan, E. C. and Shinskey, F. G. "Feedforward Analog Computer Control of a Superfractionator," Control Engineering, 1964.
- M3. Merriam, C. W. Optimization Theory and the Design of Feedback Control Systems. New York: McGraw-Hill, Inc., 1964.
- M4. Mesarovic, M. D. The Control of Multivariable Systems New York: M. I. T. Press and John Wiley & Sons, Inc., 1960.
- N1. Newton, G. C., Gould, L. A. and Kaiser, J. F. Analytical Design of Linear Feedback Controls. New York: John Wiley & Sons, Inc., 1957.
- O1. Ogata, K. State Space Analysis of Control Systems. New York: Prentice Hall, Inc., 1967.
- P1. Paige, L. J. and Swift, J. D. Elements of Linear Algebra. Mass.: Blaisdell Co., 1961.
- P2. Pagurek, B. "Sensitivity of the Performance of Optimal Control Systems to Plant Parameter Variations," I.E. E.E. trans. on Auto. Control, Vol. AC-10, pp. 495-496, 1965.

- P3. Papoulis, A. Probability, Random Variables, and Stochastic Processes. New York: McGraw-Hill, Inc., 1965.
- P4. Peterson, E. L. Statistical Analysis and Optimization of Systems. New York: John Wiley & Sons, Inc., 1961.
- P5. Preminger, J. and Rootenberg, J. "Some Considerations Relating to Control Systems Employing the Invariance Principle," I.E.E.E. trans. on Automation Control, Vol. AC-9, p. 209, 1964.
- R1. Reid, W. T. "A Matrix Differential Equation of the Riccati Type," American Journal Math., Vol. 68, pp. 237-246, 1946.
- R2. Rozonoer, L. I. "A variational Approach to the Problem of Invariance of Automatic Control Systems," Automatika and Telemekhanika, Vol. 24, No. 6, p. 680, 1963; No. 7, p. 793, 1963.
- S1. Sims, R. A. "Time Domain Identification of Zeros of a Linear System," Ph. D. Dissertation, The University of Oklahoma, 1968.
- S2. Smith, O. J. M. "Feedback Control Systems," New York: McGraw-Hill, Inc., 1958.
- S3. Solodovnikov, V. V. Introduction to the Statistical Dynamics of Automatic Control Systems. New York: Dover Publications, Inc., 1960. (First published in Russian, 1952)
- S4. Stewart, W. S., Sliepcevich, C. M. and Pucket, T. H. "Dynamics of Heat Removal from a Jacketed Agitated Vessel," C.E.P. Symposium Series, Vol. 57, No. 36, p. 119, 1961.
- T1. Tomovic, R. Sensitivity Analysis of Dynamic Systems. New York: McGraw-Hill, Inc., 1963.
- V1. Varga, R. Matrix Iterative Analysis. Prentice-Hall, Englewood Cliffs, 1962.

## APPENDIX A

### VECTOR EQUATIONS FROM TRANSFER FUNCTIONS

Most instrumentation engineers express system dynamics in the transfer function form. Therefore it is necessary to convert the transfer function into a vector differential equation in order to use the optimal controller design procedure. A three-pole, one-zero transfer function was selected as an example.

Consider the following system:

$$X(s) = \frac{K_m(s + e)}{(s+a)(s+b)(s+c)} M(s) + \frac{K_D(s+d)}{(s+a)(s+b)(s+c)} U(s) \quad (\text{A.1})$$

where  $X$  = system output variable

$M$  = control variable

$U$  = disturbance variable

$K_m, K_D$  = system gains

$a, b, c$  = system poles

$e$  = control zero

$d$  = disturbance zero

This type of configuration was found to fit the experimental heat exchanger discussed earlier. It has been found to be of sufficient order to describe the dynamics of many chemical processes.

Using standard techniques from the theory of Laplace

Transforms, we can convert the above expression into a non-homogeneous third-order ordinary differential equation.

Since we work with perturbation variables, it is assumed that all initial conditions are zero.

$$\ddot{x}_1 + \alpha_2 \dot{x}_1 + \alpha_1 \dot{x}_1 + \alpha_0 x_1 = \dot{m}_2 + \beta m_2 + \dot{u}_2 + g u_2 \quad (\text{A.2})$$

where  $x_1(t)$  = inverse laplace transform of  $X(s)$

$m_2(t)$  = inverse laplace transform of  $K_M M(s)$

$u_2(t)$  = inverse laplace transform of  $K_D U(s)$

For ease in manipulation it is convenient to combine the system gains,  $K_M$  and  $K_D$ , with their respective variables.

The subscripts used above will become apparent later.

Define the following variables:

$$\begin{aligned} \dot{x}_1 &= x_2 \\ \dot{x}_2 &= x_3 \\ \dot{m}_2 &= m_3 \\ \dot{u}_2 &= u_3 \end{aligned} \quad (\text{A.3})$$

Then the above differential equation becomes

$$\dot{x}_3 = \alpha_0 x_1 - \alpha_1 x_2 - \alpha_2 x_3 + m_3 + \beta m_2 + u_3 + g u_2 \quad (\text{A.4})$$

which can be placed in matrix form

$$\bar{\dot{x}} = B\bar{x} + C\bar{m} + D\bar{u} \quad (\text{A.5})$$

where

$$\bar{x} = \begin{bmatrix} x_1 \\ x_2 \\ x_3 \end{bmatrix} \quad \bar{m} = \begin{bmatrix} 0 \\ m_2 \\ m_3 \end{bmatrix} \quad \bar{u} = \begin{bmatrix} 0 \\ u_2 \\ u_3 \end{bmatrix}$$

$$B = \begin{bmatrix} 0 & 1 & 0 \\ 0 & 0 & 1 \\ \alpha_0 & \alpha_1 & \alpha_2 \end{bmatrix}$$

$$C = \begin{bmatrix} 0 & 0 & 0 \\ 0 & 0 & 0 \\ 0 & \beta & 1 \end{bmatrix}$$

$$D = \begin{bmatrix} 0 & 0 & 0 \\ 0 & 0 & 0 \\ 0 & g & 1 \end{bmatrix}$$

The preceding development is not the only possible way of formulating the system vector differential equation. Let  $\bar{z}(t)$  be the state variable vector which is defined by

$$\begin{aligned} z_1(t) &= x(t) - f_0 m(t) \\ z_2(t) &= \dot{x}(t) - f_0 \dot{m}(t) - f_1 m(t) \\ z_3(t) &= \ddot{x} - f_0 \ddot{m}(t) - f_1 \dot{m}(t) - f_2 m(t) \end{aligned} \tag{A.6}$$

where

$$f_0 = f_1 = 0$$

$$f_2 = 1$$

$$f_3 = \beta - \alpha_2$$

Then the system dynamics can be represented by

$$\dot{\bar{z}}(t) = B\bar{z}(t) + C\bar{m}(t) + D\bar{u}(t) \quad (\text{A.7})$$

$$\bar{x}(t) = A\bar{z}(t)$$

This equation is similar to the previous relation (A.5) for the system dynamics. In fact matrices B and D are defined exactly as in that earlier equation. The difference lies in matrices C and A.

$$C = \begin{bmatrix} f_1 & 0 & 0 \\ 0 & f_2 & 0 \\ 0 & 0 & f_3 \end{bmatrix}$$

$$A = \begin{bmatrix} 1 & 0 & 0 \\ 0 & 1 & 0 \\ 0 & 0 & 0 \end{bmatrix}$$

Matrix A referred to as the output matrix. Usually we are only interested in the output  $x(t)$ . This would require only a single entry in the output matrix located in the upper left corner element. However, if we consider constraints on the first derivative, we must add the central element.

Since we almost never have a second derivative constraint, the lower right element is neglected. If one does not need



it, there is nothing gained in carrying a full matrix in the calculations.

The above formulation of the state equations is called the standard method. It can be developed for an  $n$ th-order system. Any text on the state-variable approach covers this method (A1, D1, O1). The standard method was not repeated in the most general form here because of its complex notation.

There is another configuration which can be used. The previously discussed standard state equation form can be converted into a form where the B matrix is a Jordan matrix. This conversion can be accomplished by means of a similarity transformation

Define the following transformation

$$z = Pq$$

where P is the modal matrix. The vector, z, is state variable used in equation (A.7). Remember that the modal matrix is made from the column eigenvectors of the matrix B.

Then

$$\dot{Pq} = BPq + Cm + Du \quad (A.9)$$

$$x = APq$$

Premultiplication by  $P^{-1}$  yields


$$\dot{q} = P^{-1}BPq + P^{-1}Cm + P^{-1}Du \quad (A.10)$$

Then since P is the modal matrix of B, the similarity trans-

form  $P^{-1}BP$  results in a Jordan canonical form. The principal diagonal elements are the eigenvalues of  $B$ . Equation (A.10) is known as the normal form of the state dynamics.

Obviously, more calculation is required to obtain the normal form. However in this form the conditions for controllability and observability are easily obtained. These concepts have not been used in this work, so the normal form was not employed.

One can see that a choice of several forms of the state dynamical equations is available. Furthermore, the system can be time-scaled to make the computer calculations more reliable. Therefore, the preliminary manipulation decisions preclude building the state vector equation with the digital computer directly from the system poles, zeros, and gains.



## APPENDIX B

### DERIVATION OF CONTROLLER PARAMETER EQUATIONS

In Chapter III, a mathematical form for the solution of the continuous Dynamic Programming algorithm was postulated.

$$E[\overline{x(\mu)}^t, \mu] = I(\mu) - 2 \left( \overline{x(\mu)}^t \right)^T J(\mu) + \left( \overline{x(\mu)}^t \right)^T K(\mu) \overline{x(\mu)}^t \quad (\text{B.1})$$

The partial differential equation which must be solved is

$$\begin{aligned} \text{Min}_{m(\mu)} \{ & \langle \overline{q(\mu)}^t, \overline{\dot{q}(\mu)}^t \rangle + \langle \overline{m(\mu)}^t, \overline{\dot{\Psi} m(\mu)}^t \rangle + \left( \frac{\partial E[\overline{x(\mu)}^t, \mu]}{\partial \overline{x(\mu)}^t} \right)^T \overline{\dot{x}(\mu)}^t \} \\ & = - \frac{\partial E[\overline{x(\mu)}^t, \mu]}{\partial \mu} \end{aligned} \quad (\text{B.2})$$

The partial derivatives of  $E[\overline{x(\mu)}^t, \mu]$  needed in this equation are

$$\left( \frac{\partial E[\overline{x(\mu)}^t, \mu]}{\partial \overline{x(\mu)}^t} \right)^T = -2J^T(\mu) + 2 \left( \overline{x(\mu)}^t \right)^T K(\mu) \quad (\text{B.3})$$

$$\frac{\partial E[\overline{x(\mu)}^t, \mu]}{\partial \mu} = \dot{I}(\mu) - 2 \left( \overline{x(\mu)}^t \right)^T \dot{J}(\mu) + \left( \overline{x(\mu)}^t \right)^T \dot{K}(\mu) \overline{x(\mu)}^t \quad (\text{B.4})$$

The optimal control equation is also needed to satisfy the

minimization procedure indicated in equation (B.2).

$$\dot{m}^*(\mu) = \Psi^{-1} C^T J(\mu) - \Psi^{-1} C^T K(\mu) \overline{x(\mu)}^t \quad (\text{B.5})$$

To simplify notation, the conditional means and time arguments will be deleted from the rest of this discussion. Using equations (B.3), (B.4), and (B.5) in equation (B.2) results in

$$\begin{aligned} -\dot{I} + 2x^T \dot{J} - x^T K \dot{x} &= x^T A^T \Phi Ax + (-2J^T + 2x^T K) Du \\ &\quad - \frac{1}{4} \left( -2J^T + 2x^T K \right) C \Psi^{-1} C^T (-2J + 2Kx) \\ &\quad + (-2J^T + 2x^T K) Bx \end{aligned} \quad (\text{B.6})$$

Expanding this equation gives

$$\begin{aligned} -\dot{I} + 2x^T \dot{J} - x^T K \dot{x} &= \{J^T C \Psi^{-1} C^T J - 2J^T Du\} \\ &\quad + x^T \{+ 2KC \Psi^{-1} C^T J - 2B^T J + 2KDu\} \\ &\quad + x^T \{A^T \Phi A - KC \Psi^{-1} C^T K + 2KB\}x \end{aligned} \quad (\text{B.7})$$

This equation must hold for all values of the state variable  $x$ , so like powers of  $x$  on each side of the equation can be equated.

In order to be able to equate the quadratic terms, the terms within the braces of the right-hand side quadratic must be shown to be symmetric because the left-hand side,  $K$ ,

is symmetric. The first three terms are already symmetric so it remains to be shown that the matrix,  $2KB$ , can be manipulated into a symmetric form.

$$2KB = (KB + B^T K) + (KB - B^T K) \quad (\text{B.8})$$

The first term on the right-hand side of this equation is symmetric, while the second term is skew-symmetric. It will be shown that the quadratic form of the skew-symmetric matrix is zero.

Consider two arbitrary vectors  $y$  and  $z$ , which are related by

$$y = Bz \quad (\text{B.9})$$

$$\text{Then } z^T (KB - B^T K) z = z^T KBz - z^T B^T Kz \quad (\text{B.10})$$

$$\text{or } z^T (KB - B^T K) z = z^T Ky - y^T Kz = 0 \quad (\text{B.11})$$

because  $K$  is a symmetric matrix. Therefore the symmetry of the quadratic term has been demonstrated.

The equations which determine the parameters are

$$\dot{I}(\mu) = J^T(\mu) D \mu - J^T(\mu) C \Psi^{-1} C^T J(\mu) \quad (\text{B.12})$$

$$\dot{K}(\mu) = K(\mu) C \Psi^{-1} C^T K(\mu) - B^T K(\mu) - K(\mu) B - A^T \Phi_A \quad (\text{B.13})$$

$$\dot{J}(\mu) = K(\mu) C \Psi^{-1} C^T J(\mu) - B^T J(\mu) + K D \overline{(\mu)}^t \quad (\text{B.14})$$

The boundary conditions for this equation follow directly from equation (3.6)

$$I(T) = 0; \quad J(T) = 0; \quad K(T) = 0 \quad (\text{B.15})$$

Merriam (M3) arrived at the same results by way of a complicated summation notation operation. Because of typographical errors in his presentation, and the difference in

nomenclature, the equations are presented here. One of the probable reasons why there has not been any applications of this technique has been the complicated summation notation which was used to present the original idea.

## APPENDIX C

### SOLVING THE MATRIX RICCATI EQUATION

In order to obtain the feedback controller as shown in Chapter III, a matrix Riccati equation must be solved. Reid (R1) has presented a method for solving the matrix Riccati equations by using an associated system of linear matrix equations.

Consider the matrix Riccati equation presented as equation (3.13) in Chapter III.

$$\dot{K}(\mu) = -K(\mu)C \Psi^{-1} C K(\mu) + B^T K(\mu) + K(\mu)B + A^T \Phi A \quad (C.1)$$

where all the matrices are  $n \times n$  square matrices. The matrix elements are continuous on the finite interval  $t \leq \mu \leq T$ . The associated system of linear matrix equations is

$$\dot{Y}(\mu) = B Y(\mu) - C \Psi^{-1} C^T z(\mu) \quad (C.2)$$

$$\dot{z}(\mu) = -A^T \Phi A Y(\mu) - B z(\mu) \quad (C.3)$$

The boundary conditions for these equations are

$$Y(T) = I, \text{ the identity matrix} \quad (C.4)$$

$$z(T) = K(T) \quad (C.5)$$

The matrix  $Y(\mu)$  is nonsingular on the interval in question.

The solution to the matrix Riccati equation is given by

$$K(\mu) = z(\mu) y^{-1}(\mu) \quad (C.6)$$

This can easily be verified by differentiating this expression and substituting for the derivatives of  $z(\mu)$  and  $y(\mu)$  from equations (C.2) and (C.3).

In order to solve for  $z(\mu)$  and  $y(\mu)$ , it is convenient to define the following system.

$$\dot{W}(\mu) = GW(\mu) \quad (C.7)$$

where

$$W(\mu) = \begin{bmatrix} y(\mu) \\ z(\mu) \end{bmatrix} \quad (C.8)$$

$$G = \begin{bmatrix} B & \vdots & -C \Psi^{-1} C^T \\ \dots & \dots & \dots \\ -A^T & \Phi A & -B^T \end{bmatrix} \quad (C.9)$$

$W(\mu)$  is a vector containing an element and  $G(\mu)$  is a  $2n \times 2n$  matrix. In any case, the equation (C.7) is a simple homogeneous linear matrix differential equation. The solution of this equation is well known

$$W(\mu) = \varphi(\mu-T) W(T) \quad (C.10)$$

where  $\varphi(\mu-T) = e^{G(\mu-T)}$ , the matrix exponential.

Divide the matrix exponential into four  $n \times n$  matrices

$$\varphi(\mu-T) = \begin{bmatrix} \varphi_{11}(\mu-T) & \vdots & \varphi_{12}(\mu-T) \\ \dots & \dots & \dots \\ \varphi_{21}(\mu-T) & \vdots & \varphi_{22}(\mu-T) \end{bmatrix} \quad (C.11)$$

The associated vectors can be written as



$$y(\mu) = \varphi_{11}(\mu-T) y(T) + \varphi_{12}(\mu-T) z(T) \quad (C.12)$$

$$z(\mu) = \varphi_{21}(\mu-T) y(T) + \varphi_{22}(\mu-T) z(T) \quad (C.13)$$

Substituting the boundary equations for the associated vectors given in equations (C.4) and (C.5) and then solving for the feedback parameter using equation (C.6) results in

$$K(t+\tau) = [\varphi_{21}(\tau) + \varphi_{22}(\tau) K(T)] \cdot [\varphi_{11}(\tau) + \varphi_{12}(\tau) K(T)]^{-1} \quad (C.14)$$

where  $\tau = \mu - T$

Since only the "steady-state" value of  $K$  is desired, the above equation is used in a stepping procedure. Notice that the steps are taken in the negative  $\tau$  direction. In this manner the previously calculated  $K(t+\tau)$  is used as  $K(T)$  in each successive step. This technique is a convenient method since the matrix exponential which is a function of the stepping interval  $T$  need only be calculated once. The procedure is continued until

$$\frac{K(t+\tau) - K(t)}{K(t)} < \epsilon$$

where  $\epsilon$  is some previously determined error bound.

This procedure is not the only method of obtaining the steady state value of the matrix Riccati equation. MacFarlan (M1) has presented a method which needs the system eigenvectors and eigenvalues. Due to the inability to calculate eigenvectors precisely by digital computer methods, this method does not seem to be more useful than the stepping

procedure. Blackburn (B8) has recently presented a method which uses the Newton-Raphsen iterative technique. Again this does not seem to be a major improvement because of the limitations of the Newton-Raphsen technique.

This discussion presents only highlights of the mathematical concepts involved in solving the matrix Riccati equation. More detail can be gathered from some of the references cited in the Bibliography (K1, L3, O1)

## APPENDIX D

### SOLUTION OF THE OPTIMAL FEEDFORWARD EQUATION

In order to obtain the feedforward portion of the optimal controller, equation (3.31) must be evaluated. This equation is limited to time-invariant systems as discussed in Chapter III.

$$S = - \int_0^{\infty} \phi(-\epsilon) KDU(\epsilon) d\epsilon \quad (D.1)$$

The separable portion of the conditional mean of the load disturbance signal,  $U(\epsilon)$ , is easily found for gaussian disturbances. A zero mean is used because of the perturbation form of the system dynamics. Since this is the type of signal of interest in this work, equation (2.10) of the mathematical background chapter provides the method of obtaining  $U(\epsilon)$ .

$$U(\epsilon) = \frac{\Theta(\epsilon)}{\Theta(0)} \quad \text{for } \epsilon > 0 \quad (D.2)$$

This equation is the ratio of the autocorrelation functions of the disturbance. The autocorrelation function for gaussian signals has the following mathematical form.

$$\Theta_u(\epsilon) = \bar{u} e^{-\alpha\epsilon} \quad \text{for } \epsilon > 0 \quad (D.3)$$

where  $\alpha$  = frequency

$\bar{u}$  = mean square amplitude

Therefore,

$$U(\epsilon) = e^{-\alpha\epsilon} \quad (D.4)$$

For a single input nth order system this quantity would be an n x n matrix which contained the exponential terms in the diagonal elements.

$$U(\epsilon) = e^{-\alpha\epsilon} \begin{bmatrix} 0 & \dots & \dots & \dots & 0 \\ \vdots & \cdot & \cdot & \cdot & \vdots \\ \vdots & \cdot & \cdot & \cdot & \vdots \\ \vdots & \cdot & \cdot & \cdot & \vdots \\ \vdots & \cdot & \cdot & \cdot & \vdots \\ \vdots & \cdot & \cdot & \cdot & \vdots \\ \vdots & \cdot & \cdot & \cdot & \vdots \\ \vdots & \cdot & \cdot & \cdot & \vdots \\ 0 & \dots & \dots & \dots & 0 \end{bmatrix} = e^{\alpha\epsilon} \tilde{U} \quad (D.5)$$

The number of diagonal elements used depends on the number of zeroes in the system transfer function. Substituting this equation into equation (D.1) gives

$$S = - \int_0^{\infty} e^{[B^T - KC \Psi^{-1} C^T K] \epsilon} K D e^{-\alpha\epsilon} \tilde{U} d\epsilon \quad (D.6)$$

or

$$S = - \int_0^{\infty} e^{[B^T - KC \Psi^{-1} C^T K - \alpha I] \epsilon} K D \tilde{U} d\epsilon \quad (D.7)$$

Since we are dealing with stable systems

$$S = [ \alpha I + KC \Psi^{-1} C^T K - B^T ]^{-1} K D \tilde{U} \quad (D.8)$$



Equation (D.1) becomes

$$S = - \int_0^{\infty} e^{P\epsilon} K D e^{\bar{\alpha}\epsilon} d\epsilon \quad (D.10)$$

where  $P = [B^T - KC \Psi^{-1} C^T K]$

Bellman (B4) has shown that the above equation is the solution of the matrix equation

$$PS + S\bar{\alpha} = KD \quad (D.11)$$

provided the integral exists for all  $KD$ . Furthermore the necessary and sufficient condition that this integral exist is that  $\lambda_i + \mu_j = 0$  where  $\lambda_i$  and  $\mu_j$  are the characteristic roots of  $P$  and  $\bar{\alpha}$  respectively (B4). For physically realizable systems the above conditions are always met because the characteristic roots of these matrices are always negative.

Rearranging equation (D.11) into a form convenient for trial and error solution gives

$$S = P^{-1}KD - P^{-1}\alpha S \quad (D.12)$$

The feedforward gain,  $S$ , on the right-hand side of this equation is used to calculate a new matrix  $S$ . This procedure would be continued until some convergence criteria is satisfied.

Actually equation (D.11) may be solved directly.

Rewriting

$$[PXI + IX\alpha^{-T}] S = KD \quad (D.13)$$

$$\text{or } S = [PXI + IX\alpha^{-T}]^{-1}KD \quad (D.14)$$

The symbol,  $\chi$ , indicates the first power Kroneker product and is defined as

$$A\chi B = (a_{ij}B) \quad i, j = 1, \dots, N \quad (D.15)$$

Note that the Kroneker product of two  $N$ -dimensional matrices is a  $N^2$ -dimensional matrix. This quadratic increase in dimensionality limits the practicality of this solution method. The trouble lies with the computer algorithms which perform the matrix inversion operation indicated in equation (D.14).

## APPENDIX E

### MATRIX EXPONENTIAL EVALUATION

The fundamental matrix of a vector differential equation must be evaluated in the controller design procedure. This matrix is also called the transition matrix, the fundamental matrix, or the matrizant. Suppose we have a vector differential equation.

$$\dot{x}(t) = AX \quad (\text{E.1})$$

where  $A$  is a constant matrix and  $X$  is a vector

The solution of this equation is

$$X(t) = e^{A(t-t_0)} X(t_0) \quad (\text{E.2})$$

The matrix,  $e^{A(t-t_0)}$ , is the fundamental matrix. An excellent reference for further discussion of the properties of this function is Coddington and Levinson (C4).

If  $A$  is a constant, the fundamental matrix,  $e^{tA}$ , can be defined by a convergent power series

$$e^{At} = \sum_{i=0}^{\infty} \frac{(At)^i}{i!} \quad (\text{E.3})$$

In the actual calculation of this function, only the first thirty-six terms are used. The reason for this truncation and a corresponding condition to insure accuracy will be developed now.

The IBM 360 computer carries about seven significant



digits in the single precision mode. So in order to get an answer correct to three places to the right of the decimal, no term of the series should exceed  $10^4$ . The largest term of the  $e^t$  series is the one where  $i$  is the smallest integer such that  $\frac{t}{i+1} < 1$ . Therefore  $\frac{t^i}{i!}$  should be less than  $10^4$ .

This argument can be applied to the fundamental matrix by using some type of norm. A conservative norm which can be used is

$$\| |tA| \| = \text{Min} \left\{ \max_j \sum_i |t a_{ij}|, \max_i \sum_j |t a_{ij}| \right\} \quad (\text{E.4})$$

Then if  $\| |tA| \| < 10$  we have sufficient accuracy for our calculations.

To compute  $e^{at}$  for  $at$  which is too large, define  $\tau = \frac{t}{2^k}$  such that  $\| |\tau A| \| < 10$ . We can use the property

$$e^{A+B} = e^A e^B \quad (\text{E.5})$$

then

$$(e^{\tau A})^{2^k} = (e^{2\tau A})^k = e^{2^k \tau A} = e^{tA} \quad (\text{E.6})$$

The computation of a fundamental matrix for a large argument was not needed in the control design used in this thesis because only the regulator problem was considered. When a servomechanism problem is attacked, this method would be invaluable.

In the computer program listing in Appendix I, the exponential evaluation is carried out by the subroutine XPEVAL. The norm calculation is done in the XNORM sub-

routine. The subroutine STPSZ uses the norm to calculate a time step which would insure accuracy as discussed above.

## APPENDIX F

### MEAN SQUARE CALCULATION

In Chapter II, equation (2.15) relating the spectral density function to the signal mean value was presented.

$$\theta_{xx}(0) = \frac{1}{j} \int_{-j\infty}^{j\infty} P(s) P(-s) \phi_{dd}(s) ds \quad (F.1)$$

From the even property of the spectral density function, the above equation can be re-written as

$$\theta_{xx}(0) = \frac{1}{j} \int_{-j\infty}^{j\infty} P(s) D(s) P(-s) D(-s) ds \quad (F.2)$$

Since the system dynamics are to be represented by ordinary differential equations, the transform representation consists of the ratio of two polynomials. Therefore the integral of equation (F.2) can be rewritten in separated polynomial form.

$$\phi_{xx}(s) = \frac{c(s) c(-s)}{d(s) d(-s)} \quad (F.3)$$

where

$$c(s) = \sum_{i=0}^{n-1} c_i s^i$$

$$d(s) = \sum_{i=0}^n d_i s^i$$

$n$  = system order

Because of the generality of this particular form, several general methods of solution of equation (F.2) has been postulated. Newton, Gould, and Kaiser (N1) have presented tables for evaluating systems up to order  $n=10$ . In order to use their tables, large computer subroutines would have to be generated. The method given by Laning and Battin (L1) and Fuller (F1) is in a more suitable format for computer implementation.

Expand the numerator of equation (F.3) to obtain the following form

$$c(s) c(-s) = \sum_{i=0}^{n-1} g_i s^{2i} \quad (\text{F.4})$$

Then the mean square can be calculated from the equation on the next page. The denominator determinant is the well-known  $n$ th-order Hurwitz determinant which is associated with stability criteria for the characteristic (denominator) polynomial. Notice that the numerator determinant is the same determinant but with its first row replaced by the coefficients used in equation (F.4).

The computer program which does this calculation is listed in Appendix I.

$$\theta_{xx}(0) = \frac{(-1)^{n-1}}{2d_n}$$

$g_{n-1}$	$g_{n-2} \dots g_0$
$d_n$	$d_{n-2} \dots 0$
$d_{n-1}$	$d_{n-3} \dots 0$
.....	
0	0 ..... $d_0$
$d_{n-1}$	$d_{n-3} \dots 0$
$d_n$	$d_{n-2} \dots 0$
0	$d_{n-1} \dots 0$
0	$d_n \dots 0$
.....	
0	0 ..... $d_0$

(F.5)

APPENDIX G

THEORETICAL MODEL OF THE EXPERIMENTAL PROCESS

Energy balances around the old system, coolant system, and the reactor wall provide a mathematical model of the experimental heat transfer process. The resulting equations are

$$(\rho V C_p)_f \dot{T}_f^* = h_i A_i T_w^* - h_i A_i T_f^* + C_{pf} T_{in} W^* - C_{pf} W^* T_f^* \quad (G.1)$$

$$(\rho V C_p)_w \dot{T}_w^* = h_i A_i T_f^* + \frac{h_o A_o}{2} T_{co}^* - (h_i A_i + h_o A_o) T_w^* \quad (G.2)$$

$$(\rho V C_p)_c \dot{T}_{co}^* = 2h_o A_o T_w^* - h_o A_o T_{co}^* + 2C_{pc} T_{ci} W_c^* - 2C_{pc} W_c T_{co}^* - h_o A_o T_{ci} \quad (G.3)$$

where

- |                               |                                |
|-------------------------------|--------------------------------|
| $\rho$ = density              | subscripts f = oil             |
| V = Volume                    | w = wall                       |
| $C_p$ = Specific heat         | c = coolant                    |
| $T^*$ = temperature           | i = inside                     |
| h = heat transfer coefficient | o = outside                    |
| A = heat transfer area        | in = oil in                    |
| W = flow rate                 | ci = coolant in                |
| Q = heat loss                 | ss = steady state              |
|                               | superscript * = total variable |

In order to arrive at the above equations, several assumptions were made.

- A. The temperature of each subsystem (coolant, wall, oil) is constant within the heat transfer vessel. This is the perfect mixing assumption.
- B. Oil and coolant inlet temperatures are constants.
- C. All physical properties, such as heat capacities, heat transfer coefficients, and densities remain constant.

These equations can be changed to a perturbation form

$$T_f^* = T_f + T_{fss}^* \quad (G.4)$$

$$T_w^* = T_w + T_{wss}^* \quad (G.5)$$

$$T_{co}^* = T_{co} + T_{co,ss}^* \quad (G.6)$$

$$W^* = W + W_{css}^* \quad (G.7)$$

$$W_c^* = W_c + W_{css}^* \quad (G.8)$$

Substituting these definitions into the model equation results in

$$\begin{aligned} (\rho V C_p)_f \dot{T}_f = & - (h_i A_i + C_{pf} W_{ss}) T_f + h_i A_i T_w + (C_{pf} T_{in} \\ & - C_{pf} T_{fss}) W - C_{pf} W T_f \end{aligned} \quad (G.9)$$

$$(\rho V C_p)_w \dot{T}_w = h_i A_i T_f - (h_i A_i + h_o A_o) T_w + \frac{h_o A_o}{2} T_{co} \quad (G.10)$$

$$\begin{aligned}
 (\rho V C_p)_c \dot{T}_c &= 2h_o A_o T_w - (h_o A_o + 2C_{pc} W_{css}^*) T_{co} - 2C_{pc} \\
 &\quad (T_{coss}^* - T_{ci}) W_c - 2C_{pc} W_c T_w
 \end{aligned} \tag{G.11}$$

A standard procedure in handling these non-linear models is to expand them in a Taylor Series around the steady-state value and retain only the first order terms. Since we are interested in controlling the process around this steady-state, this linearization is usually not a disastrous assumption.

Using the constants listed in table (G.1) and taking the Laplace transform of the above equations gives the following transfer function

$$T_w = \frac{0.156(s + 0.329)W - 0.207(s + 0.569)W_c}{(s + 0.117)(s + 0.45)(s + 0.583)} \tag{G.12}$$

This equation is presented in the scaled frequency domain where the frequency variable,  $s$ , is in units of radians per ten real time seconds for use in the analog simulation.

The system is a net second order system. The identified model was found to be second order too, but the parameters are considerably different. The reason for this discrepancy lies in the assumptions made in deriving the theoretical model. The linearization is questionable in light of the step response trajectories shown in Figures



(5-6) and (5-7). Another assumption that probably is not very good is that the coolant side is perfectly mixed. This illustrates the pitfall of reliance on theoretical models.

Table G-1

## List of System Constants

Symbol	Nomenclature	Value	Units	Source
$C_{pc}$	coolant heat capacity	0.54	BTU/lb <sup>o</sup> F	1
$C_{pw}$	wall heat capacity	0.037	BTU/lb <sup>o</sup> F	1
$C_{pf}$	oil heat capacity	0.405	BTU/lb <sup>o</sup> F	2
$h_i$	oil side heat transfer coefficient	27.	BTU/hr <sup>o</sup> F ft <sup>2</sup>	3
$h_o$	coolant side heat transfer coefficient	87.	BTU/hr <sup>o</sup> F ft <sup>2</sup>	3
$A_i$	inside heat transfer area	0.322	ft <sup>2</sup>	2
$A_o$	outside heat transfer area	0.444	ft <sup>2</sup>	2
$T_{ci}$	coolant inlet temperature	42.	<sup>o</sup> F	3
$T_{fss}$	oil steady state temperature	158.	<sup>o</sup> F	3
$T_{in}$	oil inlet temperature	172.	<sup>o</sup> F	3
$T_{wss}$	steady state wall temperature	88.	<sup>o</sup> F	3
$V_c$	coolant volume	0.0102	ft <sup>3</sup>	2
$V_f$	oil volume	0.0170	ft <sup>3</sup>	2
$V_w$	wall volume	0.0153	ft <sup>3</sup>	2
$W_{ss}$	steady state oil flow	165.	lb/hr	3
$W_{css}$	steady state coolant flow	44.	lb/hr	3
$\rho_c$	coolant density	77.3	lb/ft <sup>3</sup>	1
$\rho_f$	oil density	53.0	lb/ft <sup>3</sup>	2
$\rho_w$	wall density	640.5	lb/ft <sup>3</sup>	2
$Q_L$	heat loss	0.04	BTU/sec	3

Sources: 1. Handbook; 2. Laboratory measurements; 3. Steady state data.

## APPENDIX H

### NOMENCLATURE

A	= output matrix (1.2)
$A_H$	= heat transfer area of the coil (4.1)
B	= system matrix (1.1)
C	= control signal matrix (1.1)
$C_P$	= heat capacity of the fluid (4.1)
D	= disturbance matrix (1.1)
$e(\mu)$	= scalar performance index (2.21)
$E[x(\mu), \mu]$	= minimum scalar performance index (2.23)
E	= expected value of x (2.1)
$f(x, t)$	= probability density (2.1)
$f(y/t)$	= conditional probability density (2.2)
F	= flow rate (4.1)
G(t)	= partitioned matrix
h	= functional notation (2.20)
I(u)	= scalar element (3.8)
J(u)	= n-element feedforward vector (3.8)
K(u)	= symmetric n x n feedback matrix (3.8)
$K_D$	= disturbance gain (4.5)
$K_M$	= control signal gain (4.5)
m(t)	= control vector (1.2)
M	= allowable closed set of control signals
$m^*$	= optimal control signal (3.22)
M(s)	= control signal in frequency domain

$P_D$	= disturbance transfer function (3.28)
$P_M$	= control signal transfer function (3.28)
$q(t)$	= output vector (1.2)
$Q_C$	= feedback matrix (1.3)
$Q_D$	= feedforward matrix (1.3)
$Q_D^*$	= process time delay feedforward controller (4.46)
$Q_C^*$	= process time delay feedback controller (4.47)
$\bar{Q}_C$	= control time delay feedback controller (4.61)
$Q_D$	= control time delay feedforward controller (4.60)
$R$	= steady state deviation term in controller (3.16)
$S$	= feedforward parameter (3.16)
$s$	= frequency in radians per unit time
$t$	= time
$T$	= terminal time boundary (3.3)
$u(t)$	= disturbance vector (1.1)
$U_H$	= overall heat transfer coefficient (4.1)
$\mu^2$	= mean square amplitude (4.8)
$U(s)$	= disturbance in frequency domain
$V$	= volume of the tank (4.1)
$W$	= frequency (2.14)
$W(t)$	= partitioned vector
$x(t)$	= state variable vector (1.1)
$x(s)$	= state variable in frequency domain (1.2)
$y$	= associated vector
$z$	= associated vector

- $Z$  = relative sensitivity coefficient (4.37)  
 $Z$  = sensitivity coefficient (4.34)

Greek Letters

- $\beta$  = first order pole (4.5)  
 $\sigma$  = variable of integration (3.13)  
 $\epsilon$  = parameter error bound  
 $\mu$  = dummy time variable  
 $\tau$  = time delay (4.1)  
 $\Phi$  = output weighting factor (3.3)  
 $\Phi_{xx}$  = spectral density (2.4)  
 $\phi$  = fundamental matrix (3.25)  
 $\Psi$  = control weighting factor (3.3)  
 $\delta\delta(s)$  = feedback noise (4.29)  
 $\rho$  = density of the fluid (4.1)  
 $\Theta_x$  = autocorrelation function of  $x$  (2.3)  
 $\nu$  = frequency in radians per unit time (4.8)

## APPENDIX I

## COMPUTER PROGRAMS FOR CONTROLLER CALCULATION

This appendix contains the computer program listings used to calculate the parameters of the optimal controller equation. These programs were written in Fortran IV and used on the IBM Model 360-40 computer located in the Merrick Computer Center of the University of Oklahoma.

Explanation of input format is provided within the programs via comment statements. The output is obvious from headings built into the output format statements.

C	PROGRAM 200	HARRY WEST	MAIN0020
C	OPTIMAL FEEDBACK GAIN CALCULATION PROGRAM		MAIN0030
C	READ IN MATRICES ROW BY ROW		MAIN0010
C	REMEMBER THAT PHI IS ACTUALLY PHI-INVERSE		MAIN0040
C	REMEMBER THAT THE THETA MATRIX IS ACTUALLY A*THETA*ATRANSPOSE		MAIN0050
C			MAIN0060
	COMMON G(12,12),XP(12,12)		MAIN0070
	DIMENSION B(6,6),C(6,6),PHI(6,6),THETA(6,6),CPH(6,6),CPC(6,6)		MAIN0080
	DIMENSION XP11(6,6),XP12(6,6),XP21(6,6),XP22(6,6),SSK(6,6),E(6,6)		MAIN0090
	DIMENSION SSS(6,6),ULOGIC(6,6),D(6,6),XKD(6,6),S(6,6),SJ(6,6)		
	READ(5,100) N,T,EPSL,FREQ		MAIN0140
	EPS=0.000001		
	DO 800 I=1,N		MAIN0150
	READ(5,101)(B(I,J),J=1,N)		MAIN0160
800	CONTINUE		MAIN0170
	DO 801 I=1,N		MAIN0180
	READ(5,101)(C(I,J),J=1,N)		MAIN0190
801	CONTINUE		MAIN0200
	DO 805 I=1,N		
805	READ(5,101)(D(I,J),J=1,N)		
	DO 806 I=1,N		
806	READ(5,101)(ULOGIC(I,J),J=1,N)		
	DO 803 I=1,N		MAIN0240
	READ(5,101)(PHI(I,J),J=1,N)		MAIN0220
803	CONTINUE		MAIN0260
	WRITE(6,102)		MAIN0270
	WRITE(6,106) N		MAIN0280
	CALL MATPRT(N,B,6)		MAIN0290
	WRITE(6,103) N		MAIN0300
	CALL MATPRT(N,C,6)		MAIN0310
	WRITE(6,112) N		
	CALL MATPRT(N,D,6)		
	WRITE(6,113) N		
	CALL MATPRT(N,ULOGIC,6)		
	WRITE(6,104) N		MAIN0320
	CALL MATPRT(N,PHI,6)		MAIN0330

807	CONTINUE		MAIN0210
	DO 802 I=1,N		MAIN0250
	READ(5,101)(THETA(I,J),J=1,N)		MAIN0230
802	CONTINUE		MAIN0360
	N2=2*N		MAIN0370
	CALL MULTIP(N,C,PHI,CPH,6)		MAIN0380
	DO 200 I=1,N		MAIN0390
	DO 200 J=1,N		
200	E(I,J)=C(J,I)		
	CALL MULTIP(N,CPH,E,CPC,6)		MAIN0410
	DO 201 I=1,N		MAIN0420
	IPN=I+N		MAIN0430
	DO 201 J=1,N		MAIN0440
	JPN=J+N		MAIN0450
	G(I,J)=B(I,J)		MAIN0460
	G(I,JPN)=-1.0*CPC(I,J)		MAIN0470
	G(IPN,J)=-1.0*THETA(I,J)		MAIN0480
	G(IPN,JPN)=-1.0*B(J,I)		MAIN0490
201	CONTINUE		MAIN0500
	CALL XNORM(N,GNORM)		MAIN0510
	CALL STEPSZ(GNORM,T,TAU,KK)		MAIN0550
	CONTINUE		MAIN0560
C	***** USE NEGATIVE TAU *****		
	TAU=-TAU		
245	CONTINUE		MAIN1050
	CALL XPEVAL(N2,TAU)		MAIN0830
	DO 248 I=1,N		MAIN0850
	DO 248 J=1,N		MAIN0860
	XP11(I,J)=XP(I,J)		MAIN0870
	XP12(I,J)=XP(I,J+N)		MAIN0880
	XP21(I,J)=XP(I+N,J)		MAIN0890
	XP22(I,J)=XP(I+N,J+N)		MAIN0900
248	CONTINUE		MAIN0910
	CALL SSKAL(XP11,XP12,XP21,XP22,N,ITER,EPSL,SSK)		MAIN0920
	WRITE(6,119)		
	WRITE(6,117) TAU,EPSL,ITER		MAIN0935



```

WRITE(6,105) N
CALL MATPRT(N,THETA,6)
CALL MULTIP(N,SSK,D,CPH,6)
CALL MULTIP(N,CPH,ULOGIC,XKD,6)
CALL MULTIP(N,SSK,CPC,CPH,6)
DO 206 I=1,N
DO 206 J=1,N
206 CPH(I,J)=CPH(I,J)-B(J,I)
DO 202 I=1,N
202 CPH(I,I)=CPH(I,I)+FREQ
CALL INVERT(CPH,N,EPS,SINGUL)
IF(SINGUL-1.0) 204,203,203
203 CONTINUE
STOP
204 CONTINUE
CALL MULTIP(N,CPH,XKD,S,6)
DO 205 I=1,N
DO 205 J=1,N
205 S(I,J)=-S(I,J)
CALL MATPRT(N,SSK,6)
WRITE(6,114) N
CALL MATPRT(N,S,6)
CONTINUE
CALL MULTIP(N,PHI,E,CPC,6)
CALL MULTIP(N,CPC,S,SJ,6)
WRITE(6,115) N
CALL MATPRT(N,SJ,6)
CALL MULTIP(N,CPC,SSK,CPH,6)
WRITE(6,116) N
CALL MATPRT(N,CPH,6)
WRITE(6,118)
GO TO 807
100 FORMAT(15,3F12.7)
101 FORMAT(6F10.4)
102 FORMAT(1H1,2X,'STEADY STATE RICCATI'   HH WEST'//)
103 FORMAT(/2X,'C MATRIX FOLLOWS'15,'DIMEN')

```

MAIN0340  
MAIN0350

MAIN0940

MAIN

```

104 FORMAT(/2X,'PHI MATRIX FOLLOWS',I5,'DIMEN')
105 FORMAT(/2X,'THETA MATRIX FOLLOWS',I5,'DIMEN')
106 FORMAT(2X,'B MATRIX FOLLOWS',I5,'DIMENSION')
107 FORMAT (1H1,2X,'GNORM=',E15.5)
108 FORMAT(I5)
109 FORMAT(1H0,2X,'EXP TIME STEP',F10.4,'DESIRED T=',F10.4,'KK=',I5/)
110 FORMAT(1H1,2X,'EXP FOR DESIRED T=',F10.4,2X,'EVAL AT TAU',F10.4/)
111 FORMAT(6E12.4)
112 FORMAT(/2X,'      D      MATRIX FOLLOWS',I5,'DIMEN')
113 FORMAT(/2X,'LOGICAL U  MATRIX FOLLOWS',I5,'DIMEN')
114 FORMAT(/2X,'SPARAMETER MATRIX FOLLOWS',I5,'DIMEN')
115 FORMAT(/2X,'OPTMAL FEEDFORWARD GAINS ',I5,'DIMEN')
116 FORMAT(/2X,'OPTMAL FEEDBACK   GAINS ',I5,'DIMEN')
117 FORMAT(2X,'TAU=',E12.4,2X,'ERROR=',F10.4,2X,'ITER=',I5/)
118 FORMAT(1H0,20X,'END OF DATA SET')
119 FORMAT(1H1,2X,'STEADY STATE  KALMAN METHOD')

```

```

STOP
END

```

```

SUBROUTINE XPEVAL(N2,TAU)
COMMON G(12,12),XP(12,12)
DIMENSION ACALC(12,12),XIDNT(12,12),XACALC(12,12),GTAU(12,12)

```

```

C
C
C
C

```

```

      SINCE WE HAVE SET A LIMIT ON THE TIME STEP, WE HAVE A GUIDE TO
      HOW MANY TERMS OF EXPONENTIAL SERIES IS TO BE USED   (37 TERMS)
      ZERO THE WORKING MATRICES

```

```

DO 229 I=1,12
DO 229 J=1,12
XP(I,J)=0.0
ACALC(I,J)=0.0
XACALC(I,J)=0.0
XIDNT(I,J)=0.0
229 GTAU(I,J)=0.0
DO 230 I=1,N2
DO 230 J=1,N2
GTAU(I,J)=TAU*G(I,J)
IF(I-J)232,231,232

```

```

EXPV0010
EXPV0020
EXPV0030
EXPV0040
EXPV0050
EXPV0060
EXPV0100
EXPV0110
EXPV0120
EXPV0130
EXPV0140
EXPV0150
EXPV0160
EXPV0170
EXPV0190
EXPV0200
EPPV0210
EXPV0220

```

231	XIDNT(I,J)=1.0	EXPV0230
	GO TO 233	EXPV0240
232	XIDNT(I,J)=0.0	EXPV0250
233	ACALC(I,J)=GTAU(I,J)	EXPV0260
230	XP(I,J)=ACALC(I,J)+XIDNT(I,J)	EXPV0270
235	CONTINUE	EXPV0320
	DO 240 I=2,36	EXPV0330
	X=I	EXPV0340
	XI=1.0/X	EXPV0350
	CALL MULTIP(N2,GTAU,ACALC,XACALC,12)	EXPV0360
	DO 239 J=1,N2	EXPV0400
	DO 239 K=1,N2	EXPV0410
	ACALC(J,K)=XI*XACALC(J,K)	EXPV0420
239	XP(J,K)=XP(J,K)+ACALC(J,K)	EXPV0430
240	CONTINUE	EXPV0480
	WRITE(6,200)	
200	FORMAT(80X,'XPEVAL')	
201	FORMAT(20X,I3,10X,E14.5)	
	RETURN	
	END	
	SUBROUTINE MATPRT(N,A,MDIM)	EXPV0490
	DIMENSION A(MDIM,MDIM)	EXPV0500
C		MATP0010
C	THIS IS A SPECIAL MATRIX PRINT SUBROUTINE FOR THIS PROGRAM	MATP0020
C	MDIM = 12 FOR 2N MATRIX                    6 FOR TH E N MATRIX	MATP0030
	DO 105 I=1,N	MATP0040
	IF(MDIM-12)100,101,101	MATP0050
100	WRITE(6,110) (A(I,J),J=1,N)	MATP0060
	GO TO 102	MATP0070
101	WRITE(6,111) (A(I,J),J=1,N)	MATP0080
102	CONTINUE	MATP0090
105	CONTINUE	MATP0100
110	FORMAT(1X,6E15.5)	MATP0110
111	FORMAT(1X,12E11.4)	MATP0120
	RETURN	MATP0130
	END	MATP0140
		MATP0150
		MATP0160

<pre> SUBROUTINE XNORM(N,GNORM) COMMON G(12,12),XP(12,12) DIMENSION GAB(12,12),SUMR(12),SUMC(12) N2=2*N DO 201 I=1,12 SUMR(I)=0.0 SUMC(I)=0.0 201 CONTINUE DO 202 I=1,N2 DO 202 J=1,N2 202 GAB(I,J)=ABS(G(I,J)) DO 203 I=1,N2 DO 203 J=1,N2 SUMR(I)=SUMR(I)+GAB(I,J) SUMC(I)=SUMC(I)+GAB(J,I) 203 CONTINUE RMAX=AMAX1(SUMR(1),SUMR(2),SUMR(3),SUMR(4),SUMR(5),SUMR(6), 1SUMR(7),SUMR(8),SUMR(9),SUMR(10),SUMR(11),SUMR(12)) CMAX=AMAX1(SUMC(1),SUMC(2),SUMC(3),SUMC(4),SUMC(5),SUMC(6), 1SUMC(7),SUMC(8),SUMC(9),SUMC(10),SUMC(11),SUMC(12)) GNORM=AMIN1(RMAX,CMAX) WRITE(6,200) 200 FORMAT(80X,'XNORM ') RETURN END SUBROUTINE STEPSZ(GNORM,T,TAU,KK) KK=0 TMAX=10.0/GNORM IF( T-TMAX) 210,210,211 211 KK=KK+1 DIV=1.0 DO 214 J=1,KK 214 DIV=DIV*2.0 TAU =T/DIV IF(TAU-TMAX)212,212,211 210 TAU=T </pre>	<pre> NORM0010 NORM0020 NORM0030 NORM0040 NORM0050 NORM0060 NORM0070 NORM0080 NORM0090 NORM0100 NORM0110 NORM0120 NORM0130 NORM0140 NORM0150 NORM0160 NORM0170 NORM0180 NORM0190 NORM0200 NORM0210  NORM0220 NORM0230 STEP0010 STEP0020 STEP0030 STEP0040 STEP0050 STEP0060 STEP0070 STEP0080 STEP0090 TTEP0100 STEP0110 </pre>
---	---

212	CONTINUE	STEP0120
	WRITE(6,200)	
200	FORMAT(80X,'STEPSZ')	
	RETURN	STEP0130
	END	STEP0140
	SUBROUTINE SSKAL(XP11,XP12,XP21,XP22,N,ITER,EPSL,SSK)	SKAI0010
C		SKAI0030
C	CALCULATES STEADY STATE FEEDBACK GAIN USING THE KALMAN EQUATION	SKAI0040
C	WE ARE USING A STEP PROCEDURE TO CONVERGE TO THE STEADY STATE	SKAI0050
C	** THE IMPORTANT THING TO NOTICE IS THAT THE TAU ARGUMENT OF	SKAI0060
C	THE FUNDAMENTAL MATRIX IS NEGATIVE**	SKAI0070
C		SKAI0080
	DIMENSION XP11(6,6),XP12(6,6),XP21(6,6),XP22(6,6),SSK(6,6)	SKAI0100
	DIMENSION SSK1(6,6),SSK2(6,6),SSKN(6,6)	SKAI0110
	DO 250 I=1,N	SKAI0120
	DO 250 J=1,N	SKAI0130
250	SSK(I,J)=0.0	SKAI0140
	ITER=0	SKAI0150
251	CONTINUE	SKAI0160
	CALL MULTIP(N,XP22,SSK,SSK1,6)	SKAI0170
	CONTINUE	SKAI0180
	CALL MULTIP(N,XP12,SSK,SSK2,6)	SKAI0190
	DO 252 I=1,N	SKAI0200
	DO 252 J=1,N	SKAI0210
	SSK1(I,J)=XP21(I,J)+SSK1(I,J)	SKAI0220
252	SSK2(I,J)=XP11(I,J)+SSK2(I,J)	SKAI0230
	EPS=0.0000001	SKAL0240
	CALL INVERT(SSK2,N,EPS,SINGUL)	SKAI0250
	IF(SINGUL-1.0) 254,255,255	SKAI0260
255	CONTINUE	SKAI0270
	WRITE(6,201)	
	RETURN	SKAL0280
254	CONTINUE	SKAI0290
	CALL MULTIP(N,SSK1,SSK2,SSKN,6)	SKAI0330
	CALL CNVTST(SSKN,SSK,N,SSKTST)	SKAI0340
C	TO AVOID ROUND OFF, WE FORCE SYMMETRY	SKAI0350

DO 256 I=1,N	SKAI0360
DO 256 J=1,N	SKAI0370
256 SSK(I,J)=(SSKN(I,J)+SSKN(J,I))/2.0	SKAI0380
IF(SSKTST-EP SL) 258,258,259	SKAI0390
259 ITER=ITER+1	SKAI0400
TAU=TAU+T	SKAI0410
GO TO 251	SKAI0460
258 CONTINUE	SKAI0470
WRITE(6,200)	
200 FORMAT(80X,'SSKALZ')	
201 FORMAT(25X,'IT BLEW UP IN SSKAL')	
RETURN	SKAI0480
END	SKAI0490
SUBROUTINE CNVTST(SSKN,SSK,N,SSKTST)	CONV0010
DIMENSION SSKN(6,6),SSK(6,6)	CONV0020
SUMNM=0.0	CONV0030
SUMDM=0.0	CONV0040
C TEST THE CONVERGENCE OF THIS ITERATION	CONV0050
DO 255 I=1,N	CONV0060
SUMNM=SUNNM+ABS(SSKN(I,I)-SSK(I,I))	CONV0070
SUMDM=SUNDM+ABS(SSKN(I,I))	CONV0075
255 CONTINUE	CONV0090
SSKTST=SUNNM/SUNDM	CONV0100
RETURN	CONV0110
END	CONV0120
SUBROUTINE INVERT (A,N,EP S,SINGUL)	INV00010
C	INV00020
C SUBROUTINE INVERT INVERTS A MATRIC IN IT'S OWN SPACE USING THE	INV00030
C GAUSS-JORDAN METHOD WITH COMPLETE MATRIX PIVOTING. I.E. AT EACH	INV00040
C STAGE THE PIVOT HAS THE LARGEST ABSOLUTE VALUE OF ANY ELEMENT IN	INV00050
C THE REMAINING MATRIX. THE COORIIINATES OF THE SUCCRSSIVE MATRIX	INV00060
C PIVOTS USED AT EACH STAGE OF THE RECUCTION ARE RECORDED IN THE	INV00070
C SUCCESSIVE ELEMENTS POSITIONS OF THE ROW CIKYMN UBDEX VECTIRS	INV00080
C R ABD C . THESE ARE LATER CALLED UPON BY THE PROCEDURE PERMUTE WHI	INV00090
C REARRANGES THE ROWS AND COLUMSS OF THE MATRIX. IF THE MATRIX IS	INV00100
C SINGULAR THE PROCEDURE EXITS TO AN APPROPRIATE LABEL IN THE MAIN	INV00110

```

C      PROGRAM. SINGLE = 1.
INTEGER SINGUL,I,J,K,L,PIVI,PIVJ,P,R(6),C(6)
SINGUL = 0
REAL PIVOT,A(6,6)
SET ROW AND COLUMN VECTORS
DO 1 I=1,N
R(I)=I
C(I)=I
CONTINUE
FIND INITIAL PIVOT
PIVI=1
PIVJ=1
DO 3 I=1,N
DO 3 J=1,N
IF (ABS(A(PIVI,PIVJ)) .GE. ABS(A(I,J))) GO TO 2
PIVI=I
PIVJ=J
CONTINUE
CONTINUE
C      START REDUCTION
DO 8 I=1,N
L=R(I)
R(L)=R(PIVI)
R(PIVI)=L
L=C(I)
C(L)=C(PIVJ)
C(PIVJ)=L
INTEGER ICNT,ICNT1,ICNTJ
ICNT=R(I)
ICNT1=C(I)
IF (ABS(A(ICNT,ICNT1)) .GE. EPS) GO TO 4
WRITE (6,9) I,(R(IJ),C(IJ)),IJ=1,N)
SINGUL=1
CALL MATPR1(N,A,6)

```

```

INV00120
INV00130
INV00140
INV00150
INV00160
INV00170
INV00180
INV00190
INV00200
INV00210
INV00220
INV00230
INV00240
INV00250
INV00260
INV00270
INV00280
INV00290
INV00300
INV00310
INV00320
INV00330
INV00340
INV00350
INV00360
INV00370
INV00380
INV00390
INV00400
INV00410
INV00420
INV00430
INV00440
INV00450
INV00460

```

```

4 RETURN
  CONTINUE
  DO 5 J=1,N
    JK=N-J+1
    IF (JK.EQ.1) GO TO 5
    ICNTJ=C(JK)
    A(ICNT,ICNTJ)=A(ICNT,ICNTJ)/A(ICNT,ICNTJ)
    CONTINUE
5  A(ICNT,ICNTJ)=1./A(ICNT,ICNTJ)
    PIVOT=0
    DO 7 K=1,N
      IF (K.EQ.1) GO TO 7
      DO 6 J=1,N
        JK=N-J+1
        IF (JK.EQ.1) GO TO 6
        ICNTJ=C(JK)
        ICNTK=R(K)
        H=A(ICNT,ICNTJ)*A(ICNTK,ICNTJ)
        A(ICNTK,ICNTJ)=A(ICNTK,ICNTJ)-H
        IF (I.GE.-K. OR. I.GE.-JK. OR. ABS(PIVOT).GE. ABS(A(ICNTK,ICNTJ)))
          1 GO TO 6
          PIV1=K
          PIVJ = JK
          PIVOT=A(ICNTK,ICNTJ)
6  CONTINUE
    A(ICNTK,ICNTJ)=-A(ICNT,ICNTJ)*A(ICNTK,ICNTJ)
    CONTINUE
7  CONTINUE
8  CONTINUE
  REARRANGE ROWS
  CALL PERMUT(A,R,C,N,0)
  REARRANGE COLUMNS
  CALL PERMUT(A,C,R,N,1)

```

```

INV00480
INV00490
INV00500
INV00510
INV00520
INV00530
INV00540
INV00550
INV00560
INV00570
INV00580
INV00590
INV00600
INV00610
INV00620
INV00630
INV00640
INV00650
INV00660

```

```

INV00690
INV00700
INV00710
INV00730
INV00740
INV00750
INV00760
INV00770
INV00780
INV00790
INV00810
INV00820
INV00830

```



	RETURN	INVO0850
C		INVO0860
9	FORMAT (1H1,23H THE MATRIX IS SINGULAR ,5H I = 15,(2110))	INVO0870
	END	INVO0880
	SUBROUTINE PERMUT(A,S,D,N,JJ)	PER00010
C	PERMUTE IS A PROCEDURE USING JENSEN'S DEVICE WHICH EXCHANGES ROWS	PER00020
C	OR COLUMN SOF A MATRIX TO ACHIEVE A REARRANGEMENT SPECIFIED BY THE	PER00030
C	PERMUTATION VECTORS S,D. ELEMENTS OF S SPECIFY THE ORIGINAL SOURCE	PER00040
C	LOCATIONS WHILE ELEMENTS OF D SPECIFY THE DESIRED SESTINATION	PER00050
C	LOCATIONS. NORMALLY A AND B WILL BE CALLED AS SUBSCRIPTED VARIABLE	PER00060
C	OF THE SAME ARRAY. THE PARAMETERS J,K NOMINATE THE SUBSCRIPTS	PER00070
C	OF THE DIMENSION AFFECTED BY THE PERMUATION, P IS THE 4ENSEN	PER00080
C	PARAMETER. AS AN EXAMPLE OF THE USE OF THIS PROCEDURE SUPPOSE R,C	PER00090
C	TO CONTAIN THE ROW AND COLUMN SUBSCRIPTS FO THE SUCCESSIVE MATRIX	PER00100
C	PIVOTS USED IN A MATRIX INVERSION OF AN ARRAY A. I.E. R(1),C(1)	PER00110
C	ARE THE RRLATIVE SUBSCRIPTS OF THE FISST PIVOT, R(2),C(2) OF THE	PER00120
C	SECOND PIVOT AND SO ON. THE TWO CALLS , CALL PERMUTE(A(J,P), A(K,P	PER00130
C	),J,K,R,C,N,P) AND CALL PERMUTE((A(P,J),A(P,K),J,K,C,R,N,P) WILL	PER00140
C	PERFORM THE REQUIRED REARRANGEMENT OF TOWS AND COLUMNS RESPECTIVEL	PER00150
	REAL A(6,6),W	PER00160
	INTEGER J,K,N,P,S(6),D(6),TAG(6),LOC(6),I,T,TAGJ,TAGK	PER00170
C	SETUP INITIAL VECTOR TAG NUMBER AND ADDRESS ARRAYS	PER00190
	DO 1 I=1,N	PER00210
	TAG(I)=I	PER00220
	LOC(I)=I	PER00230
1	CONTINUE	PER00240
C		PER00250
C	START PERMUTATION	PER00260
C		PER00270
	DO 4 I=1,N	PER00280
	T=S(I)	PER00290
	J=LOC(T)	PER00300
	K=D(I)	PER00310
	IF (J.EQ.K) GO TO 3	PER00320
	IF(JJ.EQ.1) GO TO 5	
	DO 2 P=1,N	

	W=A(J,P)	
	A(J,P)=A(K,P)	
	A(K,P)=W	
2	CONTINUE	
	GO TO 6	
5	CONTINUE	
	DO 7 P=1,N	
	W=A(P,J)	
	A(P,J)=A(P,K)	
	A(P,K)=W	
7	CONTINUE	
6	CONTINUE	
	TAG(J)=TAG(K)	
	TAG(K)=T	
	TAGJ=TAG(J)	
	TAGK=TAG(K)	
	LOC(T)=LOC(TAGJ)	
	LOC(TAGJ)=J	
3	CONTINUE	PER00380
4	CONTINUE	PER00390
	RETURN	PER00400
	END	PER00410
	SUBROUTINE MULTIP(N,B,C,A,MDIM)	PER00420
	REAL A(MDIM,MDIM),B(MDIM,MDIM),C(MDIM,MDIM)	PER00430
	INTEGER N,I,J,K	PER00440
		PER00450
		PER00460
		PER00470
		MUL00010
C		MUL00030
C		MUL00040
C	THIS PROCEDURE MULTIPLIES TWO MATRICES B AND C	MUL00050
C	SUCH THAT A(I,J)=B(I,K)*C(K,J) AND STORES	MUL00060
C	THE RESULT IN A.	MUL00070
C		MUL00080
	DO 1 I=1,N	MUL00090
	DO 1 J=1,N	MUL00100
	A(I,J)=0	MUL00110
	DO 1 K=1,N	MUL00120
1	A(I,J)=A(I,J)+B(I,K)*C(K,J)	MUL00130
	RETURN	MUL00140